UrbanRain23

12th International Workshop on Precipitation in Urban Areas
29 Nov - 2 Dec 2023, Sporthotel Pontresina, Switzerland
https://urbanrain.ethz.ch/

Book of Abstracts

in alphabetical order by corresponding author

P. Molnar

Institute of Environmental Engineering
ETH Zurich, Switzerland

Zurich, 2023

Impact of rainwater trees on urban cooling: 1st case study in Lyon (France)

L. Alonso [1], F. Renard* [2]

1 L&F Enviroconsulting, France
2 University of Lyon, University Jean Moulin Lyon 3, France

*Corresponding author: florent.renard@univ-lyon3.fr

Abstract

Sanitation and stormwater management have been fundamental urban issues since the early 19th century. For a long time, the most common strategy was to rely heavily on the sewerage system, whatever the type of effluent. However, this paradigm has been challenged since the 1990s. Lyon (France) was a pioneer in this field, with the creation in 1999 of the Field Observatory of Urban Water Management (OTHU[1]). This is a research laboratory for observing urban discharges and their impact on receiving systems, particularly during rainfall, in the Lyon region. The aim is to propose new solutions for wastewater treatment design and management. It is a research federation involving 9 research establishments in Lyon. This new type of management is all the more important in view of the effects of climate change, and in particular the assessment of rain-generating synoptic circulations leading to increased rainfall (Renard and Alonso, 2018). This intensification of rainfall saturates the sewage networks, which in Lyon's urban center are mostly combined sewers. This leads to direct discharges of wastewater into the natural environment, mainly the main rivers (Rhône and Saône). At the same time, more frequent and longer heatwave periods are having an impact on both human populations and ecosystems.

The need to manage rainwater locally, directly at the point of precipitation, to reduce the volume of runoff reaching the networks, is becoming increasingly apparent. This also helps to cool the city, which is crucial in the context of climate change, particularly in the context of soil impermeabilization and the disappearance of green spaces in recent decades. The Lyon metropolitan area is therefore determined to reduce soil waterproofing and encourage the infiltration of rainwater at source. One of the most effective solutions is to develop rain trees (sometimes also called stormwater trees or rainwater trees – Carlyle-Moses et al., 2020 ; Livesley et al., 2016). The rain tree is a tree whose planting pit has been sized on the surface to capture part of the rainwater runoff, and is concave in shape (fig. 1).

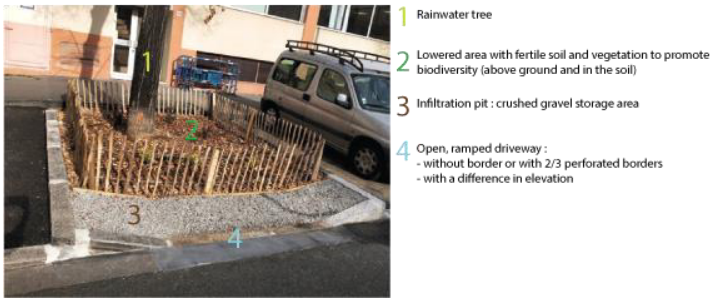

Fig 1: Rain tree operation (adapted from Caltran et al., 2022)

This concept can also be used in urban redevelopment projects to disconnect runoff from the combined sewer system and infiltrate it locally. From this point of view, rain trees fall into the category of nature-based solutions. They are natural tools, helping to reduce local flood risks by intercepting

[1] http://www.graie.org/othu/index.htm

precipitation through their canopy, limiting runoff through infiltration and also contributing to urban cooling through evapotranspiration. In addition, run-off water promotes tree growth and biodiversity, including that of the soil (Caltran et al., 2022). The aim of this study is therefore to assess the cooling impact of rain trees in tackling urban overheating and improving thermal comfort, by means of in situ measurements of climatic parameters and comparison of redeveloped areas with reference areas. Two areas in central Lyon were redesigned to transform existing alignment trees into rain trees: the Vauban site and the Récamier site. These sites are compared to control areas with tree stands that have not been reworked, located on the same street, with the same urban morphology conditions. The climatic parameters measured using professional measuring equipment calibrated in a certified laboratory are air temperature, relative humidity, mean radiant temperature and the thermal comfort index wet bulb globe temperature (WBGT). The WBGT is an index of the environment that is considered along with metabolic rate to assess the potential for heat stress, among those exposed to hot conditions. It combines the measurement of two derived parameters: natural wet-bulb temperature and black globe temperature (ISO 7243:2017[2]). The surface temperature of tree bases is also measured, in order to compare the effect of soil requalification.

38 mobile pedestrian measurement campaigns with continuous recording were carried out to measure these parameters, on warm days with no wind, in the morning, afternoon, evening and night, between June and August 2022. The Mann-Whitney test is a non-parametric test for comparing two independent samples. It is used to compare the climatic parameters and thermal comfort index between the areas requalified as rain trees and the unrestructured control sites. The measured parameters (air temperature, relative humidity, mean radiant temperature, surface temperature and thermal comfort) were studied using the Mann-Whitney statistical test, between areas requalified using rain trees and control areas. The p-value was found to be insignificant for all parameters. These results are due to the fact that these are mainly young trees on the Juliette Récamier street. They therefore do not yet provide significant shade, and their biomass is insufficient to influence the surrounding microclimatic parameters. As for the sites on rue Vauban, the vegetation at the base of the trees is still developing. It is therefore still too early to see any influence on the parameters measured. Furthermore, the summer of 2022 in Lyon was marked by extremely dry weather conditions. These did not favor evapotranspiration and contributed to potential cooling. To conclude, the rain tree concept is a highly effective way of managing urban water, particularly during heavy rainfall. However, it needs to be monitored over time to assess its impact on urban thermal comfort, in the context of climate change.

References

Caltran H., Sanabria J., Goubier P., Nait Barka H., Henry A. (2022), Livret techniques Les arbres de pluie, (ed) Métropole Grand Lyon, 28 pp.

Carlyle-Moses, D.E., Livesley, S., Baptista, M.D., Thom, J., Szota, C. (2020), Urban Trees as Green Infrastructure for Stormwater Mitigation and Use. In: Levia, D.F., Carlyle-Moses, D.E., Iida, S., Michalzik, B., Nanko, K., Tischer, A. (eds) Forest-Water Interactions. Ecological Studies, vol 240. Springer, Cham.

Livesley, S.J., McPherson, E.G. and Calfapietra, C. (2016), The Urban Forest and Ecosystem Services: Impacts on Urban Water, Heat, and Pollution Cycles at the Tree, Street, and City Scale. J. Environ. Qual., 45: 119-124.

Renard, F. Alonso, L. (2018), A comparison of two weather type classifications for evidence of climate trends on intense rainfall in the context of local climate change, in Peleg, N., and Molnar, P. (2019) Rainfall monitoring, modelling and forecasting in urban environments, 11th International Workshop on Precipitation in Urban Areas (UrbanRain18), Pontresina, Switzerland. ETH-Zürich, Institute of Environmental Engineering, pp. 144

[2] https://www.iso.org/obp/ui/#iso:std:iso:7243:ed-3:v1:en

The sensitivity of urban surface water flood modelling to the temporal distribution of rainfall

M. Asher*[1,2], M. Trigg[1], C. Birch[2], S. Böing[2], R. Villalobos-Herrera[3]

1 School of Civil Engineering, University of Leeds, UK
2 School of Earth and Environment, University of Leeds, UK
3 University of Costa Rica, Civil Engineering, San José, San Pedro, Costa Rica

*Corresponding author: gy17m2a@leeds.ac.uk

Abstract

Surface water flooding (SWF) arises when rainfall overwhelms the capacity of drainage systems causing excess water to flow overland rather than soaking into the ground or entering the sewer system. The risk posed globally by SWF to people and properties is growing due to rapid urbanisation and the intensification of rainfall due to climate change. Whilst tools to model urban flood risk have also been rapidly developing, there remains a knowledge gap around the sensitivity of urban hydraulic modelling methods to the temporal distribution of rainfall in the model input.

Flood risk analysis is often based upon event-based flood modelling, in which the flood response of a catchment to an individual 'design storm' event is simulated. The design storm must have a depth, corresponding to a specified return period, as well as a duration and a temporal profile representing variations in intensity over the duration of the storm (known as a hyetograph). Often in SWF modelling studies only one hyetograph is considered (Sharma et al, 2021)

In the UK, recent evidence suggests that the industry standard hyetograph is not very representative of real events. This hyetograph, defined in the Flood Estimation Handbook (FEH), is symmetrical and with a single peak in intensity (Fig 1, black line). In contrast, study of a large set (~72,000) of observed UK extreme precipitation events suggests that the peak in intensity more frequently occurs closer to the start or the end of real events (Villalobos-Herrera, 2022). The importance of accounting for this hyetograph variability in SWF modelling is investigated here.

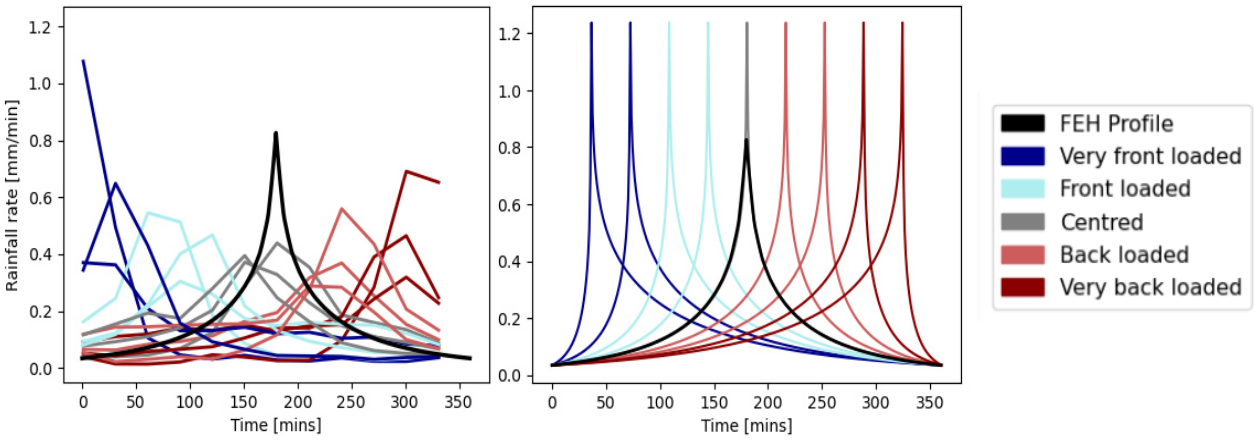

Fig 1: Hyetograph profiles used in model sensitivity testing. Left are profiles based on observed extremes, and right are idealised profiles. Both are constructed for a 6 hour duration, 100 year return period event in the test catchment. The standard FEH profile is also included for reference.

Specifically, an urban catchment in the north of England that is prone to surface water flooding is used to test model sensitivity to variations in the hyetograph. A 2D rain-on-grid Hec-Ras model is run over a 23km^2 catchment in the north of England which contains a mixture of urban and rural land uses. Over multiple model runs, the rainfall accumulation (60mm) associated with a 100 year return period event for a 6 hour duration in this catchment is consistently applied. For each model run the hyetograph used to distribute this depth over time is altered, using two sets of experimental hyetographs. The first is a set of fifteen physically realistic profiles, derived from the work on observed extremes (Villalobos-Herrera, 2022) (left, Fig 1). The second is a set of nine idealized profiles, derived from approximating the method used to construct the FEH profile and then applying systematic variations to shift the peak in time (right, Fig 1). The outputs are analyzed in respect to the total flooded extent (the area which undergoes flooding at some point during the model run time); the flood severity (in terms of the depth, velocity, and hazard rating of the flooded area); and the timing of the flood peak within the channel.

We demonstrate that SWF modelling is sensitive to the way rainfall is distributed over time. Experiments with idealised profiles (right, Fig 1) demonstrate a consistent trend towards more extensive (right, Fig 2) and more severe SWF in response to later peaks in intensity. Distributing the rainfall volume over time using the observed profiles (left, Fig 1) result in even greater differences in flooding outcomes (left, Fig 2). The same rainfall volume was found to result in an 18% greater total flooded area when distributed over time using a realistic back loaded profile, compared to using a realistic front loaded profile. Failing to represent the variety of temporal distributions found in extreme events may lead to misrepresentation (either over or under) of the surface water flood risk.

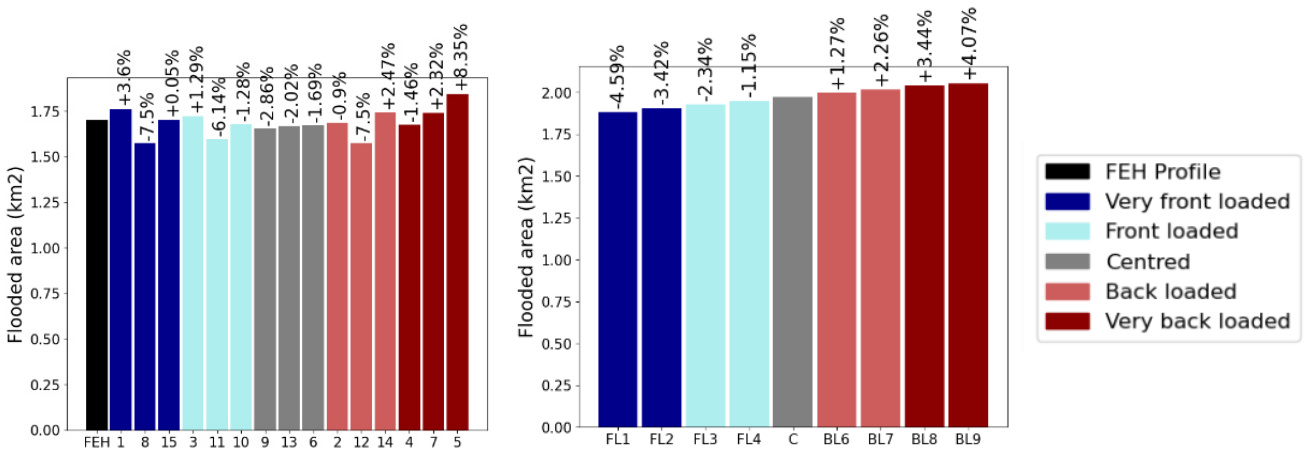

Fig 2: The total area (km^2) flooded at any point during the model run period. For the observed profiles (left) and the idealised profiles (right). For the observed profiles the percentage differences are shown relative to the FEH profile, and for the idealised profiles relative to the centered profile,

References

Sharma, A., Hettiarachchi, S. and Wasko, C., 2021. Estimating design hydrologic extremes in a warming climate: alternatives, uncertainties and the way forward. Philosophical Transactions of the Royal Society A, 379(2195), p.20190623.

Villalobos-Herrera, R., Blenkinsop, S., Guerreiro, S.B., Fowler, H.J. Flood estimation methods in the UK need new temporal profiles. (in preparation) (2022)

Error components in rainfall retrieval from collocated commercial microwave links

A. Špačková[1], M. Fencl[1], V. Bareš*[1]

1 Dept. of Hydraulics and Hydrology, Czech Technical University in Prague, the Czech Republic

*Corresponding author: vojtech.bares@cvut.cz

Abstract

Commercial microwave links (CMLs) operating in telecommunication networks can serve as rainfall sensors. However, the diversity of such opportunistic sensors and their errors are difficult to handle. This analysis empirically evaluates errors of CML observations in a real network without reference to rainfall measurements. Independent collocated CMLs at twelve sites within a real telecommunication network in Prague enable us to assess the effect of hardware homogeneity and measurement consistency. The evaluation considers 33 rainfall events in the non-winter periods of the years 2014 to 2016, monitored at 1-min temporal resolution with signal quantization of 0.3 dB. The study evaluates eight sites of identical frequency band CMLs and six sites of different frequency band CMLs. Discrepancies between collocated CMLs of the same frequency are only due to hardware characteristics and enable us to evaluate the hardware homogeneity, whereas the discrepancies of CML pairs of different frequencies are due to hardware inhomogeneity and a different interaction of microwaves to the propagation medium.

As the CML observation of rainfall is indirect, signal attenuation needs to be transformed to rainfall intensity. The processing utilises the power-law relationship of the specific attenuation and rainfall intensity. The specific attenuation (attenuation per link-path distance) is estimated from the total path loss with separation of the dry-weather attenuation (baseline) and the wet antenna attenuation (WAA), caused by the water film forming on antenna radomes. This study applies centred 10-day moving average of the total loss for baseline separation and the WAA model optimized to minimum root mean squared error with rain gauge-adjusted weather radar (Špačková et al., 2023).

Figure 1 (left) shows scatterplots of rainfall intensities of independent collocated CMLs for sites where operate at identical frequency bands. The correlation ranges from 0.97 to 0.99 and RMSE is between 0.4 and 0.9 mm h^{-1}. The double-mass curves of the cumulative rain of the CML pairs are displayed in Figure 1 (right) to explore the systematic component of the measurement deviations. The curves are parallel to the diagonal, indicating synchronized systematic errors of the independent sensors. However, changes in the trend of systematic errors can be observed. For example, by the pair at site 10a, link 2 observes systematically lower rain rates than link 1 up to rainfall depths around 200 mm, however, this trend then changes resulting in very low relative error. Overall, the pairs have a relative error between 0.01 and 0.18.

Figure 2 (left) shows scatterplots of the rainfall intensities of independent collocated CMLs at sites where operate at different frequency bands. The correlation ranges between 0.96 and 0.99 and RMSE between 0.6 and 1.7 mm h^{-1}. Overall, the performance worsened compared to the pairs operating at identical frequency bands. The double-mass curves of cumulative rain (Fig. 2 right) show the CMLs operating at higher frequency bands (links 2) with tendency to overestimate a CMLs operating at a lower frequency band (links 1). The worst match between CML pairs is observed at site 4b, where the 32 GHz CML overestimates the 25 GHz CML, more than others with a relative error of 0.69. An identical setup (32 and 25 GHz CMLs) at site 5b does not mirror such a strong tendency for overestimation having a relative error of only 0.12. Furthermore, there are also step increases along three double-mass curves (sites 2b, 5b, and 11b). The increases are associated with a systematic underestimation of rainfall intensity by links 1, while links 2 perceive low rainfall intensities for a long time. Overall, the pairs have a relative error between 0.12 and 0.26

excluding site 4b. The relative error is higher than in the case of sites with identical frequency CMLs in the pair.

This study investigates the consistency between CMLs by comparing pairs of independent collocated devices operating at the same and different frequency bands without reference rainfall measurements. The systematic errors are more pronounced for collocated CMLs operating at different frequency bands. The CMLs operated at higher frequency tend to observe higher rain rates than those operated at lower frequencies. Overall, the observations are in very good agreement, which confirms the homogeneous behaviour of the hardware in the real network.

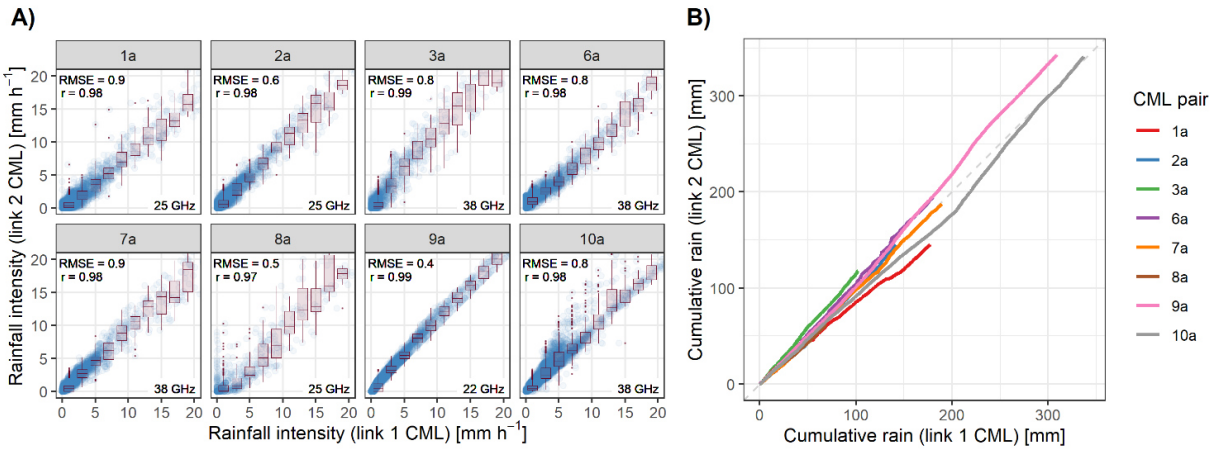

Fig 1: (left) Scatter plot of the CML-derived rainfall intensity (up to 20 mm h^{-1}) for eight collocated CML pairs having identical frequencies. The boxplots show a spread when binned to 2 mm h^{-1} bins by link 1. The performance metrics (correlation and RMSE in mm h^{-1}) are in the top left corner and the frequency band is indicated in the bottom right corner for each site. (right) Double-mass curves.

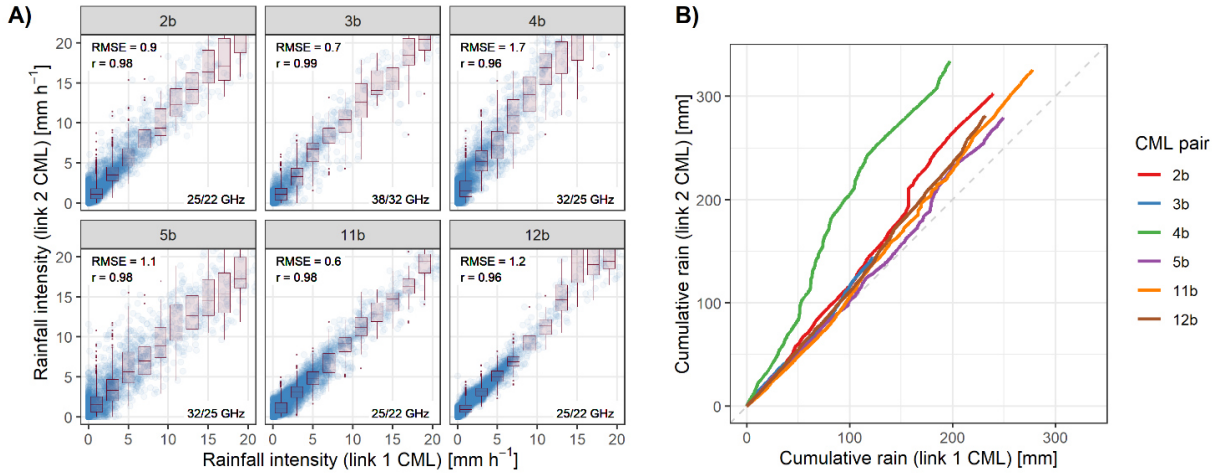

Fig 2: (left) Scatter plot of the CML-derived rainfall intensity (up to 20 mm h^{-1}) for six collocated CML pairs having different frequencies. The boxplots show a spread when binned to 2 mm h^{-1} bins by link 1. The performance metrics (correlation and RMSE in mm h^{-1}) are in the top left corner and the frequency band is indicated in the bottom right corner for each site. (right) Double-mass curves.

References

Špačková, A., Fencl, M., and Bareš, V. (2023), Evaluation of error components in rainfall retrieval from collocated commercial microwave links, Atmos. Meas. Tech. Discuss. [preprint], https://doi.org/10.5194/amt-2022-340, in review.

Globally applicable workflow for urban pluvial risk estimates in data-scarce environments

J. Blagojevic*[1], A. Paschalis[2], P. Molnar[1]

1 Institute of Environmental Engineering, ETH Zurich, Switzerland
2 Department of Civil and Environmental Engineering, Imperial College London, United Kingdom

*Corresponding author: blagojevic@ifu.baug.ethz.ch

Abstract

New precipitation data sets with global coverage provide an accessible and low-cost means for water resource and water-hazard risk management in data-scarce regions, or comparative studies with global coverage. These precipitation data sets, often derived from satellite observations tend to underestimate the short-duration, high-intensity rainfall events. Generating design-useful Intensity-Duration-Frequency (IDF) curves from such global data sets, especially for shorter duration rainfall events on the order of 1-hr or less, is often characterized by underestimation compared to the ground truth. Such underestimation exceeds what can be expected by spatial scale incompatibilities, often considered using areal reduction factors. Using the global data sets for pluvial flood risk analysis consequently leads to lower flood risk estimates.

In this paper, we develop a methodology to obtain hourly-scale IDF curves, suitable for flood inundation modelling, for ungauged areas using global datasets. To achieve that, high time-resolution, satellite remote sensing rainfall data (GSMaP) is used to train a stochastic rainfall generator model (point process Bartlet-Lewis model). The weather generator is then used to statistically disaggregate daily global precipitation data (GPCC) via stochastic ensemble simulation. The disaggregated data is used to generate more accurate IDF curves, which underpin pluvial flooding risk assessments based on realistic short duration rainfall intensities. The discrepancies in flood inundation risk estimates in urban environments, due to rainfall intensity underestimation, are demonstrated using a 2-d hydrodynamic model. All the analysis steps are executed using publicly available data sets following FAIR principles. The proposed workflow yields globally applicable rough estimates of pluvial flood risk, more representative than when using the readily available global IDF studies or IDF curves derived directly from global precipitation datasets.

How well can a new high-resolution atmospheric reanalysis ALADIN reforecast heavy precipitation?

V. Bližňák*[1], P. Zacharov[1], M. Kašpar[1], R. Kvak[1,2]

1 Institute of Atmospheric Physics, CAS, Prague, Czech Republic
2 Charles University, Faculty of Science, Prague, Czech Republic

*Corresponding author: bliznak@ufa.cas.cz

Abstract

Information on precipitation distribution at high horizontal and temporal resolution is of great importance in several fields, such as climatology, hydrology, water management, spatial planning, etc. One of the tools that can be used to obtain information about the spatiotemporal precipitation distribution in the past is atmospheric reanalyses. They are calculated using numerical weather prediction (NWP) models with or without assimilation of the observed data and provide consistent three-dimensional time series of the state of the atmosphere, typically over several decades to centuries. However, most current reanalyses lack either high horizontal or temporal resolution and are therefore not sufficiently capable of simulating high precipitation totals.

The new atmospheric reanalysis ALADIN provides precipitation reforecasts since 1989 in a high horizontal (2 km) and temporal (1 h) resolution. The non-hydrostatic nature of the NWP model and its very fine resolution allow the simulation of heavy precipitation including local convective precipitation over a large area (i.e. most of Europe) and over a long period (i.e. 30 years). The presented contribution will assess this capability based on observed precipitation representing two types of adjusted radar-derived precipitation estimates used as ground truth in the warm parts of the years 2013-2019. The first dataset was prepared using only Czech weather radar and rain gauge network data (Sokol, 2003; Bližňák et al., 2018). The second dataset was calculated for most of Europe using a combination of data from Operational Programme for the Exchange of Weather Radar Information (OPERA), which is a pan-European weather radar composite, daily rain gauge records from the European Climate Assessment & Dataset (ECA&D) database and cloud mask derived from Meteosat Second Generation measurements (Overeem et al., 2023).

Heavy precipitation will be selected from the datasets using defined criteria and their location and total amount will be evaluated for two different NWP model runs. The first one ALADIN/Reanalysis includes the full assimilation of the observed data every 6 hours using the 4D-VAR assimilation scheme. The second one ALADIN/Evaluation Run uses only the boundary conditions from the ERA-5 global reanalysis and the prognostic data are not modified in any way. Comparing the two runs will provide us with information about the level of physical description in the NWP model as well as the effect of assimilation on the resulting precipitation fields.

An example of the spatial distribution of precipitation originating from a mesoscale convective system that occurred between 1 June 2013, 2200 UTC and 2 June 2013, 0200 UTC over the Czech Republic, is shown in Fig. 1. The figure comparing the four precipitation products shows well that both model runs are capable of predicting high precipitation, but their location and timing can be a difficult task. An objective qualitative and quantitative evaluation of simulated precipitation based primarily on a fuzzy approach will provide valuable feedback to NWP model developers regarding precipitation accuracy.

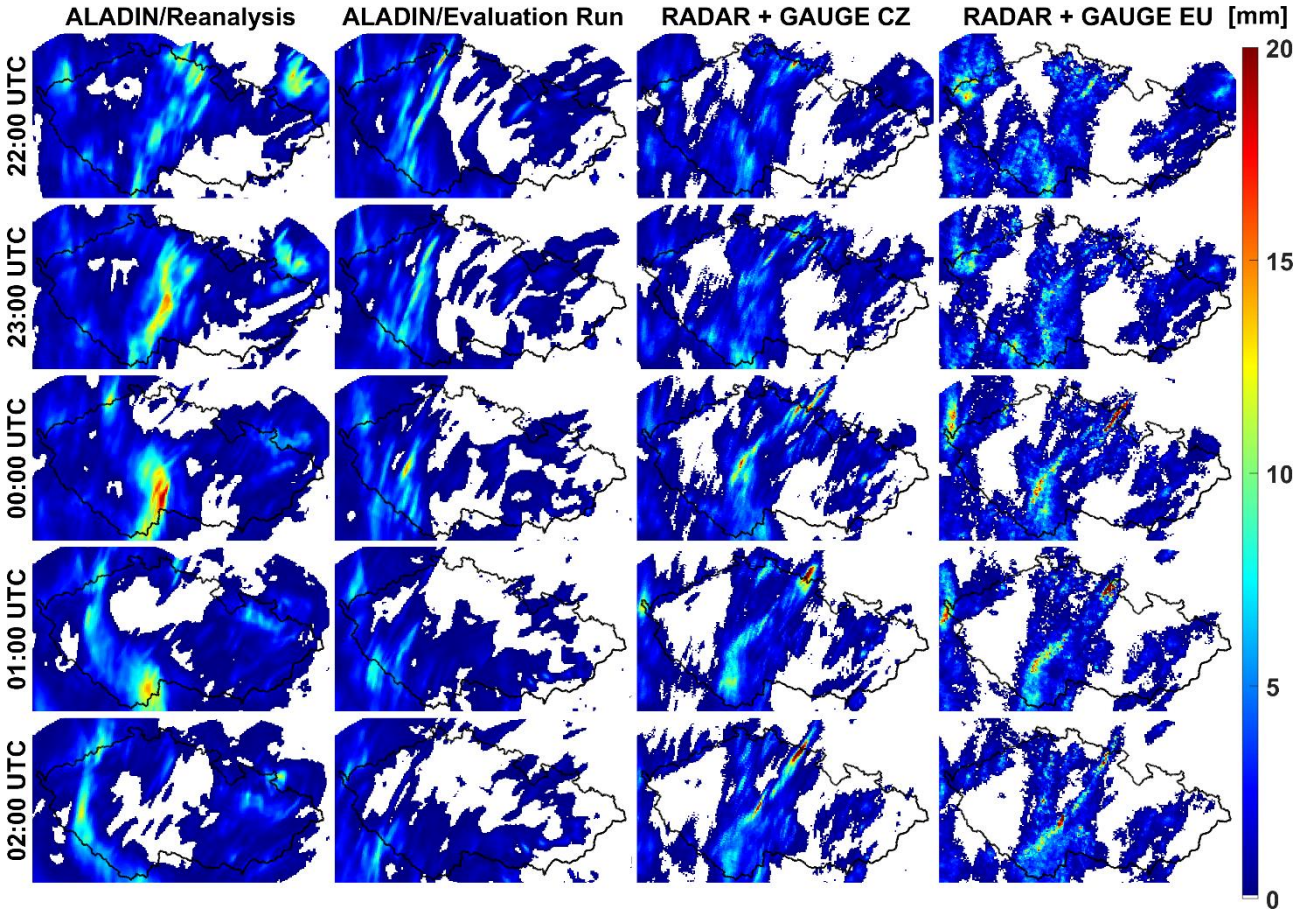

Fig 1: Spatial distribution of precipitation originating from a mesoscale convective system that occurred between 1 June 2013, 2200 UTC and 2 June 2013, 0200 UTC over the Czech Republic. The ALADIN/Reanalysis and ALADIN/Evaluation Run of 1-h precipitation totals are shown in the first and second columns, respectively. Observations represented by adjusted radar-derived precipitation estimates of 1-h precipitation totals based on Czech (RADAR + GAUGE CZ) and Europe (RADAR + GAUGE EU) data are displayed in the third and fourth columns, respectively.

References

Bližňák, V., Kašpar, M., and Müller, M. (2018), Radar-based summer precipitation climatology of the Czech Republic, Int. J. Climatol., 38, 677-691.

Overeem, A., van den Besselaar, E., van der Schrier, G., Meirink, J. F., van der Plas, E., Leijnse, H. (2023), EURADCLIM: the European climatological high-resolution gauge-adjusted radar precipitation dataset, Earth Syst. Sci. Data, 15, 1441-1464.

Sokol Z. (2003), The use of radar and gauge measurements to estimate areal precipitation for several Czech river basins, Stud. Geophys. Geod., 47, 587–604.

Thermo-dynamical impacts of cities on cloud formation and precipitation

A. Brandi*[1], G. Manoli[1]

[1] Laboratory of Urban and Environmental Systems (URBES), Ecole Polytechnique Fédérale de Lausanne, Switzerland

*Corresponding author: aldo.brandi@epfl.ch

Abstract

The impact of landscape modifications produced by urban environments is manifest as a complex system of thermo-dynamical land-atmosphere interactions. The abundance of paved impervious surfaces results in a greater absorption of solar radiation and reduced water retention that affect the partitioning of net radiation between sensible and latent heat fluxes. The excess of sensible heat flux results in a positive thermal anomaly over urban environments compared to their surrounding non-built areas (the well know urban heat island effect, UHI) and in well mixed and deeper urban boundary layers. In the absence of strong synoptical forcing, the thermal gradient produced by the UHI has the potential to promote an associated local circulation characterized by surface level convergence that promotes inflow of cooler air from the surrounding countryside (Findlay and Hirt, 1969). In addition, increased surface drag of three-dimensional urban building morphologies can slow down regional wind flow over urban environments and promote surface level air mass convergence.

Recent extensive observational studies over European (Theeuwes et al., 2019) and U.S. (Vo et al., 2023) cities showed that urban environments increase cloud cover formation and there is growing evidence that landscape modifications introduced by urban environments can also result in increased rainfall (Huang et al., 2022). Precipitation in urban environments is associated with the potential to provide both vital resources and natural hazards. On one hand, rainfall can be harvested and used to respond to the water needs of the continuously growing global urban population. On the other, the limited ability of urban surfaces to absorb precipitation, increases the potential for surface runoff and the risk of flooding.

Despite the increased risk associated with projected increase in extreme precipitation frequency and intensity associated with urbanization and climate change, there is still limited understanding of the physical processes affecting urban boundary layer dynamics involved in cloud cover formation and precipitation. Here we use a suite of idealized and real case scenario Weather Research and Forecast model simulations to conduct controlled experiments aimed at identifying and elucidating the role of individual and combined key components of thermo-dynamical processes in affecting cloud cover and precipitation over urban environments.

References

Findlay, B. F., & Hirt, M. S. (1969). An urban-induced meso-circulation. Atmospheric Environment (1967), 3(5), 731 537-542.

Theeuwes, N. E., Barlow, J. F., Teuling, A. J., Grimmond, C. S. B., & Kotthaus, S. (2019). Persistent cloud cover over mega-cities linked to surface heat release. *Npj Climate and Atmospheric Science*, *2*(1), 15.

Vo, T. T., Hu, L., Xue, L., Li, Q., & Chen, S. (2023). Urban effects on local cloud patterns. *Proceedings of the National Academy of Sciences*, *120*(21), e2216765120.

Huang, J., Fatichi, S., Mascaro, G., Manoli, G., & Peleg, N. (2022). Intensification of sub-daily rainfall extremes in a low-rise urban area. *Urban Climate*, *42*, 101124.

Improving the generalizability of urban pluvial flood emulators to untrained cities and rainfall

T. Cache*[1], M. S. Gomez[1], T. Beucler[1], J. P. Leitão[2], N. Peleg[1]

1 Institute of Earth Surface Dynamics, University of Lausanne, Lausanne, Switzerland
2 Eawag, ETH Zurich, Zurich, Switzerland

*Corresponding author: tabea.cache@unil.ch

Abstract

Urban pluvial flooding represents a global and increasing threat to people and infrastructures as cities grow and their climate changes. Specifically, cities can modify rainfall space-time properties and are vulnerable to the intensification of short-duration rainfall extremes caused by global warming. However, our understanding of the joint effect of urbanization and climate change on future urban pluvial floods' magnitude and frequency is still limited and requires to be evaluated in a stochastic framework to consider the natural climate variability along with different possible urban development and climate change scenarios. Adopting such a stochastic framework is computationally costly and beyond the capabilities of most hydrologists and research units. Data-driven models have received growing attention for emulating urban flood maps as they overcome the bottleneck of large computational costs of high-resolution physically based simulations in cities but their lack of generalizability (i.e., the prediction inability in un-trained scenarios) to both terrain and rainfall events limits their application in urban climate change studies. Therefore, we develop a new deep-learning model that can be applied to unseen urban areas and different rainfall events without being retrained. The proposed CNN-LSTM model combines the patch- and resizing-based options from recent studies in order to preserve the high-resolution terrain features while including large-scale information. We further develop the model to consider spatially varying rainfall across the city as urban areas are highly sensitive to space-time rainfall variability. The results show that the model outperforms other state-of-the-art urban flood emulators.

SPEI based severity-area-frequency curves for drought monitoring

A. Cancelliere*[1], N. Palazzolo[1], D.J. Peres[1]

1 Department of Civil Engineering and Architecture, University of Catania, Italy

*Corresponding author: antonino.cancelliere@unict.it

Abstract

Standardized Precipitation Evapotranspiration Index (SPEI) is a widely used multiscalar standardized drought index based on the difference between precipitation and potential evapotranspiration for different aggregation time scales (Vicente-Serrano et al., 2010). Probabilistic analysis of the evolution of spatial features of SPEI may provide useful information for drought management planning. Furthermore, monitoring of the spatial extent of an ongoing drought provides useful information in order to timely implement adequate mitigation measures, since similar/different drought patterns in different areas may affect feasibility of interbasin water transfers. To this end, the areal extent of the region affected by drought $Ad_t(z_0)$, can be employed, which expresses the percentage of the area of the investigated region where the SPEI is below the threshold z_0.

In this work, analytical approximations of the probability distribution of areal extent $Ad_t(z_0)$ are derived as a function of the statistical characteristics of the underlying SPEI field, and in particular of its spatial correlation structure. More specifically, let's assume a region with m stations (or m grid points) and related influence areas (or cell size) a_k. With reference to SPEI observations in station (cell) k at time t, $Z_{k,t}$, let's introduce the indicator variable $I_{k,t}$ function of a drought threshold z_0: $I_{k,t} = 0$ if $Z_{k,t} > z_0$ and $I_{k,t} = 1$ if $Z_{k,t} \le z_0$. Note that $I_{k,t}$ is an implicit function of the underlying SPEI field and of z_0. Then the areal extent will be $Ad_t(z_0) = \sum_{k=1}^{m} a_k I_{k,t}$.

In the general case of cross correlated SPEI, expected value and variance of $Ad_t(z_0)$ can be derived as a function of the stochastic properties of the underlying SPEI field and of z_0 as:

$$[Ad_t] = \quad (z_0) \tag{1}$$

$$\mathrm{Var}[Ad_t] = \quad (z_0)[1 \quad (z_0)] + 2\sum_{k=1}^{m}\sum_{j=k+1}^{m} a_k a_j \left[p_{k,j} \quad {}^2(z_0)\right] \tag{2}$$

where $\Phi(.)$ is the standard normal cdf and $p_{k,j}=P[Z_{k,t} \le z_0, Z_{j,t} \le z0]$. Note that given the normality of SPEI (in marginal sense), it is reasonable to assume a bivariate standard normal to compute the former probability, which therefore will be only function of the cross correlation between $Z_{k,t}$ and $Z_{j,t}$.

Derivation of the exact distribution of $Ad_t(z_0)$ can be cumbersome. Therefore, here an analytical approximation (exact from a second order moment point of view) is derived. More specifically, observing that $Ad_t(z_0)$ is by definition bounded between 0 and 1, a beta distribution is considered (Johnson et al., 1995), whose first and second moments are assumed equal to the expected value and variance of $Ad_t(z_0)$ given by eqs. (1) and (2):

$$f_{Ad_t}(a) = \frac{1}{B(\delta,\xi)} \cdot a^{\delta-1}(1-a)^{\xi-1} \tag{3}$$

The condition on the first and second moment leads to:

$$= \propto_A^2 \cdot \left(\frac{1 \quad \propto_A}{\frac{2}{A}} \right) \quad \propto_A \tag{4}$$

and

$$= \frac{(1 \quad _A) \times}{_A} \tag{5}$$

where μ_A and σ^2_A are the expected value and variance of $Ad_t(z_0)$) as in eqs. (1) and (2) and they are implicitly function of z_0.
The developed methodology has been applied to characterize probabilistically drought areal extent in Sicily island, Italy, one of the largest islands in the Mediterranean sea with a surface of≅ 25000 km^2. Reanalysis Era5Land precipitation and potential evapotranspiration gridded data at the monthly time scale from 1950 to present time, have been used for SPEI calculation.

The derived pdf given by combining eqs. (1)-(5) enables to map probabilities in a ($z0$, $Ad_t(z_0)$) plane. On the same plane, the severity area $Ad_t(z_0)$ curves observed in a given month can also be plotted. As an example in Fig. 1 the observed SPEI 12 months $Ad_t(z_0)$ curves are shown with reference to March 2022, May 1997 and March 1973. From the plot it can be inferred that in March 2002 90% of the region was affected by SPEI-12 values below z_0=-2, which is indicative of very dry conditions extended in space. On the other hand, the curve related to May 1997 reveals that the whole region was in near mean conditions since the SPEI-12 values varied between z_0=-0.5 and z_0=0.5. Similarly, the curve related to March 1973 indicates very wet conditions for the whole region since 100% of the region was affected by SPEI-12 values above z_0=3. On the same plot, the probabilities of observing less severe conditions (computed making use of the pdf in eq. (3)) is shown in a color scale which enables to assess the severity of the observed drought areal extent in probabilistic terms. As an example, from the plot it can be inferred that probabilities of observing drought areal extents for varying z_0 above those observed in March 2002 is very small, which confirms the severity of the drought that occurred in 2002 in the island.

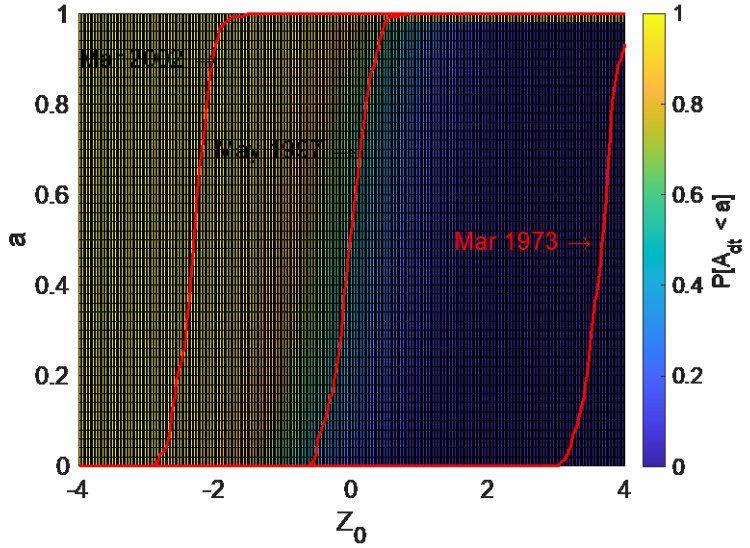

Fig. 1: SPEI-12 severity-area curves $Ad_t(z_0)$ computed for different months in Sicily (red lines) and probabilities of observing a smaller drought areal extent (color map).

References

Johnson, N. L., Kotz, S., & Balakrishnan, N. (1995). Continuous univariate distributions, volume 2 (Vol. 289). John wiley & sons.

Vicente-Serrano, S. M., Beguería, S., & López-Moreno, J. I. (2010). A multiscalar drought index sensitive to global warming: the standardized precipitation evapotranspiration index. Journal of climate, 23(7), 1696-1718.

Estimation of flooded areas from post-event survey and mitigation scenarios using permeable pavement solutions: a case study in the Italian territory

A. Cauteruccio*[1], E. Chinchella[1], G. Boni[1], L.G. Lanza[1]

1 Dept. of Civil, Chemical and Environmental Engineering (DICCA), University of Genova, 16145, Genoa, Italy

*Corresponding author: arianna.cauteruccio@edu.unige

Abstract

The Italian territory is increasingly prone to damage due to flooding events as a consequence of increasing urbanization. The imperviousness of soil reduces the infiltration process resulting in increased flood hazard, while the growth of population and its economic welfare enhance the exposure and vulnerability with a resulting amplification of the risk associated with flooding events. The National project “Return – multi-Risk sciEnce for resilienT commUnities undeR a changiNg climate” addresses this topic within the activity of work package 2: “Flood risk under environmental and climatic changes”.

During the three years of the project, the envisaged activities include the collection of post-event datasets composed of rainfall measurements (from in-situ and remote sensors), extension of the flooded areas, water depth and velocity, assets at risk, damage estimation, surface and subsurface drainage network information in terms of size and maintenance degree, etc. The collected information will support future mitigation strategies and/or warning systems based on an easy-to-perform flooding simulation model.

The present work focuses on the urban flooding event occurred in the Sampierdarena district of the town of Genoa (Italy), on September 24th, 2022. Rain gauge measurements at the five-minute resolution were collected as well as the extension of the flooded areas and the occurred damages. The post-event survey was conducted based on photographs, videos and reports made available by citizens, authorities and operators present during the emergency interventions. From the available documentation, selected reference locations were identified to derive water depth values needed to reconstruct at least the extension of the flooded area.

Fig 1: The urban district of Sampierdarena (left hand side – from GoogleMaps), and flooding features on a street (central picture – from genova24.it) and a commercial activity (right hand side – from imperiapost.it).

With the aim to provide an easy-to-use procedure to reconstruct the extension of the flooded area, for use by civil protection and/or the municipality, the estimated water levels at the reference locations were implemented in a Geographic Information System (GIS) and using the Digital Terrain Model (DTM) the morphologically expected extension of the flooded areas was derived. The proposed methodology allows to reconstruct the flooded areas a-posteriori and to predict the flood prone areas under the assumption of total failure of the sub-surface drainage system, as shown by Lanza et al. (2023) for the investigated rainfall event and study area.

The same analysis was conducted by introducing storm water retention scenarios within the investigated area using permeable pavements and green areas mainly replacing pedestrian sidewalks and traffic islands. The proposed permeable pavement solutions (see Figure 2) were recently installed in another district of the town within a reconversion project (see Cauteruccio and Lanza 2022) and their hydrological performance were investigated in a testbed facility available at the hydraulic laboratory of the University of Genova. Different rainfall intensity and bed slope combinations were tested, and laboratory results were interpreted in terms of both surface and subsurface runoff coefficients.

Fig 2: Two permeable pavement solutions installed in the laboratory testbed, with a honeycomb grid and resin-gravel pavement (left-hand panel) and with meadow (right-hand panel).

The estimation of the flooded areas with the associated water volumes after the application of the derived retention coefficients allows to quantify the benefit introduced by the adoption of permeable solutions as a mitigation strategy to reduce the risk of flooding in a highly urbanized district. Results will be presented in terms of the expected and observed (reconstructed) flood hazard maps, as well as in the form of non-dimensional ratios between summary parameters in the present configuration and the proposed scenarios.

Acknowledgements

This study was carried out within the RETURN Extended Partnership and received funding from the European Union Next-GenerationEU (National Recovery and Resilience Plan – NRRP, Mission 4, Component 2, Investment 1.3 – D.D. 1243 2/8/2022, PE0000005)

References

Lanza, L.G., Cauteruccio, A., and Chinchella, E. (2023), Opportunistic rain sensors and flood modelling to assess the risk of failure of surface drainage in urban areas, EGU General Assembly 2023, Vienna, Austria, 24–28 Apr 2023, EGU23-9567, https://doi.org/10.5194/egusphere-egu23-9567.

Cauteruccio, A., and Lanza, L.G. (2022). Rainwater Harvesting for Urban Landscape Irrigation Using a Soil Water Depletion Algorithm Conditional on Daily Precipitation. Water, 14, 3468. https://doi.org/10.3390/w14213468

Unravelling the contrasting microphysical features of clouds and precipitation for Mumbai and Chennai - the urban coastal megacities of India

Kaustav Chakravarty[1*] and G.Pandithurai[1]

1 Indian Institute of Tropical Meteorology (IITM), Pune, India

*Corresponding author: kaustav@tropmet.res.in

Abstract

In the recent decades, many urban areas all around the world, has witnessed the increasing threat of heavy rainfall and flooding. With the increase of population, as the cities continues to expand, the impact of urbanization creates unique problems related to land use, transportation, agriculture, housing, pollution etc. which in turn have measurable impact on weather and climate processes over these regions. Looking into this scenario, the present study tried to highlight the morphology of the vertical structure of clouds and microphysical features of precipitation during the inter-seasonal phases of monsoon over Mumbai- a rapidly expanding urban coastal megacity of India, which is situated on western part of the Indian sub-continent. The city of Mumbai, also considered as the financial capital of India experiences heavy rainfall spells during the pre-monsoon and monsoon periods from the cloud systems originating from the eastern and western part of the region respectively. The study will also portray the cause and the impact of these severe rainfall events of Mumbai which creates severe flooding at the city quite frequently during the monsoon times. In addition to above, the study also compares the microphysical features of rainfall pattern of Mumbai to that with Chennai – the other urban megacity of India which is situated on the eastern coast of India peninsula. Chennai also gets flooded with the severe rainfall spells from the north-east monsoon during the month of December-February. The analysis has been done by using the dataset from Joss-Waldvogel Disdrometer placed at Mumbai and Chennai along with the S-band Doppler Weather Radar.

The preliminary results over Mumbai shows that the city receives rainfall primarily from easterly winds during the pre-monsoon time which then shifts to the south-westerly direction during the monsoon period. Looking into the diurnal variation of rainfall, three distinct rainfall peaks was noted for the pre-monsoon period. The corresponding vertical profile of radar reflectivity shows that these rainfall peaks are complimented with clouds of reflectivity more than 40 dBz and the presence of severe lightning flashes. But in case of monsoon month, no such distinct diurnal variations are visible over these regions. The dominance of urban convective environment in the pre-monsoon period and the impact of moisture supply from the marine sources over the city during the monsoon months are considered to be one of the contributing factors for the contrasting diurnal pattern of rainfall for these inter-seasonal phases of monsoon. Correspondingly, the giant cloud condensation nuclei (GCCN) from the bursting of sea salt aerosol in the Arabian Sea also plays a significant role in the enhancement of warm rain processes in the coastal urban region during the monsoon months. In addition to that while looking into the microphysical characteristic of rainfall, it has been found that the raindrops of diameter 2.5 mm and above dominate the pre-monsoon months with respect to the monsoon period. The convective urban environment characterized by higher localized CAPE aids vigorous thermals leading to smaller drops shifting aloft and thereby allowing bigger drops to precipitate locally during the pre-monsoon season over Mumbai.

Correspondingly, while comparing the cities of Mumbai and Chennai together, the impact of the south-west and north-east monsoon respectively in conjunction with the interplay of the continental and maritime effect on the microphysics of precipitation over these cities is strongly

visible in the analysis. The study reveals that the rainfall evolving from the continental clouds along with contrasting surface temperature produces distinct diurnal

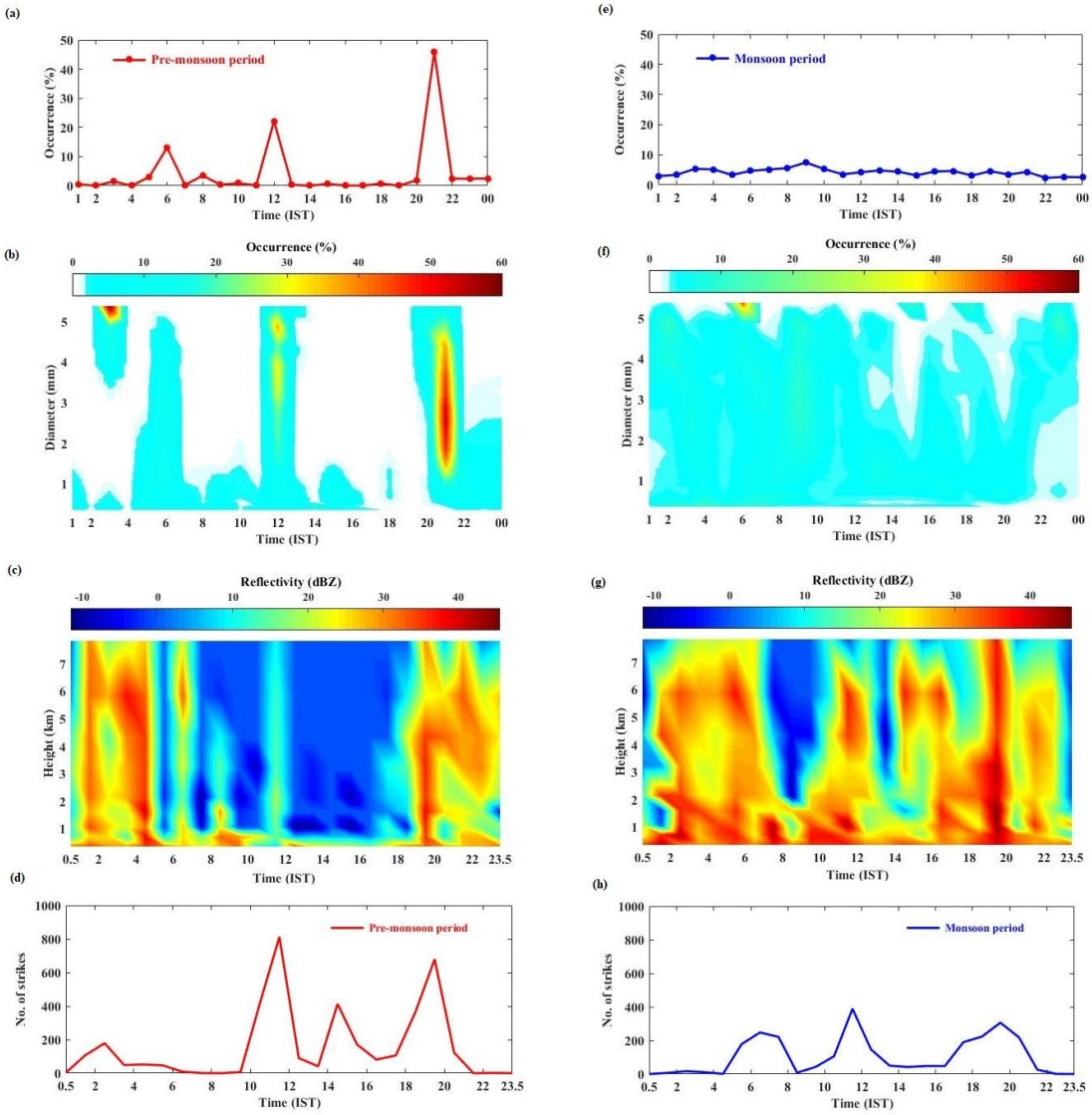

Fig 1: (a) Diurnal variation of rainfall (b) raindrop size distribution (c) vertical profile of radar reflectivity and (d) lightning occurrences during the pre-monsoon period over Mumbai. The same parameters for the monsoon months are obtained in Fig (e) – (h) respectively. (IST = Indian standard time)

variation for the summer (winter) rainfall over Chennai (Mumbai) while such variations are not visible for the maritime clouds. It has been observed that the drops of larger diameter along with higher radar reflectivity dominated the summer rainfall of Chennai with respect to Mumbai. While for the winter rainfall, such distinct variations are visible only for higher rainfall regimes from 16 mm/h and above where the domination of larger drops is visible for the Mumbai rainfall. Thus the difference in surface temperature which in turn escalates the convective environment in the atmosphere can be termed as one of the important factors responsible for this inter-seasonal variability of precipitation microphysics.

Thus on the whole it can be said that this high-spatiotemporal-resolution dataset of two heavily populated cities of India has provided a new, comprehensive insight regarding the microphysical characteristics of precipitation over the two urban-coastal stations of India which acts as a reference point for the precipitation pattern of south-west and north-east monsoon rainfall over the Indian sub-continent.

Assessing the wind-induced bias for the OTT Parsivel^2 optical gauge using CFD and particle tracking.

E. Chinchella*[1,2], A. Cauteruccio[1,2], L.G. Lanza[1,2]

1 University of Genova, Dep. of Civil, Chemical and Environmental Engineering (DICCA), Italy
2 WMO Measurement Lead Centre "B. Castelli" on Precipitation Intensity, Italy

*Corresponding author: enrico.chinchella@edu.unige.it

Abstract

Amongst precipitation measurement instruments, the so called Non-Catching type Gauges (NCGs) (see Lanza et al., 2021 for a review) are quickly gaining market share, notwithstanding their higher cost and complexity. These instruments, also called in some case disdrometers, provide information about precipitation microphysical properties and being contactless with no funnel and no moving parts, require less maintenance than traditional gauges. They are often used as ground reference for validating radar and satellite measurements (see e.g., Barros et al. 2014). NCG measurements are however affected by wind, which impacts on the gauge body and produces strong velocity gradients that may divert incoming hydrometeors away from the gauge sensing area. This is a well-known bias of traditional catching gauges and is recently being investigated for more complex NCGs, that often present non radially symmetric shapes.

In this work, the wind-induced bias on the OTT Parsivel^2 measurements is evaluated by means of Computational Fluid Dynamics (CFD) simulation with Lagrangian Particle Tracking (LPT) using the OpenFOAM software. CFD results provide the velocity field – generated by wind – close to the gauge body. Simulations are run by solving the Unsteady Reynolds-Averaged Navier Stokes (URANS) equations, using a local time-stepping approach and a k-ω SST turbulence model. Various combinations of the wind speed and direction are simulated. Numerical results show a significant disturbance – close to the gauge sensing area – for a wind direction parallel to the gauge laser beam (Figure 1a). Minimal disturbance is instead observed when the wind direction is transversal to the laser beam. Strong turbulence generation – visualized using the Q criterion – also occurs in the wake of the instrument body (Figure 1b).

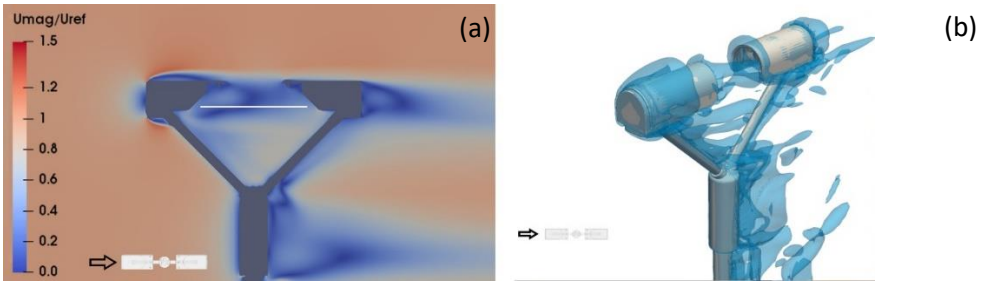

Fig 1: Magnitude velocity field around the Parsivel^2 for undisturbed wind speed U_{ref} = 5 m/s parallel to the laser beam (a). Turbulent structures close to the gauge body (b).

Hydrometeors trajectories are then computed using the simulated velocity field as input to the LPT model. Drops of diameters between 0.25 mm and 8 mm are released inside the computational domain along regular grids. Simulations are run until all trajectories reach the gauge, exit the domain, or fall significantly below the sensing area. From the simulated trajectories, the catch ratio (CR) of each monodisperse rainfall component is computed for the investigated combinations of wind speed and direction. The CR is the ratio between the number of trajectories that reaches the gauge sensing

area and the number of drops that would have reached the same area in undisturbed conditions (as if the instrument was transparent to wind and precipitation).

CRs are presented as a function of the particle Reynolds number (see Figure 2a). For a wind direction parallel to the laser beam, some limited overcatch of small drops occurs at low wind speed (1 and 2.5 m/s), while severe underestimation occurs at high wind speed. When the wind direction is transversal to the laser beam, limited bias is present with some overcatch in the case of high wind speed. CRs are fitted with an appropriate function allowing to adjust measurements once the wind speed and direction is known at the gauge installation site.

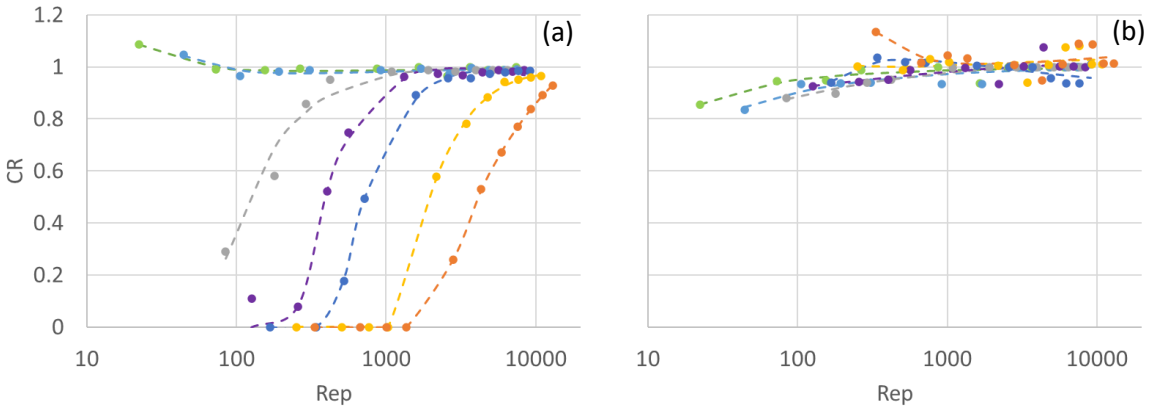

Fig 2: Catch ratios as a function of the particle Reynolds number for a wind direction parallel (a) and transversal (b) to the laser beam.

This disparity in the number of drops of different diameter sensed by the gauge also introduces a bias in the Drop Size Distribution (DSD) when measured in windy conditions. For some combinations of wind speed and direction, small drops are not sensed altogether, significantly affecting the shape of the DSD. The drop fall velocity is also affected, and especially the small size drops are slowed down by the wind-induced disturbance.

By choosing a DSD the bias on integral precipitation properties can also be evaluated. The Collection Efficiency (CE) is obtained by integrating the CRs over the whole diameters range. The CE is the ratio between the precipitation volume sensed by the gauge and the actual precipitation volume. Non negligeable overestimation of the rainfall volume is observed at a wind direction of 45° with respect to the laser beam, except for very low wind speed where the bias is limited. Another integral property often sought from NCGs measurements is radar reflectivity. Performance is evaluated by considering the Radar Retrieval Efficiency (RRE), defined as the ratio between the radar reflectivity computed from the DSD sensed by the gauge in windy conditions and the theoretical radar reflectivity. Very limited bias occurs for wind parallel to the laser beam in case of very high wind speed, while the bias is negligeable for other combinations of wind speed and direction. This is because radar reflectivity is mostly associated with medium size drops, which are weakly affected by wind.

In conclusion, wind introduces significant bias in the Parsivel^2 measurements of microphysical and integral properties of liquid precipitation. Adjustments are possible using the results of this work, based on ancillary measurements of wind speed and direction.

References

Lanza, L. G., Merlone, A., Cauteruccio, A., Chinchella, E., Stagnaro, M., Dobre, M., ... & Parrondo, M. (2021). Calibration of non-catching precipitation measurement instruments: A review. Meteorological Applications, 28(3), e2002. https://doi.org/10.1002/met.2002

Barros, A. P., Petersen, W., Schwaller, M., Cifelli, R., Mahoney, K., Peters-Liddard, C., Shepherd, M., Nesbitt, S., Wolff, D., Heymsfield, G., Starr, D. (2014). NASA GPM-Ground Validation: Integrated Precipitation and Hydrology Experiment 2014 Science Plan.

Towards conclusive climate projections for precipitation

P.H. Dias Kovalczuk[1,2], D. Schertzer*[1], I. Tchiguirinskaia[1]

1 Hydrology Meteorology and Complexity (HM&Co), Ecole des Ponts ParisTech, Champs-sur-Marne, France
2 Instituto Militar de Engenharia, Rio de Janeiro, Brasil

*Corresponding author: Daniel.Schertzer@enpc.fr

Abstract

How will rainfall evolve in the context of climate change? Policy-makers, especially urban planners and managers, are eager to know the answer. Unfortunately, the IPCC reports acknowledge that they are still faced with huge uncertainties in the precipitation projections: the projected change is very often less than the natural internal variability.

Royer et al (2008) have shown that this uncertainty is caused by the contradictory trends in mean intermittency C1 and the multifractality index α, that are fundamental parameters of Universal Multifractals (Schertzer and Lovejoy, 1987). Direct analyses of precipitation rates are therefore inconclusive. On the contrary, they pointed out that a refined analysis using the maximum probable singularity γ_s (Hubert et al., 1993; Douglas and Barros, 2003) can disentangle the two behaviours and lead to conclusive assessments.

By using Euro-Cordex data, we are largely generalising the results of Royer et al (2008), which were limited to a few pixels over France. We also clarify contradictory results obtained by Brochet (2020).

References

Brochet, C., Discrete cascade disaggregation of climate models outputs. Report, Ecole des Ponts ParisTech, 28 p., 2020.

Douglas, E.M. and A. P. Barros. Probable maximum precipitation estimation using multifractals: Application in the eastern United States. Journal of Hydrometeorology, 4(6):1012–1024, 2003.

Hubert, P., Y. Tessier, P. Ladoy, S. Lovejoy, D. Schertzer, J. P. Carbonnel, S. Violette, I. Desurosne, and F. Schmitt. Multifractals and extreme rainfall events. Geophys. Res. Lett., 20:931–934, 1993.

Royer, J.F., A. Biaou, F. Chauvin, D. Schertzer, and S. Lovejoy. Multifractal analysis of the evolution of simulated precipitation over France in a climate scenario. C.R Geoscience, 340:431–440, 2008.

Schertzer, D. and S. Lovejoy. Physical modelling and analysis of rain and clouds by anisotropic scaling and multiplicative processes. J. Geophys. Res., 92(D8):9693–9714, 1987.

Future rainfall extreme values: Temperature-dependent disaggregation of climate model data

N. Ebers[1], K. Schröter[2], H. Müller-Thomy*,**[2]

[1]Coordination Unit Climate and Soil, Thuenen Institute, Germany
[2]Leichtweiß Institute for Hydraulic Engineering and Water Resources, Department of Hydrology and Water Resources Management, Technische Universität Braunschweig, Germany

*Corresponding author: h.mueller-thomy@tu-braunschweig.de
**previously published under the name H. Müller

Abstract

For urban hydrology time series with high temporal resolution are crucial. Since most climate scenarios offer daily resolution only, statistical downscaling in time seems a promising and computational effective solution. The micro-canonical cascade model (MRC, Müller-Thomy, 2020) is chosen as downscaling method since it conserves the daily rainfall amounts exactly, so the resulting 5 min time series is coherent with the daily time series used as starting point. A second advantage of the MRC are the parameters, which are solely probabilities. In comparison to other statistical downscaling methods no assumptions about future parameter changes have to be made. However, since rainfall extreme values are often linked to temperature (especially convective events, which are crucial for urban hydrology), a temperature-dependent MRC is introduced in this study. Temperature-dependence is tested for minimum temperature, mean temperature and maximum temperature, which all allow a physical interpretation of rainfall extreme values and provide deeper insights into their future changes. Since the introduction of the temperature-dependency increases the number of MRC parameters, several modifications for MRC parameter reduction are tested beforehand.

For this study 45 locations across Germany are selected. To ensure spatial coherence with the climate model data (~Δl=5 km*5 km), the YW dataset (radar-gauge-merged data) from the German Weather Service (DWD) with originally Δl=1km*1 km and Δt=5 min was aggregated in space and used for the estimation of the MRC parameters. The DWD core ensemble with six combinations of global and regional climate models is applied for the climate change analysis, for both, RCP4.5 and RCP8.5 scenario.

For the MRC parameter reduction two potentials are analyzed: i) reduction of position-dependent probabilities, and ii) scale-independency of MRC parameters. For i), the position classes, which are based on the wetness state of the time step to disaggregate and its adjacent time steps (starting, enclosed, ending or isolated), and used for the parameter estimation, are considered. It was identified before that for certain probabilities of starting and ending position similarities of MRC parameters occur. These similarities are confirmed for the study area, and validated as simplification option. For ii), the scale-dependency of MRC parameters is analyzed for scale-invariant ranges and used for simplification. In the reference model an individual parameter set is applied for each disaggregation level: 8 h→4 h, 2 h→1 h, 1 h→30 min, 30 min→15 min and 15 min→7.5 min. For i), the simplification based on the MRC parameter similarity leads to no worsening of rainfall characteristics of the disaggregated time series in comparison to the reference model. For ii), scale invariance for 8 h→1 h and 1 h→15 min leads to a minor worsening, which is taken into account as trade-off for the number of reduce parameters (48 parameters instead of 144 in the reference model).

For the temperature-dependency class widths of 5 K are chosen to include a representative number of time steps in each class. No significant influence on continuous rainfall characteristics as wet spell

amount, average intensity, wet and dry spell duration can be identified. To analyze the impact on rainfall extreme values peak-over-threshold series and 99.9 %-quantile $q_{99.9}$ are studied. While for the peak-over-threshold no significant differences can be identified, an impact on the $q_{99.9}$ is visible (Fig. 1). While the reference model without temperature-dependency (S0-P0) leads to higher overestimations for Δt=5 min for ϑ<13 °C and underestimations for ϑ>18 °C, the temperature-dependency (S0-P0-TD) reduces the deviations over the whole range to a median overestimation of 1 mm/5 min (range of observations: 4 mm/5 min<$q_{99.9}$<6 mm/5 min).

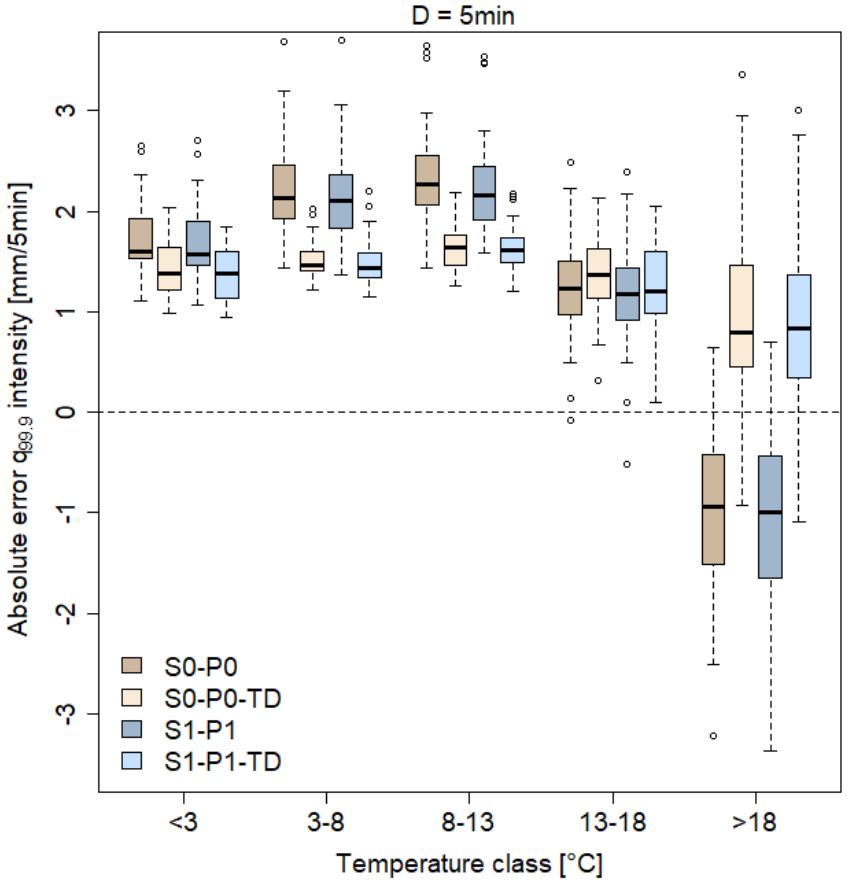

Fig 1: The impact of temperature-dependent (TD) MRC parameters on $q_{99.9}$ for reference model (S0-P0) and parameter-reduced model (S1-P1) for daily mean temperature.

Both, the reference model and the parameter-reduced cascade model, will be used for the disaggregation of the climate scenarios. The rainfall extreme values of the disaggregated time series will be analyzed regarding their relative changes from the control period C20 (1971-2000) to near-term and long-term future (NTF: 2021-2050 and LTF: 2071-2100, respectively). An additional focus will be on the comparison of the relative changes for different durations to prove if the relative changes of daily extreme values can be assumed to be representative for shorter durations D as e.g. D=5 min.

References

Müller-Thomy, H.: Temporal rainfall disaggregation: Possibilities to improve the autocorrelation, Hydrology and Earth System Sciences, 24, 169-188, 2020.

Open Data: the LAWA heavy rain portal based on more than 20 years of DWD radar data

Thomas Einfalt[1], Alrun Jasper-Tönnies[2], Benjamin Mewes[3], Marcel Alderlieste[4]

1 hydro & meteo GmbH, Lübeck, Germany
2 hydro & meteo GmbH, Lübeck, Germany
3 Okeanos GmbH, Bochum, Germany
4 HydroLogic B.V., Amersfoort, The Netherlands

*Corresponding author: einfalt@hydrometeo.de

Abstract

After two decades of radar-based rainfall observations, there have been two different approaches to get easy access to information on heavy rainfall events during this time. One algorithm for an event database was developed in North-Rhine Westphalia (NRW) by the authors and was launched in 2017 (Strehz et al., 2019), the other one was developed by the German Weather Service DWD (Lengfeld et al., 2021) and operational since 2018. Both approaches have now been combined for the benefit of all hydrological users in a web-based “Heavy Rain Documentation” application of the German LAWA (German Working Group on water issues of the Federal States and the Federal Government represented by the Federal Environment Ministry).

The RADOLAN RADKLIM dataset of the DWD is basis for the portal, which uses approximately 1000 stations for radar adjustment for the whole of Germany (Winterrath et al., 2018).

Event selection as shown in Figure 1 is using the object-oriented event definition by DWD. Events can be filtered for a time period, area, maximum number of events, so that the table and map on the web site shown above will change accordingly.

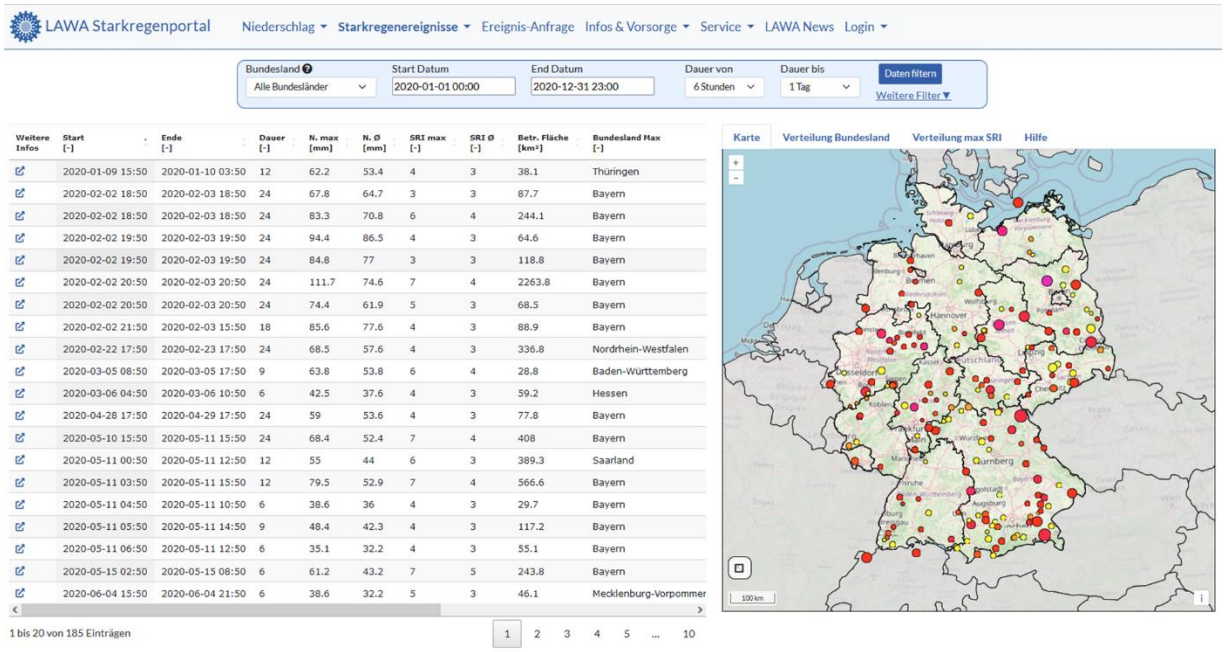

Weitere Infos	Start [-]	Ende [-]	Dauer [-]	N. max [mm]	N. Ø [mm]	SRI max [-]	SRI Ø [-]	Betr. Fläche [km²]	Bundesland Max [-]
	2020-01-09 15:50	2020-01-10 03:50	12	62.2	53.4	4	3	38.1	Thüringen
	2020-02-02 18:50	2020-02-03 18:50	24	67.8	64.7	3	3	87.7	Bayern
	2020-02-02 18:50	2020-02-03 18:50	24	83.3	70.8	6	4	244.1	Bayern
	2020-02-02 19:50	2020-02-03 19:50	24	94.4	86.5	4	3	64.6	Bayern
	2020-02-02 19:50	2020-02-03 19:50	24	84.8	77	3	3	118.8	Bayern
	2020-02-02 20:50	2020-02-03 20:50	24	111.7	74.6	7	4	2263.8	Bayern
	2020-02-02 20:50	2020-02-03 20:50	24	74.4	61.9	5	3	68.5	Bayern
	2020-02-02 21:50	2020-02-03 15:50	18	85.6	77.6	4	3	88.9	Bayern
	2020-02-22 17:50	2020-02-23 17:50	24	68.5	57.6	4	3	336.8	Nordrhein-Westfalen
	2020-03-05 08:50	2020-03-05 17:50	9	63.8	53.8	6	4	28.8	Baden-Württemberg
	2020-03-06 04:50	2020-03-06 10:50	6	42.5	37.6	4	3	59.2	Hessen
	2020-04-28 17:50	2020-04-29 17:50	24	59	53.6	4	3	77.8	Bayern
	2020-05-10 15:50	2020-05-11 15:50	24	68.4	52.4	7	4	408	Bayern
	2020-05-11 00:50	2020-05-11 12:50	12	55	44	6	3	389.3	Saarland
	2020-05-11 03:50	2020-05-11 15:50	12	79.5	52.9	7	4	566.6	Bayern
	2020-05-11 04:50	2020-05-11 10:50	6	38.6	36	4	3	29.7	Bayern
	2020-05-11 05:50	2020-05-11 14:50	9	48.4	42.3	4	3	117.2	Bayern
	2020-05-11 06:50	2020-05-11 12:50	6	35.1	32.2	4	3	55.1	Bayern
	2020-05-15 02:50	2020-05-15 08:50	6	61.2	43.2	7	5	243.8	Bayern
	2020-06-04 15:50	2020-06-04 21:50	6	38.6	32.2	5	3	46.1	Mecklenburg-Vorpommer

Fig. 1: View of the events (object-oriented view). The table on the left and the map display on the right are directly linked

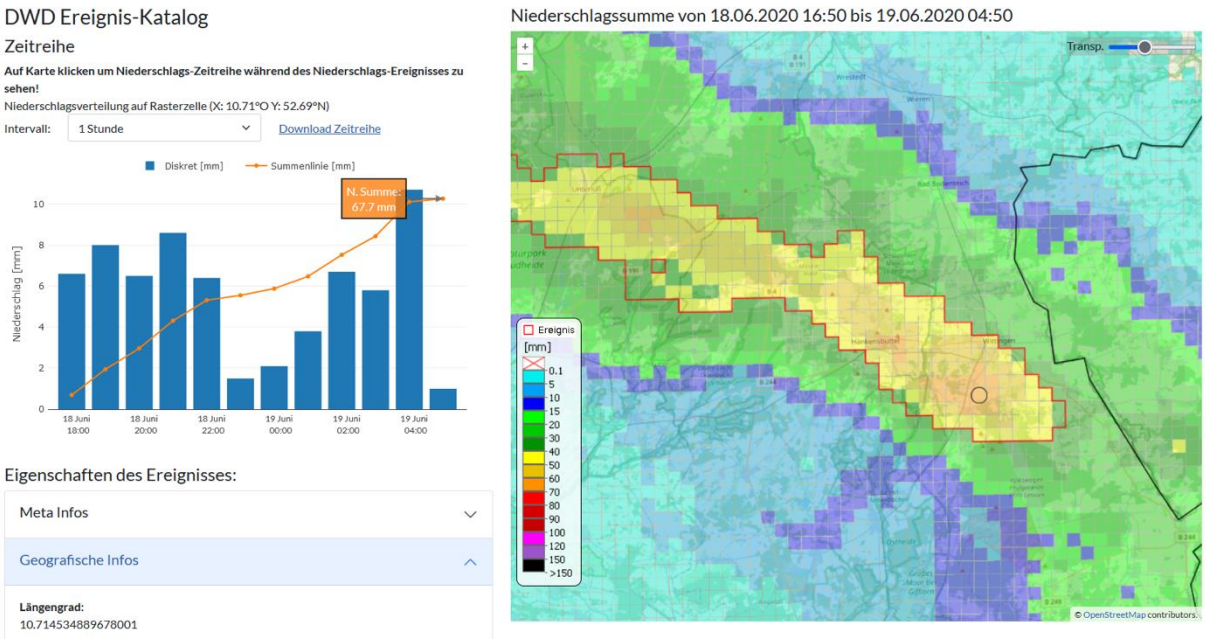

Fig. 2: View of a single event. The time series on the left and the map display on the right are directly linked

Each event is displayed as shown in Figure 2. Thus, the areal extent of the event and its spatial heterogeneity become obvious. For each pixel, the corresponding time series can be presented in different temporal resolutions. The presented data can be downloaded, timeseries can also be requested via an API. Both, the capability of showing the related time series and the possibility to download data are using the HydroNET data base.

The object-oriented events have been analysed for return period and heavy precipitation index so that their severity can be assessed. Other attributes are the topographic position index (TPI) as average value for the event area or the weather type. Such supplementary data provide the means for further analysis of each event and allow for a better comparison between individual events.

Additionally to the predefined events, individual requests for any user-defined point or any area are possible through the HydroNET data base. Such a request will produce the time series and the image for the selected area and duration time, similar to Figure 2. Such an online request does not calculate the event properties because this may require a more lengthy processing.

Acknowledgements
This work has been financed by the LAWA through the programme 'Wasser, Boden und Abfall'.

References

Lengfeld, K., Walawender, E., Winterrath, T., Becker, A. (2021). CatRaRE: A Catalogue of radar-based heavy rainfall events in Germany derived from 20 years of data. Meteorologische Zeitschrift Vol. 30 No. 6 (2021) , p. 469 - 487.

Strehz, A., Einfalt, T., Alderlieste, M. (2019) HydroNET-SCOUT – Ein Webportal zum Zugriff auf qualitätsgeprüfte Niederschlagsdaten. Tag der Hydrologie 28./29.3.2019, Karlsruhe; www.hydronet-scout.de

Winterrath, T.; Brendel, C., Hafer, M.; Junghänel, T.; Klameth, A.; Lengfeld, K.; Walawender, E.; Weigl, E.; Becker, A. (2018): RADKLIM Version 2017.002: Reprozessierte, mit Stationsdaten angeeichte Radarmessungen (RADOLAN), 5-Minuten-Niederschlagsraten (YW) DOI: 10.5676/DWD/RADKLIM_YW_V2017.002

Decomposing the effects of compound mechanisms on flood risk estimation for urban environments: A case study over Greater Boston

S. Emmanouil*[1,2], A. Langousis[3], E. Perry[4], L. Madaus[5], J.P. Hacker[5], and E.N. Anagnostou[1,2]

1 Department of Civil and Environmental Engineering, University of Connecticut, Storrs, CT, U.S.A.
2 Eversource Energy Center, University of Connecticut, Storrs, CT, U.S.A
3 Department of Civil Engineering, University of Patras, Patras, Greece
4 Jupiter Intelligence, New York, NY, U.S.A.
5 Jupiter Intelligence, Boulder, CO, U.S.A.

*Corresponding author: stergios.emmanouil@uconn.edu

Abstract

Several recent studies have stressed the need to account for the compound effects of various flood mechanisms (i.e., storm surge, riverine, and pluvial flooding) as a function of the hydrologic response of catchments. Researchers often use copula functions or conditional distribution analyses to estimate the joint exceedance probability of certain thresholds related to storm surge and spatially averaged rain rates. While accounting for the compound impact of flood-generating processes can improve risk estimation at locations where various sources intersect, in most cases, such an approach tends to lead to a misestimation of flood risk. Specifically, from a physical standpoint, the effect of each flood mechanism on the severity level of inundation is spatially variable, and the outcome is determined by the weighted combination of the causal events with weights that depend on the general characteristics of the respective region (i.e., river network, distance from the coast, rainfall climatology, etc.). In this context, the actual impact of certain flood mechanisms may be inconsequential, despite their severity (i.e., return period).

The primary goal of this study is to reveal the combinations of rainfall intensity and storm surge that may lead to different flood inundation levels over urban environments, by utilizing probabilistic and statistical techniques coupled with hydrodynamic simulations of historical and synthetic storm events. Using the Greater Boston (MA, United States) region as a case study, we decompose the factors that contribute to flood inundation levels through a stepwise refinement that focuses on the susceptibility of the respective study domain and, accordingly, neglects the effects of phenomena that would rarely cause flooding. At a conceptual level, this is equivalent to the deconvolution of the total risk from all possible combinations of storm surge and rainfall thresholds to their corresponding marginal and joint probability counterparts. Given numerous simulated events that encapsulate a broad spectrum of potential outcomes, the underlying methodology allows us to rate the importance of different flood mechanisms, estimate their recurrence rate, and, ultimately, assess their impacts. In this regard, the suggested framework could enhance the accuracy of flood risk assessment for critical infrastructure design and, therefore, support future planning for flood resilience.

Applying operational attenuation data from the telecommunication network in the city of Olomouc for predicting inflows to WWTP

M. Fencl*[1], V. Bares[1]

1 Department of Hydraulics and Hydrology, Czech Technical University in Prague, Czechia

*Corresponding author: martin.fencl@cvut.cz

Abstract

The composition and quantity of wastewater approaching the wastewater treatment plant (WWTP) during rainfall is fundamentally influenced by rainfall-runoff processes in the sewerage network catchment. Detailed distributed mechanistic models are now commonly used for modelling rainfall runoff in engineering studies, e.g. to assess the impact of connecting new development areas on the sewerage network capacity. For operational use, where minimum latency between measurement and prediction is a crucial parameter, computationally very efficient conceptual models are often more appropriate. However, the use of such models is still rather rare. One of the reasons is the lack of traditional precipitation measurements available in real time. In this respect, precipitation data obtained from a network of commercial microwave links (CMLs) can help since they are available in urbanized catchments worldwide, even in the developing countries.

CMLs are radio links widely used in mobile operator networks. They operate in the microwave band, where precipitation activity is a significant source of signal attenuation (Olsen et al., 1978). In cooperation with T-Mobile, we have previously developed an application that uses SNMP protocol to collect real-time data (dt = in 1 min) on transmitted and received signal levels of about 2500 CMLs from a substantial part of the Czech Republic (Blettner et al., 2023). Within the pilot project in the Olomouc city area (approx.. 100 km^2, 100 000 inhabitants), attenuation data from 12 selected CMLs are provided in an operational mode to the sewerage and WWTP operators using a web application enabling their conversion to rain rates, visualization, and export. The latency does not not exceed 2 min from the measurement. Previous studies reported that CMLs can very well capture rainfall temporal dynamics but their rain rate estimates are often significantly biased due to inaccurate separation of wet antenna attenuation (Pastorek et al., 2022). Reduction of this bias requires calibration against reference rainfall data and limits potential of CMLs for ungauged regions. In this contribution, we address the question if and how operational attenuation data from CMLs can be used in a conceptual rainfall-runoff model without conversion to rain rates and whether their systematic biases can be reduced by optimizing runoff model parameters.

The conceptual model is constructed and tested for the location of the city of Olomouc. The model is calibrated and validated with attenuation data from the 12 CMLs and flow data measured at the outlet of the sewer before the influent to the WWTP. Flow is measured with an ultrasonic flow meter using the velocity-area method and all the data span a period of seven months. For the model calibration we use data from April to June and the for the validation data from July to the end of October 2022. The model consists of two cascades of linear reservoirs simulating slow runoff and four cascades simulating fast runoff. The daily flow pattern is assumed to be periodic, determined by flow data from a dry season. The “rainfall” input to the model is the average specific attenuation of all CMLs. This is obtained by subtracting the background attenuation value from the total CML attenuation, dividing this value by the link length, and averaging the specific attenuation obtained from all the CMLs at each time step. Correction of wet antenna attenuation is not introduced. The data are aggregated to a regular 5 min time step. The runoff model is calibrated by optimizing the following parameters: virtual catchment area (ha km dB^{-1}), ratio of areas generating fast and slow runoff component, retention time for both runoff components, and travel time of fast runoff through the city sewer system.

Initial testing of the model has produced good results. Figure 1 shows two hydrographs from a summer period. The model is able to reproduce very well onset of a runoff event and also slow runoff often lasting several days after rain events. The reason for plateaus observed during peak discharges are not (yet) known and the model is not designed to reproduce them. The overall evaluation (Tab. 1) shows that modelled runoff is correlated well with the measured discharge and practically unbiased in long term. When considering wet-weather periods only (flow over 750 l/s with safety window of three hours before and one day after increased flows) the correlation is slightly stronger, Nash-Sutcliffe efficiency considerably higher, and total runoff volume becomes systematically overestimated (by 10%).

Overall, the study demonstrates that CML attenuation can be directly used to for operational predictions of rainfall-runoff in a large urban catchment achieving good agreement with the measured runoff. Simple lumped model calibrated against observed discharge can efficiently compensate for large systematic errors often affecting CML rainfall observations. CMLs can be thus considered as highly reliable alternative of standard rainfall observations worldwide available in urban catchments. Further work now focuses on better understanding of artefacts (plateaus) in the reference flow measurements and transformation of the model to the space-state form enabling real-time updating of simulated flows with flow observations.

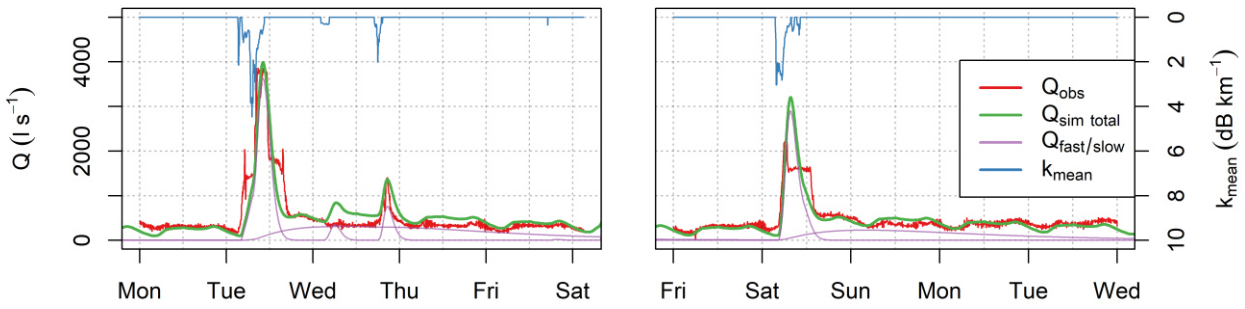

Fig 1: Two hydrographs with observed and simulated discharge and mean specific attenuation on 25 – 30th July (right) and 5-9th August 2022 (left).

Tab 1: Quantitative evaluation of the model performance.

Metric	Whole validation period	Wet-weather periods only
Pearson correlation coeff. (-)	0.75	0.78
Relative error in volume (-)	0.00	0.10
Nash-Sutcliffe Efficiency (-)	0.45	0.56

References

Blettner, N., Fencl, M., Bareš, V., Kunstmann, H., Chwala, C., 2023. Transboundary rainfall estimation from commercial microwave links (preprint). Preprints. https://doi.org/10.22541/essoar.167591117.73401471/v1

Olsen, R., Rogers, D., Hodge, D., 1978. The aRbrelation in the calculation of rain attenuation. IEEE Transactions on Antennas and Propagation 26, 318–329. https://doi.org/10.1109/TAP.1978.1141845

Pastorek, J., Fencl, M., Rieckermann, J., Bareš, V., 2022. Precipitation Estimates From Commercial Microwave Links: Practical Approaches to Wet-Antenna Correction. IEEE Transactions on Geoscience and Remote Sensing 60, 1–9. https://doi.org/10.1109/TGRS.2021.3110004

Rain gauge data quality revisited: old-fashioned or new trend?

C. Fennig*[1], T. Einfalt[1], S. Luers[1]

[1] hydro & meteo GmbH, Luebeck, Germany

* Corresponding author: c.fennig@hydrometeo.de

Abstract

Data quality plays an increasingly important role in the huge amount of data which is being collected nowadays: from traditional meteorological weather stations via weather radar (WMO JET OWR Best Practice Guide for Weather Radar, Michelson et al., 2023) to opportunistic sensing data (Seidel et al., 2023) or IoT sensors (www.opensense.org) - it becomes more and more important which data you can trust. Therefore, efforts are undertaken to prove the quality of data for their specific fields of interest.

Experience from decades of rain gauge data and from two decades of radar data have shown: The quality of rain gauge data is crucial for online applications as well as for climate trend analyses. A manual procedure for data quality control is well established but not feasible for online applications or huge data amounts. In this paper, we describe steps towards the direction of automated, radar assisted quality control of rain gauge data and ways to automatically document the data quality characteristics.

The past experience has shown that spatial-temporal behaviour of rainfall (especially of convective cells) leads to problems in automatic checks. Therefore, already existing methods of rain gauge quality control have been combined with new variability methods with the objective to only use rain gauge data for adjustment procedures, which are spatially comparable to radar data.

Automatic spatial tests with surrounding gauge stations have been extended with radar data. In addition to the values of four surrounding gauge stations in different directions, the confidence interval with median weighted mean values and standard deviations of radar data in the environment plays an important role. Now, extreme value detection is a combination of rain gauge comparisons and radar data comparisons with set thresholds for different time intervals (5, 60 and 1440 minutes). Radar data should be at least 20% of rain gauge value at the same location. Because manual checks base often on form observations of cumulative precipitation curves, consistency checks help to transfer this to automatic checks. Therefore, correlation coefficients at one location are calculated for the cumulative rain gauge and radar curve. If the result is below a defined limit, it will be documented. This method has the advantage to be independent of rain amounts and focused on form details of cumulative precipitation curves.
To evaluate the automatic rain gauge checks the results are analysed in two steps: 1. compare number of cases in error categories (s. Fig.1) and 2. control manually time series at found occurrences. The evaluation basis were 42 stations in the Berlin region (Germany) for a period of seven months. The correlation tests based on a time interval of one day.
Our first results of the extended automatic checks have shown an obvious improvement due to the inclusion of radar data. Most (ca. 80%) of the manual found errors could be detected with smart method combinations and set thresholds. This is a good base to improve rain gauge data for online use and adjustment procedures with radar data. New wrong cases in the consistency check resulted from time shifts around the change of day for example. This effect can be seen more often if the time interval is reduced.

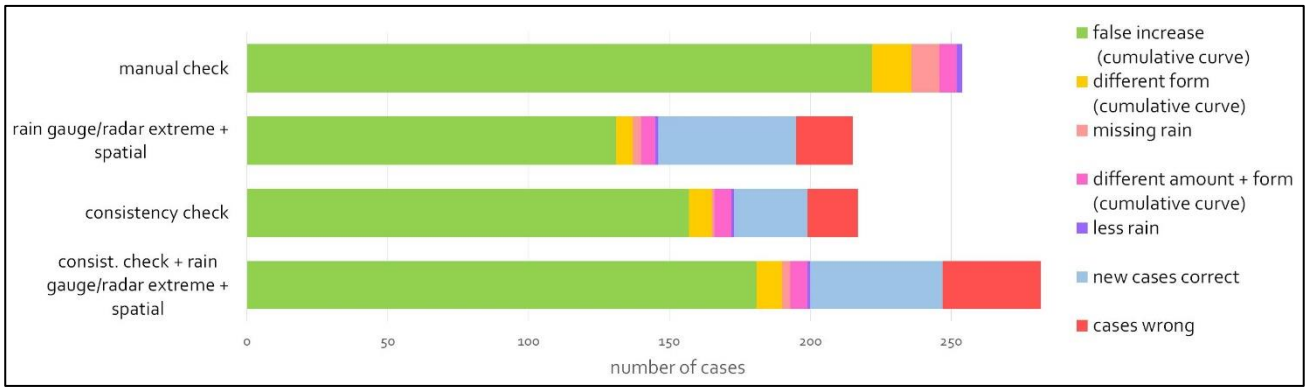

Fig. 1: Comparison of automatic and manual check results

Outlook

For online applications, such as warning systems or real-time flooding modelling, already the time of arrival of station data for further use is important for understanding successive results. Therefore, additionally to the online documentation of the quality control results for each station, a scheme like shown in Fig. 2 on the age of retrieved data is a useful and important information for documentation purposes.

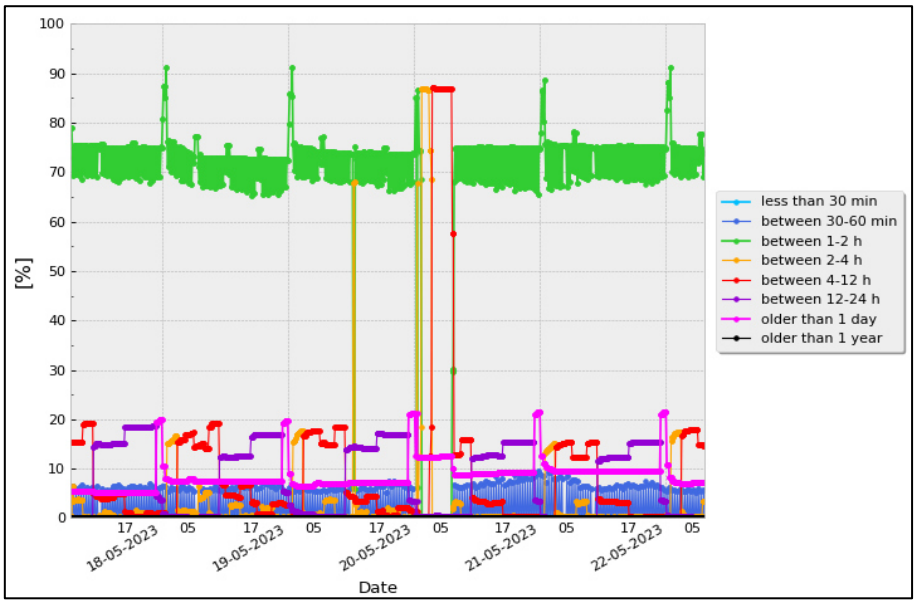

Fig. 2: Documentation of the age of retrieved station data used for radar adjustment

References

Michelson, D. et al. (2023), WMO JET OWR Best Practice Guide for Weather Radar, URL: https://community.wmo.int/en/activity-areas/weather-radar-observations/best-practices-guidance (accessed 24th May 2023)

Seidel, J. et al. (2023) Using personal weather station data for improving precipitation estimates and gauge adjustment of radar data. Abstract submitted to *UrbanRain23.*

Seventeen years of real-time hourly precipitation estimation: an improved agreement since 2016 among various conventional and remotely sensed MeteoSwiss operational products

M. Gabella*[1], I. Sideris[1], M. Boscacci[1], U. Germann[1]

1 MeteoSwiss, Locarno-Monti, Switzerland

*Corresponding author: marco.gabella@meteoswiss.ch

Abstract

Radar quantitative precipitation estimation (QPE) in complex orography is crucial for several applications: monitoring and nowcasting of precipitation, natural hazards by extreme precipitation, river flow and lake level forecasting, hydro-geological risk management, civil protection, urban and water management. In Switzerland, especially after the dual-polarization renewal and enlargement of the radar network, QPE needs and expectations are high, as are the problems. Strong back-scattering by the mountains causes severe ground clutter. Beam shielding poses great challenges: think of low-level growth in a moist troposphere or evaporation in a dry one: in such cases, what the radar detects aloft does not correspond to what happens in the shielded valley. Another problematic fact is that radar echoes are in many cases the results of backscattering by complex-shape, solid and/or mixed-phase hydrometeors and not by simple-shape, liquid rain drops.
Combining rain gauge point measurements and radar estimates can be a remedy: in addition to the radar-only product (RZC), a method has been developed that is based on kriging with external drift. It operationally produces effective real-time merging of data coming from the two complementary technological networks. This QPE product called CombiPrecip (CPC) has been operationally running since 2012; a reprocessing of the period 2005-2010 (old radar network) was also implemented.
The first part of this two-page abstract shows the agreement between the precipitation product under test and the gage reference in terms of dispersion around the mean error. There are large differences in the sampling modes of the two networks; we have tried to reduce such effects by averaging precipitation rates over one hour. All hourly amounts are grouped together according in a pool according to winter (December to February) and summer (June to August). The agreement is characterized in terms of dispersion of the weighted multiplicative error around the mean (scatter in dB, see e.g., UrbanRain18). **Table 1** shows the results for summer: it simply (extends in time and) confirms what was presented at the UrbanRain conference in Pontresina in 2018. **Table 2 shows results for winter**, which is a season with prevailing solid/mixed-phase precipitation. The first column refers to the old radar network (6-year); the other two columns to the state-of-the art network with an increasing number of both radars and gages (see Table 3).

Table 1: Performance of MeteoSwiss **summer** hourly precipitation values in terms of scatter in dB.

Product	2005-2010 3 radars		2013-2015 3-4 new radars	**2016-2022** 5 new radars
Radar (RZC)	**2.9**±0.08 dB		**2.8**±0.15 dB	**2.65**±0.16 dB
CPC leave-1-out	**2.4**±0.14 dB		**2.1**±0.08 dB	**1.83**±0.18 dB
CPC version3.5	0.3±0.07 dB		0.4±0.08 dB	0.48±0.12 dB

Table 2: Same as Table 1, but for **winter** hourly precipitation amounts.

Product	2005-2010 3 radars		2013-2015 3-4 new radars	**2016-2023** 5 new radars
Radar (RZC)	**2.8**±0.14 dB		**2.7**±0.07 dB	**2.59**±0.12 dB
CPC leave-1-out	**2.3**±0.20 dB		**1.9**±0.05 dB	**1.79**±0.11 dB
CPC version3.5	0.3±0.05 dB		0.4±0.04 dB	0.40±0.04 dB

The Swiss Confederation investments and efforts to improve and enlarge both networks are paying off. The increased performance from ~2.9 dB to ~2.6 dB of the radar-only (RZC) hourly precipitation estimates is linked to the improved visibility and better coverage thanks to the installation of the 4th and 5th radar. The significant increase in the number of gages (more robust variogram in the kriging algorithm) together with a better radar networks is reflected in an even larger improvement of the CPC using the leave-1-out (cross-validation) approach: the scatter decreases from ~2.4 dB to ~1.8 dB. Since such figures apply to both seasons, we conclude that better radar performance in summer (many more hydrometeors in the liquid phase) are counter-balanced by worse gage performance. Main causes are the well-known lack of representativeness in convective situations as well as larger uncertainty at higher precipitation rate of gages (see Table 3, which shows the average hourly precipitation rate according to rain gages, with the lowest possible threshold of 0.1 mm/h!)

Table 3: Summer and winter average (±inter-annual standard deviation) hourly precipitation rate in Switzerland since 2005 based on a telemetered rain-gage network with increasing number of sites.

Periods # of Gages	2005-2010 ~70		2013-2015 ~190	**2016-2022** ~270	**2016-2023** ~270
Summer	**1.40**±0.10 mm/h		**1.33**±0.05 mm/h	**1.58**±0.11 mm/h	---
Winter	**0.77**±0.09 mm/h		**0.72**±0.07 mm/h	**0.81**±0.10 mm/h	**0.79**±0.10 mm/h

The scatter is a meaningful score, especially for hydrological applications. However, as any score, it just illustrates part of the (dis-)agreement between the remote sensing estimates aloft and the in situ measurements at the ground. It can be complemented by the Pearson correlation coefficient or its squared value, which is the explained variance. In addition to the scatter, Table 4 presents the percentage of explained variance for the best/worst year of two radar eras: the old 3-radar network vs the state-of-the-art one that is based on 5 radars.

Table 4: Best and worst **explained variance** (in percentage) and scatter (in dB) for the **summer** season during two periods of the old (2005-10) and new (2016-23) radar network (5 systems).

	2006 worst-year during 2005-2010	2009 best-year during 2005-2010		2018 worst-year during 2016-2022	2021 best-year during 2016-2022
Radar-only (RZC)	**29**%; 2.99 dB	**49**%; 2.78 dB		**47**%; 2.94 dB	**61**%; 2.41 dB
CPC leave-1-out	**33**%; 2.62 dB	**51**%; 2.42dB		**60**%; 2.17 dB	**75**%; 1.65 dB
# of hourly data pairs	**14762**; 8182	**13584**; 8036		**34066**; 19822	**75187**; 42958

In terms of Pearson correlation, the improvement since 2016 is even more evident. Given the very different number of hourly data pairs (see last row of Table 4), the explained variance (49%) of the best year for the old radar network (2009) is certainly worse than the one (47%) of the worst year for the new network (2018). For the operational radar product, this is not the case for the scatter (2.78 dB in 2009 vs 2.94 dB in 2018). However, it is the case for the CPC product using the cross-validation approach: the best summer results with the old network (2.42) dB is worse than the worst one with the new network (2.17 dB). Similar characteristics are obtained in winter, as it will be shown at the Workshop (next December, 2023) as well as in the 5-page preprint. For what concerns CPC cross-validation, the scatter of summer 2021 (winter 2023) is exceptionally good: 1.65 (1.52) dB.
It is rewarding to see that by increasing the number of gages and radar coverage (from 3 to 5 systems), by improving radar technology and algorithms, QPE products become more reliable. It is also interesting that better performances in the radar-only QPE product causes, in turn, an even larger imporvement of CombiPrecip, which is considered to be the more accurate hourly QPE product in Switzerland. MeteoSwiss has been investing significant efforts in the development of a novel QPE based on dual-polarization information: a random forest regression is trained with data from a large database containing 6 years (from 2016 to 2021) of combined in situ measurements (e.g., precipitation, wind, temperature, relative humidity) and polarimetric radar observations. Since 2023, this innovative QPE product is now experimentally running in real-time using operational data and the results of this approach is also presented (see abstract by Gugerli et al.) at UrbanRain23.

Characterizing and simulating with blunt extension of discrete cascades rainfall anisotropy in a Universal Multifractals framework

A. Gires*[1], I. Tchiguirinskaia[1], D. Schertzer[1]

1 Hydrologie Météorologie et Complexité (HM&Co), École des Ponts, Champs-sur-Marne, France

*Corresponding author: auguste.gires@enpc.fr

Abstract

Rainfall fields exhibit extreme variability over wide range of space-time scales which make them complex to characterize, model and even measure. Another basic feature, which is also observed for most geophysical fields, is a strong anisotropy. Fortunately, scaling anisotropy has been developed for a few decades to generalise scaling in an anisotropic framework, e.g., in the simplest case iso-surfaces become self-affines ellipsoids instead of self-similar spheres. This is particularly straightforward for continuous in scale cascades (Schertzer and Lovejoy, 1987). For them, as well as for discrete in scale cascades, Universal Multifractals (UM) have been widely used to analyse and simulate such geophysical fields with the help of a very limited number of physically meaningful parameters. In order to remain in the simple framework of discrete cascades while partly overcoming their well know and often neglected no translation invariance issue, blunt cascade were introduced (Gires et al. 2020, 2023). It basically consists in geometrically interpolating over moving windows the multiplicative increments at each cascade steps. The size of the moving window in tailored according to the cascade step to remain in a scale invariant framework. Here we suggest to incorporate observed anisotropic features in 2D and 3D (space and time) blunt discrete cascade simulations.

The first step consists in characterizing anisotropy in UM framework. This is achieved by performing a 1D analysis along various directions, considering each column as a different “sample” of the process. Such methodology is implemented on high resolution space-time rainfall data collected with help of a dual polarisation X-band radar operated by HM&Co-ENPC. Changes in UM parameters with the angle of the chosen direction are observed. These variations are more or less pronounced depending on the intrinsic anisotropy of the studied time steps.

In a second step, anisotropy features are incorporated into blunt extension of discrete UM cascades simulations. This is tentatively done by using moving window shaped as ellipses instead of squares. It was found that tuning the eccentricity and orientation of the ellipses enables to introduce various levels of anisotropy within the stochastically simulated fields and to retrieve with a good level of approximation the multifractal behaviour previously observed on actual rainfall data. Applications to downscaling of rainfall field will finally be discussed.

Authors acknowledge the RW-Turb project (supported by the French National Research Agency - ANR-19-CE05-0022), for partial financial support.

References

Gires, A., Tchiguirinskaia, I. & Schertzer, D. (2020) Blunt extension of discrete universal multifractal cascades: development and application to downscaling, Hydrological Sciences Journal, 65:7, 1204-1220, DOI: 10.1080/02626667.2020.1736297

Gires, A., Tchiguirinskaia, I. & Schertzer, D. (2023) Generating a missing half of multifractal fields with a blunt extension of discrete cascades, Hydrological Sciences Journal, 68:2, 261-275, DOI: 10.1080/02626667.2022.2154160

Schertzer, D. and Lovejoy, S., 1987. Physical modelling and analysis of rain and clouds by anisotropic scaling and multiplicative processes. Journal of Geophysical Research, 92 (D8), 9693–9714. doi:10.1029/ JD092iD08p09693.

Operational implementation of a random forest approach to perform quantitative precipitation estimation with measurements from the Swiss polarimetric radar network

Rebecca Gugerli*[1,2], Daniel Wolfensberger[2], Marco Gabella[2], Marco Boscacci[2], Urs Germann[2] and Alexis Berne[1]

1 Environmental Remote Sensing Laboratory, École Polytechnique Fédérale de Lausanne (EPFL), Switzerland
2 Radar, Satellite and Nowcasting Division, Federal Office of Meteorology and Climatology MeteoSwiss, Switzerland

*Corresponding author: rebecca.gugerli@meteoswiss.ch

Abstract

Quantitative precipitation estimation (QPE) is crucial for hydrological, climatological and meteorological studies. Weather radars provide remote observations of hydrometeors with a wide-range coverage. However, an accurate retrieval of precipitation intensity from weather radar observations remains a challenge.

In this study, we present an approach using random forest regression to compile QPE maps from operational polarimetric radar observations. Random forest regression is a machine learning approach based on an ensemble of decision trees. The model "Rainforest" (RF) is trained with a database covering six years (January 2016 to December 2021) with observations from 288 rain gauges and polarimetric radar observations from five dual polarization Doppler C-band radars (Swiss weather radar network). Each radar performs plan indicator (PPI) scans at 20 elevations in 5 minutes.

The complex topography in Switzerland poses many challenges to compile an accurate QPE map. Such challenges include beam shielding, ground clutter and the complex spatial structure of precipitation. Hence, it is important to use information from the entire vertical column of radars. Here, the vertical column of radar observations that results from 20 radar sweeps are aggregated to a single value at the ground level onto a Cartesian grid by applying an exponential weighting function in the vertical.

Based on the evaluation of the feature importance, we include 13 predictors in the RF model: horizontal and vertical reflectivity (Z_h, Z_v), fraction of the contribution of each of the five radars to the grid cell ($Frac_{radar}$), height of each radar volume above the grid cell (H), static visibility of the radar volume (VIS), specific differential phase shift (K_{DP}), co-polar correlation coefficient (ρ_{hv}) and spectral width (SW). The legacy model (RFQ) presented by Wolfensberger et al. (2021) includes temperature estimates (T) given by the numerical weather prediction model COSMO-1 at each model elevation. Because of constraints in the operational implementation, this multi-layer predictor is replaced by the single-layer 0°C isothermal altitude (ISO0). The model is then trained using the extensive database of station observations and the corresponding grid cells of aggregated input variables.

Figure 1 compares the performance of RF models to already operationally implemented QPE products of MeteoSwiss. This evaluation is based on a five-fold cross-validation, in which precipitation events as defined by Wolfensberger et al. (2021) are entirely assigned to either the training or testing data set.

The operational RF model (RFO) is trained on four years (light green) and six years (dark green) of data. The RFO trained on four years allows for a direct comparison to the legacy model (RFQ),

which was trained on the same four years. RFO trained on six years of data is currently implemented on the operational testing chain at MeteoSwiss.

Overall, all the RF models show a promising performance at an hourly time resolution. RFO outperforms the single-polarized operational QPE model (RZC), and shows a similar performance to CombiPrecip CrossVal (CPC.CV). In CombiPrecip gauge and radar estimates are merged. For the sake of a fair comparison, we use CombiPrecip CrossVal in which the gauge estimate evaluated is not considered in the estimate calculation. More information on the QPE products and the scores applied can be found in Wolfensberger et al. (2021) and Germann et al. (2022).

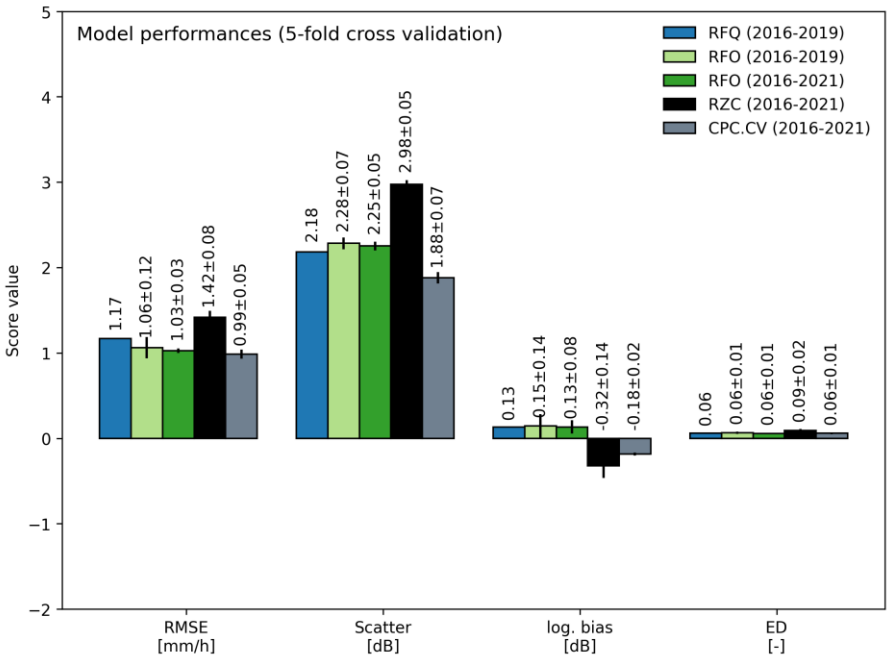

Fig 1: Performances of different models. The scores are averaged over a five-fold cross validation based on randomly-assigned precipitation events. Scores are calculated for hourly estimates with a double conditional threshold of 0.1 mm/h.

As the gauge observations of the Swiss network are logged at 10 min time steps, the temporal resolution of the radar measurements have to be aggregated from 5 to 10 min. This is done through an average over two consecutive time steps of radar volume scans. For the operational implementation, QPE maps are produced at a 5min temporal resolution by applying a temporal disaggregation scheme based on the Swiss Z-R relationship.

In summary, we present the implementation of a machine learning model for compiling operational QPE maps at a 5 min resolution on a 1x1 km2 grid in Switzerland. The new model, which runs in real-time with operational dual-polarization data, is able to outperform the currently operationally implemented radar-only QPE at MeteoSwiss. The novel approach shows great potential for meteorological and hydrological studies in complex terrain regions.

References

Wolfensberger, D., Gabella, M., Boscacci, M., Germann, U., and Berne, A. (2021) RainForest: a random forest algorithm for quantitative precipitation estimation over Switzerland, Atmos. Meas. Tech., 14, 3169–3193.

Germann U, Boscacci M, Clementi L, Gabella M, Hering A, Sartori M, Sideris IV, Calpini B. (2022) Weather Radar in Complex Orography. Remote Sensing. 2022; 14(3):503.

Modeling Areal Precipitation Risks: A Data-driven Approach to model Intensity-Duration-Area-Frequency Relationships in Switzerland

Abubakar Haruna*[1], Juliette Blanchet[2], Anne-Catherine Favre[1]

1 Univ. Grenoble Alpes, Grenoble INP, CNRS, IRD, IGE, 38000 Grenoble, France
2 Univ. Grenoble Alpes, CNRS, IRD, Grenoble INP, IGE, 38000 Grenoble, France

*Corresponding author: abubakar.haruna@univ-grenoble-alpes.fr

Abstract

The assessment of areal rainfall risk is paramount because areal precipitation is directly linked to the hydrological response of a region. Watersheds and river basins integrate precipitation over their respective areas, leading to the accumulation of runoff and subsequent flood generation. By modeling areal precipitation, better understanding of how extreme precipitation events can trigger hydrological responses can be gained, enabling more effective flood prediction and management.

The main statistical characteristics of areal precipitation, such as the return level, return period, duration, and spatial extent (area), are usually summarized in Intensity Duration Area Frequency (IDAF) curves. These models provide the mathematical link between precipitation intensities (I), durations (D), areas (A), and frequency of occurrence (F). They have various applications, including hydrological design, quantification of areal rainfall risk, storm characterization, and development of early warning systems. IDAF models extend the classical Intensity Duration Frequency models (IDF) by incorporating the spatial extent of precipitation (i.e., the area).

In this study, we develop IDAF models using the entire range of non-zero precipitation intensities, not just the extremes. We utilize the extended generalized Pareto distribution (EGPD) (Naveau et al., 2016) to model the precipitation intensities. Building upon the work of Haruna et al. (2023), who demonstrated the applicability of modeling IDF curves with the EGPD, we extend their approach to model IDAF curves. We adopt a data-driven approach (Overeem et al., 2010) to construct the IDAF models (referred to as the EGPD-IDAF model). This approach enables the linkage of EGPD parameters with duration and area based on empirically determined parametric relationships. The parameters are inferred through a global maximum likelihood estimation, and uncertainties are assessed using the block-bootstrap method.

As a case study, we focus on Switzerland, a topographically complex region spanning 42,000 km², characterized by regional precipitation variability and clear seasonality. For our analysis, we utilize 17 years of data from CombiPrecip, a radar-reanalysis product generated by merging radar and rain gauge data in an operational setting. We build the EGPD-IDAF model for the spatiotemporal range of 1-72 hours and 1 to 1000 km² at each pixel. An illustration of the modelled IDAF curves is given in Figure 1.

To evaluate the performance of the EGPD-IDAF model, we compare it to a naive approach (referred to as the base model) that fits the EGPD separately to each dataset of a given area and duration, without linking the parameters with duration. The results demonstrate that the EGPD-IDAF model is more robust and precise, indicated by narrower uncertainty bounds.

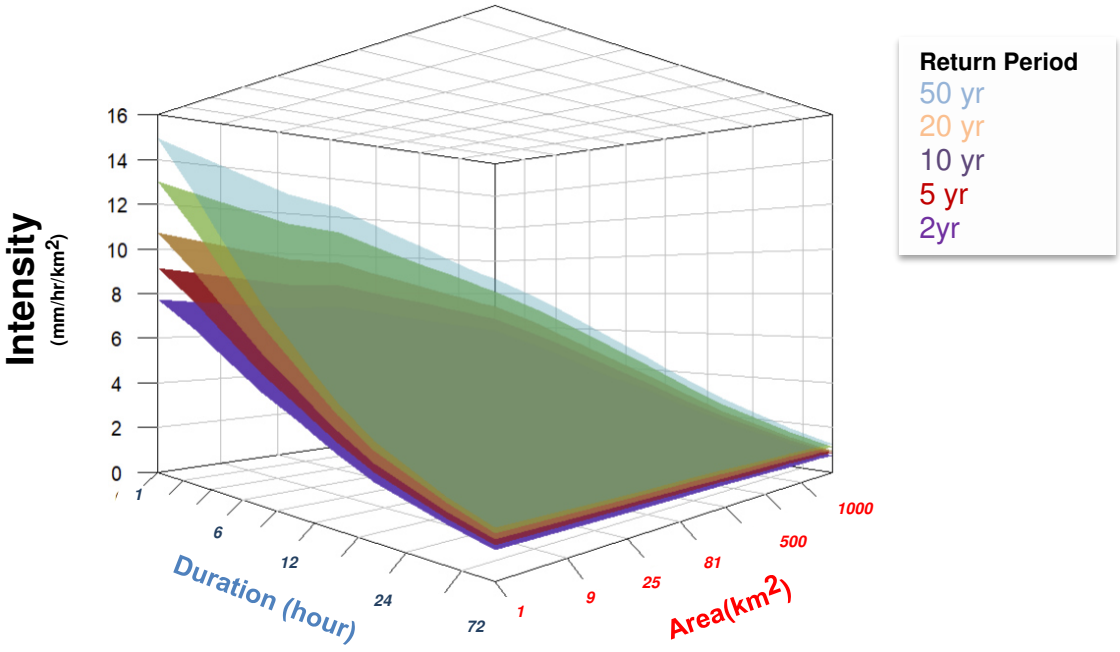

Figure 1: Illustration of autumnal IDAF curves at a location in Adelboden located in northwestern Switzerland.

Using the EGPD-IDAF model, we identify and highlight the spatial variation of areal precipitation risks in Switzerland for different durations and areas. To the best of our knowledge, this study represents the first attempt to utilize the EGPD in IDAF curve modeling. Furthermore, it discusses the use and limitations of CombiPrecip in extreme value analysis and emphasizes the challenges associated with modeling areal precipitation in a complex topographical environment.

References

Haruna, A., Blanchet, J., & Favre, A.-C. Modeling intensity-duration frequency curves for the whole range of non-zero precipitation: A comparison of models. Water Resources Research, 59, e2022WR033362. https://doi. org/10.1029/2022WR033362, 2023

Naveau, P., Huser, R., Ribereau, P., and Hannart, A.: Modeling jointly low, moderate, and heavy rainfall intensities without a threshold selection, Water Resources Research, 52, 2753–2769, https://doi.org/10.1002/2015WR018552, 2016

Overeem, A., Buishand, T. A., Holleman, I., and Uijlenhoet, R.: Extreme value modeling of areal rainfall from weather radar. «Water Resources Research, 46, https://doi.org/10.1029/2009WR008517, 2010

Melting layer prediction via surface weather and its correlation with classes of rainfall rate

S. H. Hosseini*[1], H. Hashemi[1], J. Olsson[2], H. Aspegren[3], R. Berndtsson[1]

1 Division of Water Resources Engineering, Lund University, Lund, Sweden
2 Swedish Meteorological and Hydrological Institute, Norrköping, Sweden
3 Sweden Water Research, Joint R&D company of NSVA, Sydvatten and VA SYD, Lund, Sweden

*Corresponding author: hasan.hosseini@tvrl.lth.se

Abstract

According to IPCC, extreme daily precipitation events have, with “high confidence”, increased since the mid-20th century in most global land regions. However, trends for sub-daily events have limited data and “low confidence”. Thus, management of downpours, as frequent causes of urban floods, requires developments in high-resolution data, and predictable pathways linking the events to climate change, useful for users with both adaptation and mitigation orientations. Remote sensing by scanning dual-polarization X-band weather radars (X-WRs) is a unique technique that has recently gained attention for minute and sub-km rainfall observations in Sweden. However, radar data are prone to various errors and require extensive corrections. Melting layer (ML) observations or overshooting are two major issues causing significant over/under-estimates by X-WR. This fact supports the recently demonstrated benefits of merging data from multiple elevation angles of the X-WRs (Hosseini et al., 2023). However, vertical observations by X-WRs are limited and may or may not include the ML. Thus, a more dedicated device, called Micro Rain Radar (MRR), was installed in Lund in 2021, for constant observation of the altitude range of 146–2246 m amsl with 70-m resolution normal to the earth surface. Figure 1 shows that the ML, corresponding to the peak MRR rainfall rate (RR), varies through inter and intra events.

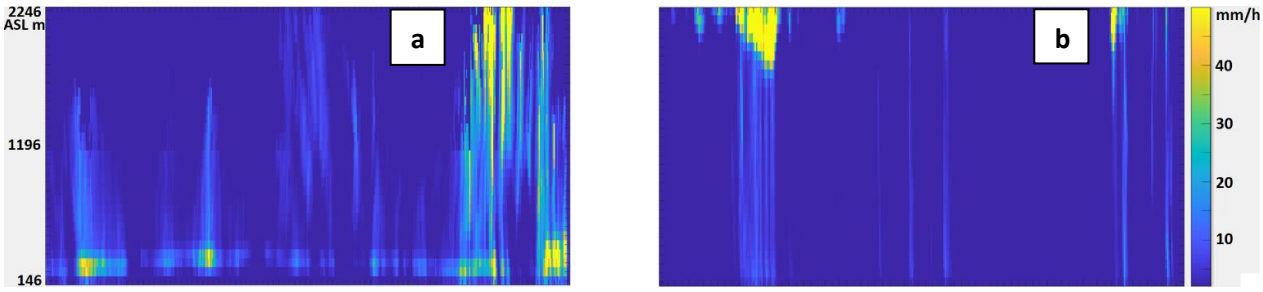

Fig 1 Time series of RR profile of the MRR in Lund (horizontal axis is time in minutes) for the period 13:10-22:00 December 3, 2021 (**a**), and 00:30-22:30 October 15, 2022 (**b**).

Brast and Markmann (2020) used multiple MRR products to manually detect the ML. They used these observations as reference for training a neural network model. Their method is accurate for cases where the ML is continuous in time, but concerns may rise about the uncertainties in the manual observations, e.g., for shorter perturbations with one or more MLs of variable prominence. The present study evaluated 15 months of minute RR profile data from the MRR in Lund for a systematic characterization and neural network prediction of the ML level (1 to 31). Since the ML can also vary spatially, areal upscaling of ML is desirable for bias-correction of the scanning X-WRs. To this aim, the ML was related to the surface temperature and wind (speed and direction) measured close (500 m) to the MRR. Selection of these surface weather parameters was based on their usually better availability and high potential in bias-correction of the RR profile against ground precipitation. Figure 2 summarizes the promising results of the study at various time scales and via different performance criteria (PCC: correlation coefficient, and MAE: mean absolute error). By modeling ML using surface weather and associating their variability to precipitation rates, improved

solutions to urban flood protection are achievable. However, further MRR data both temporally and spatially are needed to lower uncertainties of the data-driven approach.

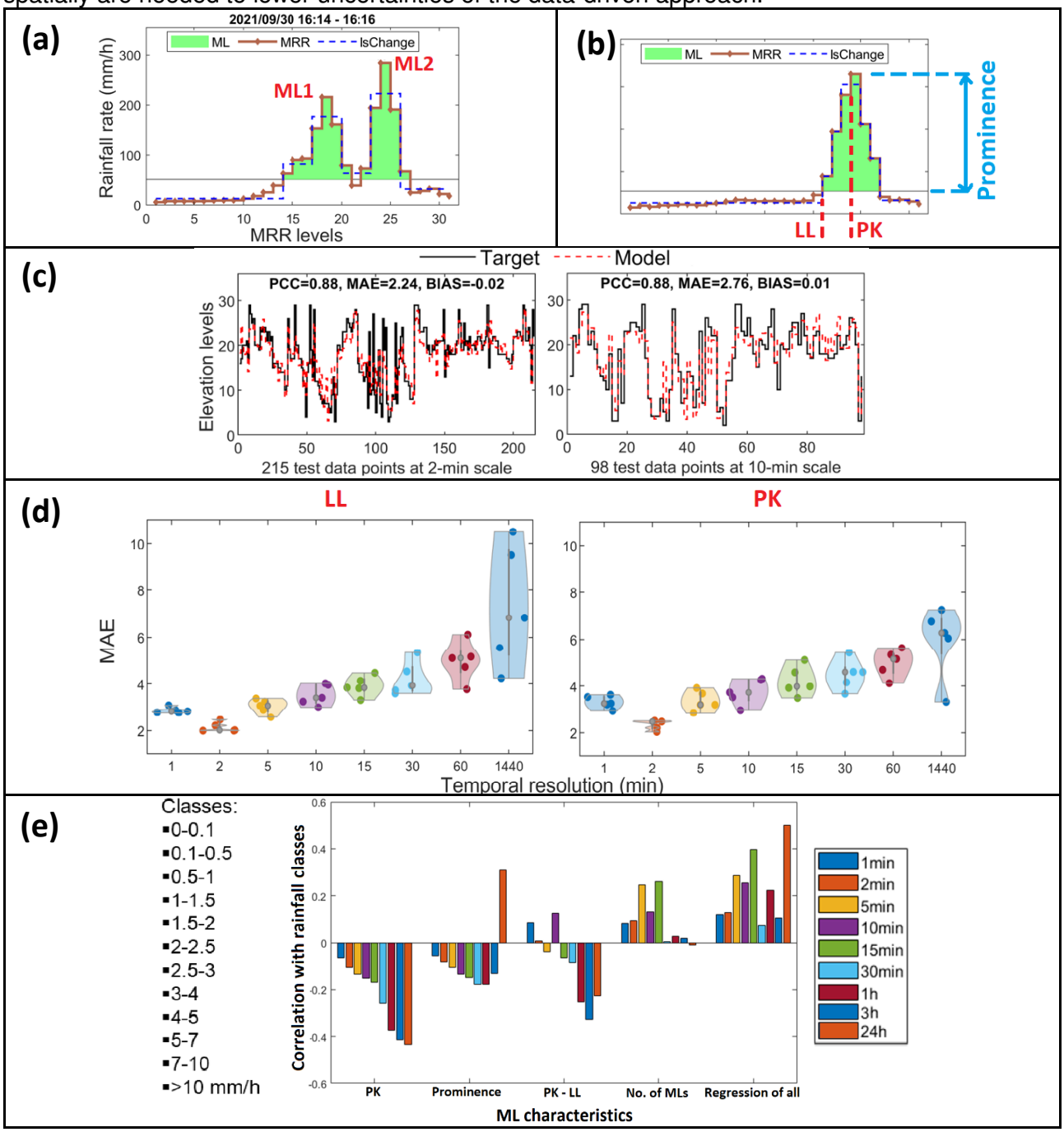

Fig 2 Detection of MLs using the IsChange algorithm in MATLAB (**a**). Definition of lower level (LL), peak (PK), and prominence of a ML (**b**). ANN modeling of LL for test data (not used in calibration) at 2 and 10-min scales (**c**). The violin plot of MAE for multi-scale LL and PK models tested by a 5-fold cross validation (**d**). Correlation between ML characteristics and precipitation classes (**e**).

References

Hosseini, S.H., Hashemi, H., Larsson, R., and Berndtsson, R. (2023), Merging dual-polarization X-band radar network intelligence for improved microscale observation of summer rainfall in south Sweden, J. of Hydrol., 129090, DOI: 10.1016/j.jhydrol.2023.129090.

Brast, M., and Markmann, P. (2020), Detecting the melting layer with a micro rain radar using a neural network approach, Atmospheric Measurement Techniques, 13, 6645–6656.

The comparison of design precipitation totals in the border region of the Czech Republic and Germany

F. Hulec*[1,2], M. Kašpar[1], M. Müller[1,2], T. Winterrath[3], T. Junghänel[3]

1 Institute of Atmospheric Physics, CAS, Prague, Czech Republic
2 Charles University, Faculty of Science, Prague, Czech Republic
3 Deutscher Wetterdienst, Offenbach am Main, Germany

*Corresponding author: hulec@ufa.cas.cz

Abstract

Extreme rainfall events significantly impact a wide range of human activities and the environment, for example, through flash floods or soil erosion. To design effective mitigation measures, especially in small catchments that are not hydrologically monitored, it is necessary to know the statistical representation of the events. It is usually expressed by the design precipitation totals, where possible in the sub-daily step, because maximum rainfall intensities are usually reached in convective storms lasting only tens of minutes to several hours. As a natural phenomenon, extreme rainfall events are not only limited to the territories of specific countries. Therefore, their consequences should be dealt with regardless national borders.

Sub-daily design precipitation totals can be derived from station or radar data. Each of these data sources has advantages and disadvantages. Station measurement time series are usually long enough for the statistics of extremes with long return periods, but the network of stations is too sparse and does not provide sufficient information on the spatial variability of precipitation. In contrast, radar data continuously cover a large area with high spatial and temporal resolution. Therefore, they can capture well the small-scale spatial dynamics and temporal variability of precipitation. However, radar measurement time series are still too short and the conversion of radar reflectivity to precipitation intensity is only approximate. In the presentation, we show the comparison and evaluation of design precipitation totals derived from station and radar measurements and also from the combination of both using available datasets from the Czech and German territory.

Data from 39 stations are used for the comparison. Czech station data provided Czech Hydrometeorological Institute after their quality control (Crhová et al., 2022). German station data are provided by German Weather Service. These data are also used as a source for KOSTRA-DWD 2020 dataset. Czech radar data come from the national radar network, which consists of two C-band Doppler radars (Bližňák et al., 2018), and their time series length is 20 years. Radar-derived precipitation estimates were before use adjusted with 1-day precipitation totals at more than 700 stations using the method by Sokol (2003). Climatological database RADOLAN is used as a source of German radar data, which time series length is 22 years. Design precipitation totals are derived using generalized extreme-value distribution as a parametric model. Regarding Czech radar data, the L-moment-based index storm procedure and region-of-influence method are applied to refine their estimates (Kyselý et al., 2011); in addition, obtained design totals are combined with design totals derived from station data by the interpolation of differences. Regarding German radar data, design totals are derived using also Pareto distribution as a parametric model, which parameters are available in RADOLAN database.

Preliminary results show that design precipitation totals derived from station data are consistent on both sides of the border, with minimal deviation in statistical characteristics. Figure 1 compares short-term design totals derived from station data with design totals derived from different radar datasets in corresponding radar pixels. It is evident that radar-derived design totals are underestimated

compared to the station-derived design totals. As expected, the best results are achieved employing adjusted radar data and regional frequency analysis, especially for longer return periods.

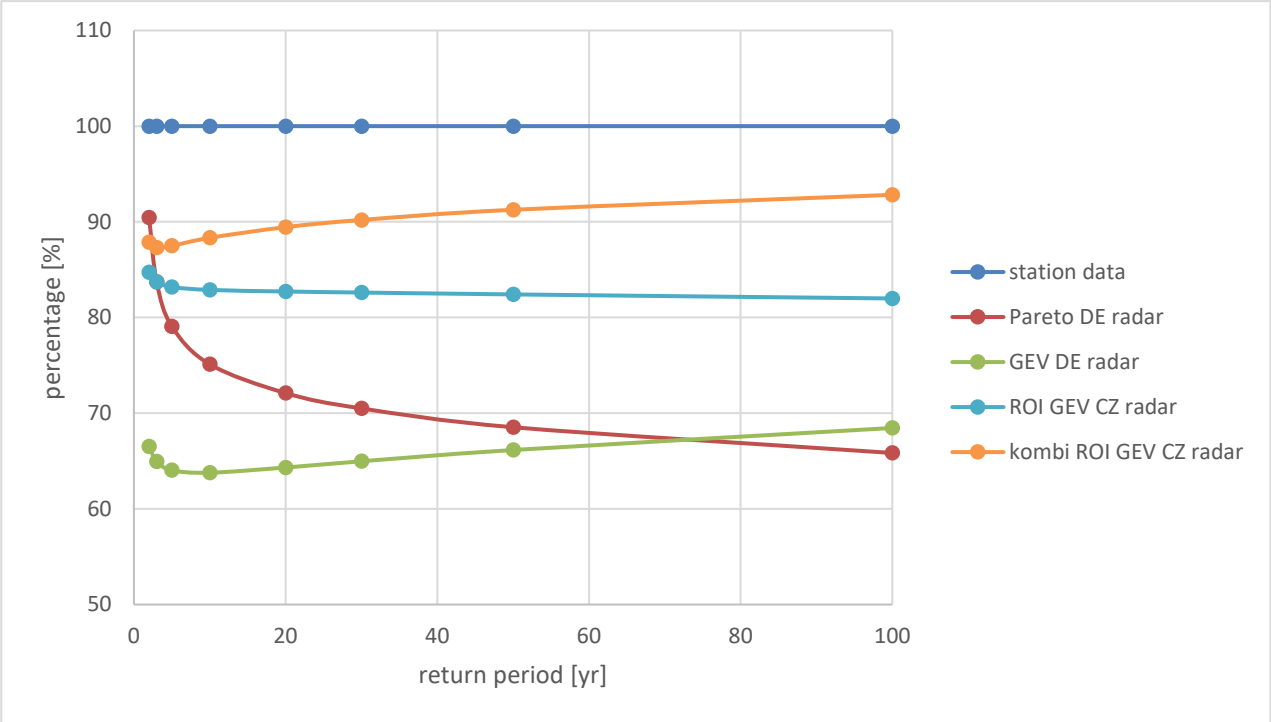

Fig 1: Percentage comparison of the means of 1-h design precipitation totals derived from different considered datasets.

References

Bližňák, V., Kašpar, M., and Müller, M. (2018), Radar-based summer precipitation climatology of the Czech Republic, Int. J. Climatol., 38, 677-691.

Crhová, L., Kliegrová, S., and Valeriánová, A. (2022), Měření srážkových intenzit na stanicích Českého hydrometeorologického ústavu (ČHMÚ) a průběh jejich zpracování (Measurement of precipitation intensities at the stations of the Czech Hydrometeorological Institute (CHMI) and the way of their processing), Meteorologické zprávy, 75, 37-43. In Czech with English abstract.

Kyselý, J., Gaál, L., and Picek J. (2011), Comparison of regional and at-site approaches to modelling probabilities of heavy precipitation, Int. J. Climatol., 31, 1457-1472.

Sokol Z. (2003), The use of radar and gauge measurements to estimate areal precipitation for several Czech river basins, Stud. Geophys. Geod., 47, 587-604.

IMERG Run Deep: Can we produce a low-latency IMERG Final run product with a deep learning based prediction model?

Ho Tin Hung*[1], and Li-Pen Wang[1]

1 Department of Civil Engineering, National Taiwan University, Taiwan

*Corresponding author: b08501134@ntu.edu.tw

Abstract

IMERG is a global satellite-based precipitation dataset produced by NASA. It provides valuable rainfall information, starting from June 2000, that facilitates the design or the operation of the disaster and risk management worldwide. In operation, NASA offers three types of IMERG Level 3 (L3) products, with different levels of trade-offs in terms of time latency and accuracy. These are Early run (IMERG-EL; 4-hour latency), Late run (IMERG-LR; 14-hour latency) and Final run(IMERG-FR; 3.5-month latency). The IMERG-FR product integrates multi-sensor retrievals and provides precipitation estimates with the highest quality among three IMERG products. It however suffers from a long processing latency, which hinders its applicability to near real-time operations.

In the past 10 years, deep learning techniques have made significant breakthroughs in various scientific fields, including short-term rainfall forecasting. Deep learning models have shown to have the potential to learn the complex variations in weather systems and to outperform the Numerical Weather Prediction (NWP) in terms of short lead-time predictability and the required computational resources for operation (Bakkay, et al., 2022). In this research, we explore the potential of deep learning (DL) in generating high-quality satellite-based precipitation product with low latency. More specifically, we investigate if DL models can learn the discrepancies between IMERG-FR and IMERG-ER products, and thus predict a IMERG-FR alike using IMERG-ER product as input; such that high-quality yet low-latency IMERG precipitation product can be obtained. A number of DL techniques are selected and tested in this work. These include Auto-Encoder (AE), ConvGRU and Deep Generative models. IMERG-FR and IMERG-ER products between 2018 and 2020 over a rectangular area centred in the UK are sampled for model training and testing. Those IMERG-FR data that are not sampled for training and testing, as well as ground rain gauge records, will be used to evaluate the performance of the predicted product. The selected experimental area includes both ocean and land regions, which enables the comparison of the model performance between two different surface conditions.

Amongst the DL models being tested, the deep generative model architecture (i.e. DGMR; see Figure 1), proposed by Ravuri, et al. (2021), appears to outperform other models. It can well learn the spatial-temporal relationship of precipitation data while accounting for the uncertainty of the IMERG-ER data. Preliminary results show that the predicted IMERG-FR alike leads to better performance measures than the baseline IMERG-ER data in terms of all categorical metrics (CSI, POD, FAR) (see Figure 2). This suggests that, as compared to IMERG-ER, the predicted IMERG-FR alike is much more similar to the original IMERG-FR. The shows great potential of the proposed work to improve the applicability of IMERG products in an operational context.

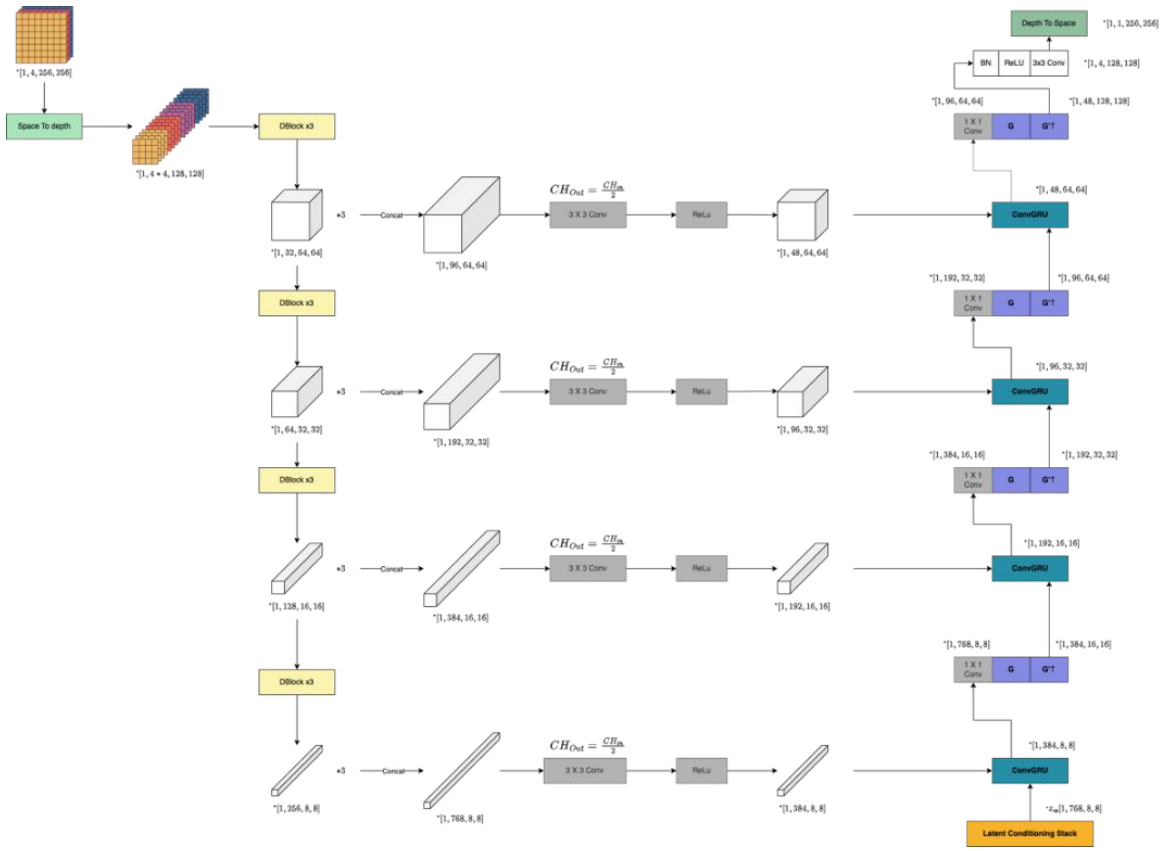

Fig 1: DGMR's Generator architecture (Ravuri, et al., 2021)

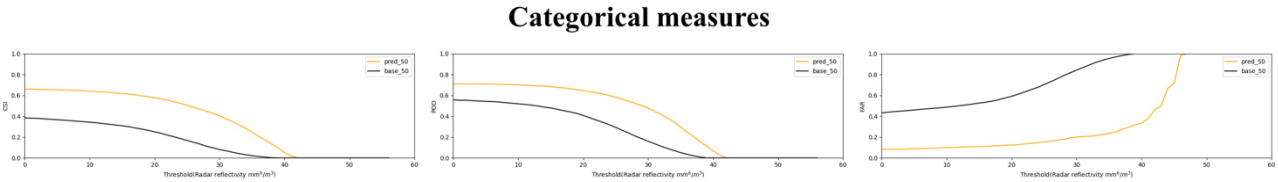

Fig 2: Medians of the selected categorical measures at different thresholds: Critical Success Index (CSI; left), Probability of Detection (POD; middle) and False Alarm Rate (FAR; right). Dark lines represent performance measures resulting from IMERG-ER, while orange lines from the IMERG-FR alike.

References

Bakkay, M. C., Serrurier, M., Burda, V. K., *et al.* Precipitaion Nowcasting using Deep Neural Network. (2022). https://doi.org/10.48550/arXiv.2203.13263

Ravuri, S., Lenc, K., Willson, M. *et al.* Skilful precipitation nowcasting using deep generative models of radar. *Nature* **597**, 672–677 (2021). https://doi.org/10.1038/s41586-021-03854-z

Enhanced urban drainage management for Melbourne Water with the Hydronet Water Control Room

B. Jackson*[1], M. Alderlieste[2] T. Einfalt[3], A. Strehz[3]

1 Water Technology, Melbourne, Australia
2 Hydrologic Systems BV, Amersfoort, The Netherlands
3 hydro & meteo GmbH, Lübeck, Germany

*Corresponding author: brian.jackson@watertech.com.au

Abstract

Melbourne Water (MW) is a Victorian Government-owned statutory authority that controls and manages much of the water bodies and supplies in metropolitan Melbourne, Victoria, Australia. MW has extensive monitoring equipment and data management systems to assist them and their partners to prepare for, respond to, and recover from potential flooding events and other urban drainage related management responsibilities across the region. However, many significant rainfall events still miss the rain gauges, leading to gaps in the understanding of the intensity, duration, timing and locality of events.

MW have thus sought to use rain gauge adjusted radar rainfall to improve the understanding of rainfall, while simultaneously evolving their technology around operational information creation and sharing of the personalised information required by staff, management and partner organizations for effective and coordinated decision making.

Therefore, the HydroNET Water Control Room (WCR) was implemented and linked to various data sources including a new HydroNET- SCOUT gauge adjusted radar rainfall product, with the intention of improving the rainfall data while simultaneously enabling easier access and use of the data without burdening system administrators and without the need for a new data warehouse.

Data Connections and HydroNET Water Control Room

HydroNET is an award winning, web-based decision support platform that provides users with smart tools overlying existing data sources and systems, allowing them to easily generate personalised dashboards, forecasts, notifications and reports.

The data sources connected to HydroNET for MW are:

- The Bureau of Meteorology's (BoM) digital forecast database (ADFD) forecast, observed weather data, including their Rainfields 3 high resolution, bias adjusted radar rainfall data and radar based high resolution, short term rainfall forecasts up to two hours ahead.
- The new HydroNET – SCOUT gauge adjusted radar rainfall product.
- The MW Flood Integrated Decision Support System for MW's rain gauge, river level gauge, tidal gauge, water quality gauge and drainage basin gauge network data.
- The MW Hydstra System for surface and underground pipe level data.
- The MW GIS servers to include geospatial background information.

Staff at MW now have numerous dashboards that can be further configured by themselves that provide them with a good overview as well as the details of all relevant data sources. An example is shown in figure 1.

HydroNET – SCOUT Gauge Adjusted Radar Rainfall Data

Under normal conditions rain gauges measure precipitation with high accuracy, but with limited spatial representativeness depending on the meteorological conditions. In contrast, radar data is ideally suited to represent spatial precipitation patterns with greater uncertainties in precipitation amounts at point scale compared to rain gauges. Carefully combining quality-controlled data from automatically reporting rain gauges and radar data yields a dataset with a high accuracy, a good temporal and spatial resolution, and a low latency, together with a good spatial coverage (Einfalt & Frerk, 2011). Therefore, a SCOUT (Einfalt et al, 1990) process was set up to adjust the BoM Rainfields 3 radar rainfall data against the MW rain gauges to provide MW with a radar rainfall product with improved calibration against rain gauges, hence providing precipitation information with good accuracy and spatial detail.

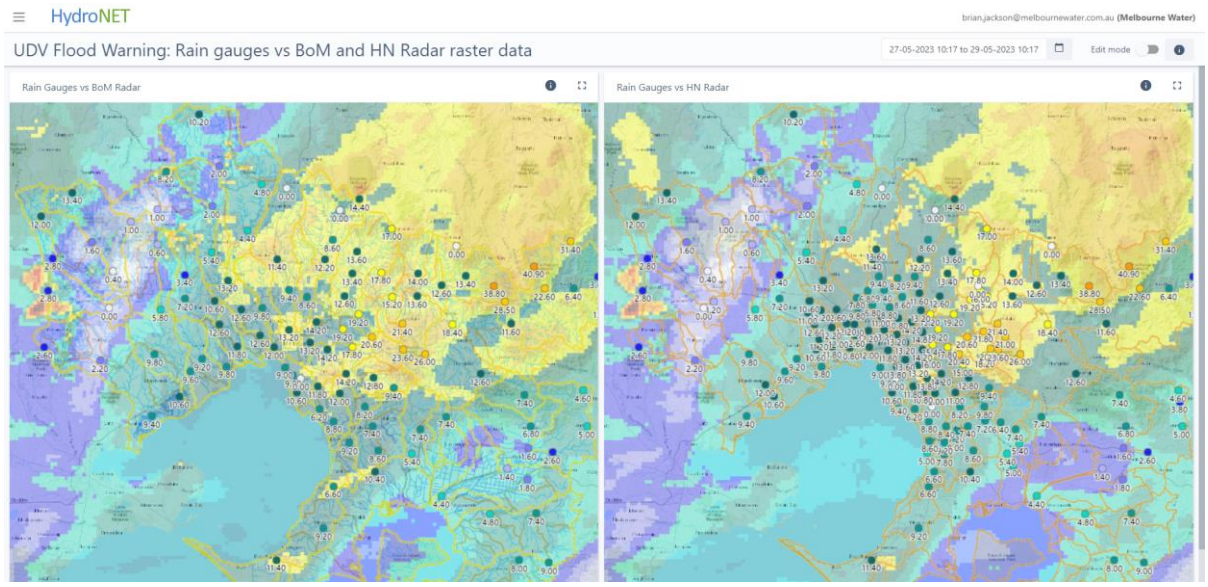

Figure 1. The BoM's Rainfields 3 Radar Rainfall data (left) vs the HydroNET – SCOUT gauge adjusted radar rainfall data (right), compared to MW's rain gauge network, as visualised in HydroNET.

Conclusions and future work

HydroNET now provides MW with simple, robust tools for accessing and sharing the live information required for various differing needs before, during and after events, based on the same underlying data. Timeseries of radar data can easily be extracted from individual pixels as well as catchment averages.

This greatly improves joint decision making. The observed and forecast radar rainfall data also provides improved understanding of the intensity, duration, timing and locality of events when compared to rain gauges alone, as has been found by several other studies (Daly, 2016; Sun, 2000). The automated catchment aggregation further improves the understanding of catchment flooding.

References

Einfalt, T.; Denoeux, T.; Jacquet, G. A radar rainfall forecasting method designed for hydrological purposes. J. Hydrol. 1990, 114, 229–244, doi:10.1016/0022-1694(90)90058-6.

Einfalt, T.; Frerk, I. On the influence of high quality rain gauge data for radar-based rainfall estimation. In Proceedings of the 12th ICUD, Porto Alegre, Brazil, 11–16 September 2011.

Daly, A. Radar Rainfall Calibration of Flood Models – the future of Catchment Hydrology? Paper presented at the Stormwater Queensland Conference, 2016.

Sun, X., Mein, R.G., Keenan, T.D. and Elliott, J.F., 2000. Flood estimation using radar and rain gauge data. Journal of Hydrology, 239(1), pp.4-18.

heavyRain - Use of IoT rain sensors to improve heavy rain forecasts in Lübeck

A. Jahnke-Bornemann*, T. Einfalt[1]

1 hydro & meteo GmbH, Lübeck, Germany

*Corresponding author: a.jahnkebornemann@hydrometeo.de

Abstract

As part of the three-year mFUND funded project "heavyRain" project (BMDV, 2022), 50 newly developed Internet-of-Things (IoT)-enabled rain sensor systems will be tested in each of four German cities (Bochum, Hagen, Lübeck, Lüdenscheid) as part of a field trial, with this paper primarily presenting the results from Lübeck to date. The low-cost IoT sensor systems from NIVUS use an infrared (IR) rain sensor established in the automotive sector, combined with a LoRaWAN transmitter and a photovoltaic element. The Long Range Wide Area Network (LoRaWAN) is a low-power wireless network protocol that is already widely used in the four cities. The sensors can distinguish dry weather and 7 classes of rain. The measured data is transmitted over the existing LoRaWAN wireless network of Stadtwerke Lübeck, the public utility company of the city of Lübeck. In case of transmission error, data could get lost as there are no intermediate buffers in the transmission chain before they reach the server, where data are checked and made available for further use.

This field trial will show the extent to which the sensors are useful to supplement precipitation measurements in the future. Although the stations are single point measurements, a large number of densely placed sensors can improve to capture the spatial structure of precipitation events. The sensors are very responsive and react to even small amounts of rainfall. Another advantage is the low initial cost and the ease of installation and handling, which allows many units to be installed over a larger area. The self-sufficient power supply and self-cleaning sensor dome allow for very long maintenance intervals and less manpower is needed. We identified the data transmission and the quality of the sensors as possible weak points of the system.

Fig 1: The NIVUS rain sensor system with infrared sensor, PV element and LoRaWAN sender.

Sensor quality tests were carried out in the laboratory, before the sensors were installed. Tests were carried out with defined amounts of water on several devices in order to assign them to precipitation classes and to determine the variance of the measurement.

Particular attention was paid to the search for suitable sites, and evaluation criteria were developed in order to achieve the best possible results in the urban environment. Based on the specifications

of the WMO for the installation of rain sensors, 4 location categories were defined, that result from the points given after evaluation of 9 characteristics for each location (Tab 1). The sites were distributed throughout Lübeck, considering the main wind direction. The distances to the closest sensors vary from a few meters to 6 kilometers in peripheral areas. Most sensors will be installed in cooperation with the city of Lübeck on streetlamps at a height above 250 cm to make theft and vandalism more difficult. Some sensors will be installed near existing rain gauges.

Tab 1: Characteristics for determination of location category.

Characteristic	**Possible options (Points)**
Installation height of the instrument	1 m to 1.5 m (3), 1.5 m to 5 m (2), more than 5 m (1), less than 1 m (0)
Splash water	None (3), sporadically, e.g., from the mast (2), Regular splashing of water from any source (0)
Pollution	None (3), typical city environment (2), additional sources, e.g. dust and pollen (1)
soil condition	grass or gravel soil (3), Texture between grass and asphalt (2), asphalt (1)
Obstacles in the angle above the sensor	None (3), Small restrictions like wires and cables (2), larger objects like traffic signs on the mast (1), shielding e.g. by trees (0)
Obstacles in the horizontal field of view of the sensor	No obstacles or far enough away (3), The obstacles are at a distance that is at least equal to the height of the obstacle, angle is at most 45° (2), <60°, up to 180° solid angle, at least h/2 distance (1), > 180° solid angle and at the same time >60°, closer than h/2 to the sensor (0)
Slope	level ground (3), inclinations < 30° (2), inclinations > 30°(1)
Turbulence	Uniform obstacles at sufficient distance (3), somewhat heterogeneous obstacles (2), obstacles vary in height (1)
Infrared light	None (3), Infrared light sources far enough away (2), regular infrared light input (0)

In order to analyze the usefulness of the sensors, it is planned to quality prove each sensor data set and do a plausibility check and comparison of the precipitation time series with each other. (Fennig, 2023). In addition, a comparison with data from other point measurements from nearby stations from other operators is planned This can include the tracking of interesting rain events in both sources and comparison of the results. Besides that, a precipitation field is to be interpolated from the sensor measurements with methods like IDW or Kriging. Different temporal resolutions are considered and compared with precipitation fields from other sources (radar, satellite). It is also planned to analyze data from neighboring sensors over a longer period to determine drift effects of sensor type. The influence of other precipitation types, such as hail, can also be studied.

The result will provide a good estimate of the data quality. We expect that with a large-scale distribution of sensor systems and well-chosen locations, the small-scale structures of precipitation events on the order of 0.5 to 1 km can be better captured, thus allowing for a finer forecast grid for nowcasting. It seems interesting to compare the results of this field trial with studies where other devices have been used, in particular, it is worth comparing with the results on NetAtmo systems described in Bárdossy (2023).

References

Fennig, C., T. Einfalt, S. Luers (2023), Rain gauge data quality revisited: old-fashioned or new trend? Conference Abstract, UrbanRain23, ETH Zurich.

Bárdossy, A., Seidel, J., and El Hachem, A. (2021), The use of personal weather station observations to improve precipitation estimation and interpolation. Hydrol. Earth Syst. Sci., 25, 583–601.

BMVD (2022), Heavy Rain sensor-based Artificial Intelligence Nowcast – heavyRain, https://bmdv.bund.de/SharedDocs/DE/Artikel/DG/mfund-projekte/heavyrain.html, access. 6/6/23

Spatial variability of the course of precipitation intensity during heavy rains in Czechia

M. Kašpar*[1], V. Bližňák[1], F. Hulec[1,2], M. Müller[1,2]

1 Institute of Atmospheric Physics, CAS, Prague, the Czech Republic
2 Charles University, Faculty of Science, Prague, the Czech Republic

*Corresponding author: kaspar@ufa.cas.cz

Abstract

Key variable input data for hydrological modeling are the precipitation total, its distribution in time and space, and antecedent soil moisture. In the presented contribution, we focus on the first two variables for the purposes of water management in small catchments that are rarely hydrologically monitored. An applicable approach is to evaluate the design precipitation in a sub-daily step due to the great influence of heavy short-term rainfalls there. Two characteristics are assessed: (i) the design precipitation total with a given return period and (ii) the occurrence probability of typical variants of the precipitation intensity course for a given design total. The evaluation is presented for the territory of Czechia.

To capture the naturally high spatial and temporal variability of heavy short-term rainfalls, the input dataset consists of 20-year series of precipitation intensities with a time resolution of 10 min and a spatial resolution of 1 km. The intensities were determined from 10-min weather radar-derived intensities in more than 80,000 radar pixels and adjusted by 1-day precipitation totals measured in more than 700 rain gauges (Bližňák et al., 2018).

Courses of precipitation intensity typical for the studied area are divided into 6 variants approximated by 6 synthetic storm hyetographs depicted in Fig. 1. The hyetographs were constructed by the cluster analysis of reference precipitation events with the highest 6-hour totals using 3 similarity measures quantifying the time concentrations of precipitation during the events (Müller et al., 2018). Considering the 6-h accumulation time is a compromise between the 24-h accumulation, which is too long to examine the effect of the time concentration of precipitation on the hydrological response in small catchments, and 1-h and shorter accumulations, which usually do not cover the whole event and do not allow capturing more significant changes in the intensity. Design precipitation totals with a given return period are estimated by robust procedures of the regional frequency analysis (Kašpar et al., 2021). In order to refine obtained design totals, they are further combined with design totals estimated from available ombrographic measurements by a suitable interpolation method. The generalized extreme-value distribution is selected as a parametric model in the frequency analysis. Its parameters are derived using the block maxima approach and applying the L-moment-based index storm procedure and region-of-influence method. The occurrence probability of a variant of the intensity course for a given 6-h design total is estimated by comparing the return period of the total for the variant with those for the other variants.

Figure 2 shows an example of the spatial distribution of design precipitation totals (on the left) and the corresponding occurrence probabilities of the variant of the precipitation intensity course characterized by a short period of high intensity belonging usually to torrential rains during convective storms (in the middle) and the variant characterized by relatively steady and longer-lasting rains falling from larger systems of prevailing stratiform clouds (on the right). It is obvious that the spatial heterogeneity of design totals and variant percentages amplifies with the increasing return period. Their spatial distribution is affected mainly by topography. However, the dependence of percentages on topography may differ for individual variants due to different dynamics of causal circulation conditions.

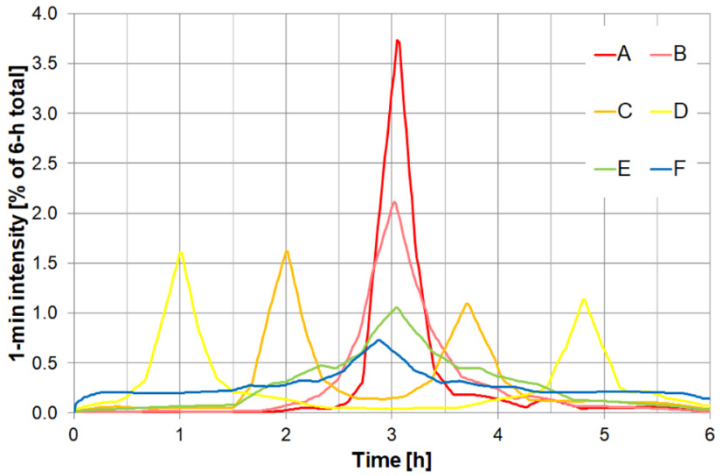

Fig 1: Six synthetic storm hyetographs typical of 6-h heavy precipitation events in Czechia.

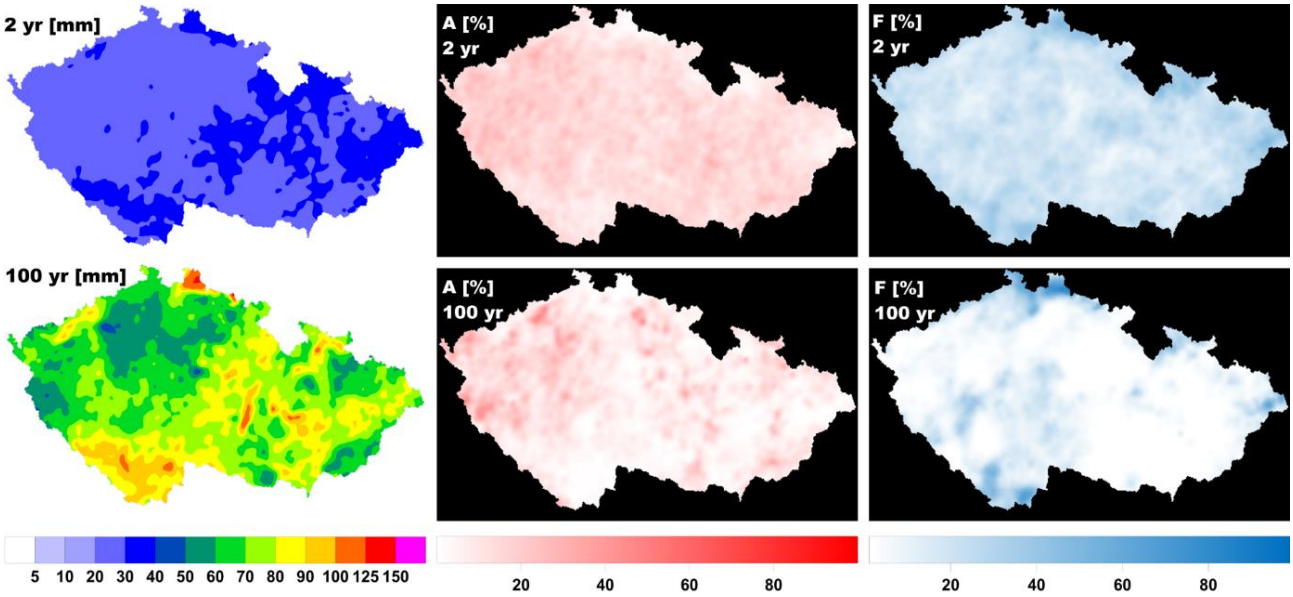

Fig 2: Six-hour design precipitation totals with the return period of 2 and 100 years (on the left) and the corresponding occurrence probabilities of two variants of the precipitation intensity course approximated by the synthetic storm hyetographs A (in the middle) and F (on the right) in Fig. 1.

References

Bližňák, V., Kašpar, M., and Müller, M. (2018), Radar-based summer precipitation climatology of the Czech Republic, Int. J. Climatol., 38, 677-691.

Kašpar, M., Bližňák, V., Hulec, F., and Müller, M. (2021), High-resolution spatial analysis of the variability in the subdaily rainfall time structure, Atmos. Res., 248, 105202

Müller, M., Bližňák, V., and Kašpar, M. (2018), Analysis of rainfall time structures on a scale of hours, Atmos. Res., 211, 38-51.

Classification of Czech urban areas by their characteristics in link to potential of retention of heavy rainfall.

P. Kavka*[1], D. Stránský[1], A. Vizina[2], M. Hanel[3]

1 The Czech Technical University in Prague, Czech Republic
2 T. G. Masaryk Water Research Institute, Czech Republic
3 The Czech University of Life Sciences, Czech Republic

*Corresponding author: petr.kavka@fsv.cvut.cz

Abstract

Urban areas are increasingly affected by extreme hydrological events such as flash floods and droughts. However, there is currently a lack of design rainfall information for safe management of flash floods, particularly for short durations (5-10 min) and for changes in rainfall extremes with shorter recurrence periods (2, 5, and 10 years). Adaptation measures are being introduced to manage water scarcity during droughts, they are not being evaluated for their effectiveness in the face of ongoing and future climate change. This contribution introduces part of ongoing project that have three main tasks. a) Estimating changes in precipitation in link to climate changes for a range of design precipitation with different recurrence intervals. Statistical models with regional/global climate model simulations are used to estimate changes in precipitation extremes with durations of 1-24 hours. A geostatistical model to describe changes in intensity-duration-frequency (IDF) curves are used for the Czech Republic. b) The impacts of rainfall extremes, the potential for retention and the need to use water from heavy rainfall also depend on the nature and extent of urban areas of the specific area under consideration. Assessing the impact of climate change on adaptation measures in urban areas and quantifying and evaluating them on pilot sites. Selection of this pilot sites are based on classification of urban areas and their contributed headwater watershed. The methodology and preliminary results are presented in this contribution. c) Adaptation measures to increase the volume of water retained in the area during heavy rainfall. The project in practical also propose typical measures to increase the volume of water retained in the area during heavy rainfall, such as temporary retention basins and flood parks. Developing a methodology for technical protection against flooding due to heavy rainfall, including the possibility of creating temporary retention volumes in the area. Methodological support for the local government and stakeholders for design of retention areas and emergency outflow paths, and document the impact of climate change and the evaluation of the balance in urbanized areas.

Methodology and Results

This contribution presents options for categorizing urbanized areas in terms of vulnerability. Classify urbanized areas are based on degree of urbanization, proportion of paved areas, overall size of the urbanized area, morphology, presence of natural and or artificial drainage paths, and link to possibilities of risks of external waters, see Table 1.
Tab 1: Urban areas characteristics.

Characteristics	Units	Description
Degree of urbanization	[%]	Percentage of paved areas
Size	km^2	Five class
Habitats	No.	Five class
Potential of pluvial floods	Degree of risks	Based on SoLC (Kavka, 2021)
Potential of fluvial floods	N100/N20/No	Based on flood risk maps
Volume of design precipitation	[mm]	1, 6, 24 h
Percent probability of heavy storms	[%]	Based on classification (Muller, 2018)

Urban drainage systems Retention and GI	Categories Categories	Combinate, Separate, No

The categorization of urbanized areas, in addition to their characteristics (described above), also includes their connection and their possible vulnerability to water generated outside the urbanized area itself. This characteristic is particularly important for less urbanised and often smallest areas in agricultural landscapes. For these needs of the possible risk of external water risks to urbanised areas, the derived headwater catchments (SoLC) up to 5km2 will be used for including their classification in terms of the possible occurrence of rapid runoff (Kavka).

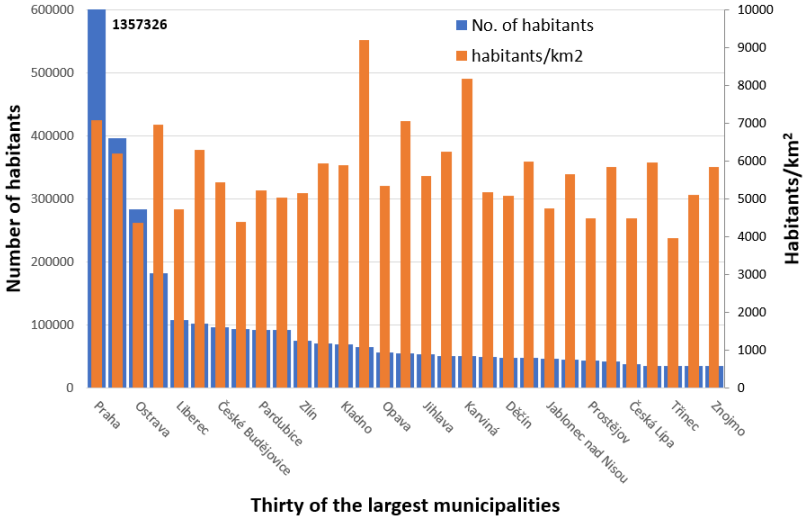

Fig 1: Thirty largest settlements in the Czech Republic by population (blue) and population per km2 (orange).

These thirty the biggest municipalities have 20% of the country's population. The average number of inhabitants in a municipality is 1732 and almost half of the people live in municipalities with less than 5000 inhabitants. This show population distribution a is a support for classification that also included connection to external waters risks. It can help to determine the appropriate types or combination of measure for specific classes of urban areas.

This research is supported by research project "Adaptation of urban areas to flash floods and droughts" (TAČR - SS06010386).

References

Kavka, P. (2021) ‘Spatial delimitation of small headwater catchments and their classification in terms of runoff risks’, Water (Switzerland), 13(23). doi: 10.3390/W13233458.

Müller, M., Bližňák, V., Kašpar, M., 2018. Analysis of rainfall time structures on a scale of hours. Atmos. Res., 211, 38–51. DOI: 10.1016/j.atmosres.2018.04.015.

Detecting futures changes in the characteristics of short-term rainfall in Slovakia

S. Kohnová*[1], G. Földes[2]

1 Slovak University of Technology, faculty of Civil Engineering, DLWRM, Bratislava, Slovakia
2 Senec tourism administration, Senec, Slovakia

*Corresponding author: silvia.kohnova@stuba.sk

Abstract

Climate warming is driving an increase in extreme precipitation across most of the globe. This phenomenon is expected to continue as the air temperature is projected to rise. Thus, there will likely be a higher frequency and intensity of extreme rainfall in the future, leading to an increased risk of floods.

Rainfall intensities and rainfall-duration-frequency (IDF) curves are of great practical importance in water resources management, e.g., for designing hydraulic structures and urban drainage systems and estimating flash flood risk. This study focused on the impact of climate change on the characteristics and design values of short-term rainfall intensities in Slovakia. To simulate future rainfall data in hourly time step, the Community Land Model (CLM 4.0.) was used (http://www.cgd.ucar.edu/tss/clm/). The CLM scenario was simulated by the IPCC scenario for A1B for the 21st century; the scenario is semi pessimistic with a 2.9°C increase in the global temperature by 2100.

For the analysis together, 31 climatological stations from the whole territory of Slovakia were selected. For each climatological station, the collected data of hourly short-term rainfall intensities were divided into three time periods: historical–observed data (1961-2020), the near future (2031-2070), and the far future (2071-2100) climate scenario data. The analyzed rainfall durations were divided into 60, 120, 180, 240, and 1440 minutes. First, the analysis of data homogeneity, trends, and breaking points in data series and the seasonality of maximal rainfall events in all durations and for all selected periods were performed. The trend analysis confirmed an increasing but insignificant trend at most climatological stations; the seasonality of maximum rainfall events revealed the future changes compared to the historical period, and the shifts in extreme rainfall occurrence between the historical and future periods are to a later date; often the shift from July to August (see Figure 1).

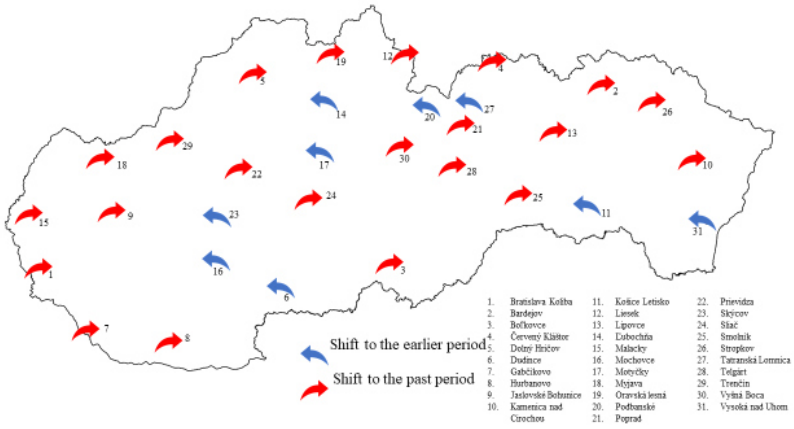

Fig 1: The shift in the occurrence of maximum short term rainfall intensities between the historical and far future periods.

Next, the simple scaling theory was adopted to estimate the IDF characteristics of short-term rainfall. The derived values of scaling exponents also confirm their change in future periods. The scaling exponents for the future periods have higher values than in the historical period. Subsequently, scaling exponents were used to derive IDF curves of short-term rainfall intensities. The design values of short-duration rainfall have been compared with an increasing character for the future.

The results showed that climate change, represented by the CLM scenario, will affect the characteristics and the design values of short-term rainfall intensities in the future. This will significantly impact water structures and the need for re-evaluation of their safety. The findings of this study also indicate the need to revise urban design guidelines to be prepared for future extreme rainfall events.

Nowcasting of heavy rainfall events with AI-based precipitation forecast models: Influence of number of model parameters and of input images on the prediction accuracy

J. Koltermann da Silva*[1], B. Burrichter[1], M. Quirmbach[1]

1 Institute of Civil Engineering, Ruhr West University of Applied Sciences, Germany

*Corresponding author: Juliana.KoltermanndaSilva@hs-ruhrwest.de

Abstract

Accurate predictions of rainfall intensities for heavy rainfall events are especially required in urbanized areas, where the catchments have short runoff concentration times and are not usually able to manage large rainfall amounts well. The most severe consequence of such events is the onset of flash floods that can cause property damages and ultimately loss of lives, as it could be experienced on several occasions during the last years. In this context, the research project KIWaSuS (AI-based warning system for heavy rain and urban flash floods) aims to increase the preparedness to such events by improving the accuracy of urban pluvial flood forecasts and, consequently, of flood warnings. In order to better inform the disaster management teams, an AI-based model for flood forecast was developed, which depicts the future situation with a high-resolution spatiotemporal sequence of flooding maps (Burrichter et al., 2023).

One of the inputs to the AI-based flood forecast model is the precipitation prediction over the study area in the city of Gelsenkirchen (Germany) for the upcoming hour. As the current precipitation nowcasting models cannot properly reproduce the dynamics behind the development of heavy rainfall events, an AI-model is being developed for precipitation nowcasting in the research project as well. Alike most models for precipitation nowcasting, radar images are used as input and the AI-based model must return the sequence of future radar images corresponding to one hour.

Radar data of the DX product of the German Weather Service (DWD) from the radar station Essen are corrected for clutter removal and signal attenuation effect, then converted into rain intensity values before being given to the AI-model as input. So that the AI-model can learn from selected historical heavy rainfall events, it must receive jointly with the input the corresponding label. For the label, DX-Offline data are used, which have a substantially higher quality than usual radar data. This dataset is extensively corrected, including correction with rainfall measurements of precipitation sensors, and is available for past radar data, covering the time period chosen for model training (2012 – 2019).

Deep learning architectures deriving from the area of image processing have shown to be applicable also to the problem of precipitation nowcasting. The most straightforward of these structures is an all convolutional network (Ayzel et al., 2019). In KIWaSuS, six Conv3D-layers totaling almost 300,000 parameters form the 3D-CNN model, which receives twelve radar images (one hour) as input to return the next twelve images for the predicted precipitation situation. Furthermore, two versions of an adapted U-Net (Ronneberger et al., 2015) architecture were tested. At first, a small U-Net with 16 Conv3D and three MaxPooling layers with twelve images as input was trained. It contains 16 filters in the first Conv3D layer, which amounts to circa 1.6 million parameters for the whole model. Then, a large U-Net with the same number of layers was tested. The difference between these U-Net models is that the second one has 64 filters in the first Conv3D and receives only six radar images as input, resulting in over 28 million parameters. Because all the three models need to forecast the next twelve radar images at once, this analysis aims to evaluate the influence of number of parameters and number of input images on the prediction accuracy for each time step and on the resultant hourly precipitation sum.

Figure 1 compares the ground truth (DX-Offline) with the forecasts of the U-Net models and of a Lagrangian Persistence nowcasting model (DenseRotation) for a heavy rainfall event with a return period of at least 100 years. This event would have triggered the highest warning level from DWD, as it surpassed 47 mm in one hour. The results with the 3D-CNN model are not shown here, because the model could not improve upon the forecast generated with the DenseRotation model.

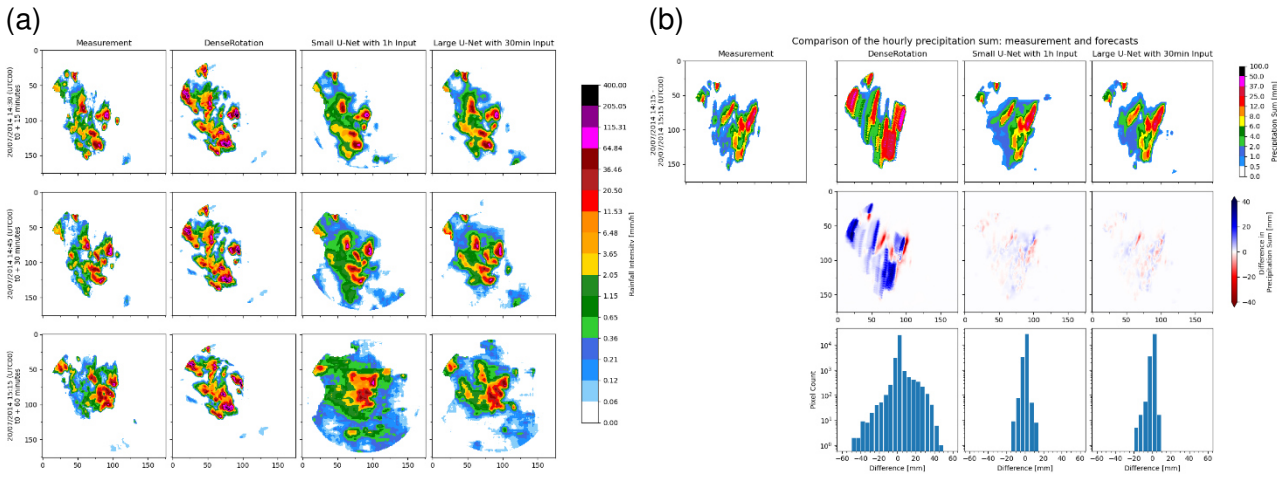

Fig 1: Comparison of the forecasts from two U-Net models and from a current usual precipitation nowcasting model with the radar measurements for a specific heavy rainfall event.

Among all tested models, the AI-models with a U-Net architecture can better predict the development of the heavy rainfall cells, even if a certain blurring effect can be perceived in their forecasts. The comparison between the small and the large U-Net models (Figure 1 (a)) indicates that the increase in the number of model parameters can reduce this effect, but also that the small U-Net can better predict pixels with relatively high rainfall intensities throughout the upcoming hour. This shows the influence of the number of input images on the forecast result. The large U-Net leads to lower overestimation in the hourly precipitation sum analysis (Figure 1 (b)), probably due to the more accurate prediction of cell contours. However, it leads to a larger underestimation of rainfall amounts in some regions compared to the smaller U-Net.

In conclusion, it is clear that the AI-models can outperform current nowcasting models based on Lagrangian Persistence. As long as a U-Net architecture is applied with an adequate minimum number of model parameters, the amount of radar images given as input seems to be more decisive for the precipitation prediction accuracy than the model size. For future model analyses and optimizations, the design with twelve radar images as input will, therefore, be maintained.

References

Ayzel, G., Heistermann, M., Sorokin, A., Nitikin, O., and Lukyanova O. (2019), All convolutional neural networks for radar-based precipitation nowcasting, Procedia Computer Science, 150, 186-192.

Burrichter, B., Hofmann, J., Koltermann da Silva, J., Niemann, A. and Quirmbach, M. (2023), A Spatiotemporal Deep Learning Approach for Urban Pluvial Flood Forecasting with Multi-Source Data. Water, 15(9), 1760.

Ronneberger, O., Fischer, P., and Brox, T. (2015), U-Net: Convolutional Networks for Biomedical Image Segmentation. In: Navab, N., Hornegger, J., Wells, W., Frangi, A. (eds) Medical Image Computing and Computer-Assisted Intervention – MICCAI 2015. MICCAI 2015. Lecture Notes in Computer Science(), vol 9351, 234-241. Springer, Cham.

Urbanization and climate change impacts on future convective precipitation in Milan, Italy

M. Koukoula*[1], H. Torelló-Sentelles[1], N. Peleg[1]

1 Institute of Earth Surface Dynamics, University of Lausanne, Switzerland

*Corresponding author: marika.koukoula@unil.ch

Abstract

Urbanization has experienced a rapid increase over the last fifty years with more than 50% of the world's population now living in cities. The amount of urban population is expected to further increase during the coming decades. Urbanization and the associated changes in land use/land cover can modify the temporal and spatial properties of precipitation. On top of that, global warming is expected to enhance the magnitude and frequency of short-duration heavy precipitation, with a consequential increase in flood hazards. Therefore, understanding how urbanization and climate change affect short-duration rainfall events is crucial for flood risk assessments and urban planning. To this end, we investigate the impact of climate change and urbanization on the space-time properties of precipitation by conducting current and future simulation scenarios over the city of Milan using the Weather Research and Forecasting (WRF) physically-based atmospheric model. The results of this study reveal that future urbanization will affect the temporal and spatial distribution of rainfall, while the combined effects of urbanization and climate change can alter significantly the structure of short-duration heavy precipitation events.

The relevance of radar rainfall on urban drainage dimensioning and performance

S. Krämer*[1], H. Leberke[1], M. Lindenberg[1], K. Maerker[2]

1 Institut für technische-wissenschaftliche Hydrologie GmbH, Germany
2 Umweltamt der Stadt Dresden, Germany

*Corresponding author: s.kraemer@itwh.de

Abstract

With the beginning of the systematic development of urban drainage systems, large numbers of rain gauges were installed in cities at an early stage in order to systematically record rainfall. Today it is known that rain gauge measurements already have high uncertainties on the order of ± 25% at the microscale level (Peleg et al 2013 among others).

The alternative are radar rainfall data, which are already available for periods of more than 20 years and thus have sufficient length from an extreme value statistics perspective for design practice. They also have a high spatio-temporal resolution which meets the requirements of urban drainage modelling. However, the quantitative accuracy of the processed radar data from the national meteorological services is not sufficient to use the radar rainfall data in rainfall-runoff models. They systematically underestimate the actual rainfall (Schleiss et al. 2020). The main cause is the attenuation of the radar signal induced by the precipitation itself, which is crucial in extreme rainfall for the relevant duration levels (D ≤ 60 min) and return periods (T ≥ 1 a). Table 1 shows the statistical rainfall heights as a function of duration and return period according to extreme value statistics of the German Weather Service (KOSTRA-DWD 2010R) for the city of Dresden and the associated specific attenuation for C-band frequencies. The shorter the duration level and the higher the return period the stronger is the influence of the attenuation. Note: due to the logarithmic scaling, an attenuation of 3 dB already includes a halving of the radar signal strength.

Tab 1: Statistical rainfall heights (h_N) in [mm] depending on duration [min] and return period [a] for the city of Dresden and specific attenuation (k) (one way) in [dB/km]

	Return period [a]								
Duration D	1 a	2 a	3 a	5 a	10 a	20 a	30 a	50 a	100 a
5 min	4.8 / 0.5	6.2 / 0.6	7.0 / 0.7	8.0 / 0.9	9.0 / 1.0	10.8 / 1.2	11.6 / 1.3	12.6 / 1.5	14.0 / 1.7
60 min	14.1 / 0.1	18.8 / 0.1	21.5 / 0.2	25 / 0.2	29.7 / 0.2	34.3 / 0.3	37.1 / 0.3	40.5 / 0.3	45.2 / 0.4

In order to meet the high urban hydrological requirements for data quality, the radar data have to be corrected in a two-step process. Following van de Beek (2016), the most important step involves a time-step correction of physical influences. These include: clutter removal, radome attenuation correction, radar signal attenuation correction, Z-R conversion, and a spatio-temporal interpolation. This correction is embedded in an ensemble-based approach to fit radar rainfall data to rain gauge observations in terms of a mean field bias correction factor. The advantage of this processing is the preservation and spatial reconstruction of rainfall structures through the attenuation correction without a bias due to uncertain rain gauge observations.

Using this methodology, a total of 210 design-relevant heavy rainfall events from the period 2000 - 2020 with a temporal resolution of 5 min and a grid resolution of 500 × 500 meters were processed for the Dresden urban area. The radar long term event time series was investigated both on the

rainfall side by extreme value statistics and on the runoff side under hydrodynamic simulation of the drainage system of the city of Dresden for the target variable surcharge of manholes.

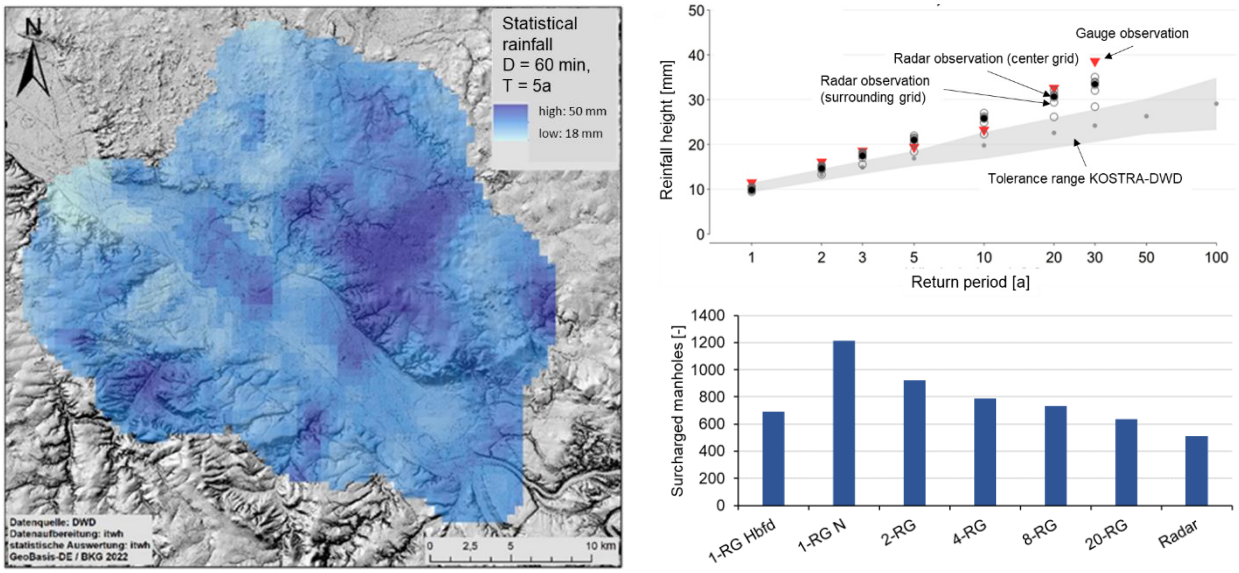

Fig 1: left: statistical radar rainfall heights for the Dresden area; right above: comparison of radar and gauge rainfall extreme value statistics based on partial times series; right bottom: surcharged manholes based on hydrodynamic simulation for the urban drainage system of the city of Dresden for different areal rainfall loads. Data basis: 210 rainfall events.

The results can be evaluated manifold and are summarized as follows:

- The extreme value statistical comparison according to (DWA-A 531) of radar and rain gauge heights depending on the duration and return period shows a plausible agreement and thus proves the validity of the chosen correction approach (Fig 1. right above).
- The spatial analysis of extreme value statistical rainfall heights on the radar grid level shows a pronounced small-scale variability (Fig. 1, left); the orographic influence of slope and valley locations is evident.
- The evaluation of areal precipitation starting from the maximum rainfall height of the rainfall structures shows on average over the 210 events already within a radius of less than 2 km a decrease of the relative rainfall height to 75% and up to 5 km a decrease to 50%.
- The choice of rainfall load for hydrodynamic verification of drainage system, here: Number of surcharged manholes for a surcharge frequency 1 in 3 years has a significant influence on the assessment of hydraulic performance. As the spatial resolution of rainfall information increases, the number of surcharged manholes decreases (Fig. 1, right bottom).

The results demonstrate the high relevance of radar rainfall data for hydraulic dimensioning and assessment of urban drainage system performance.

This research was part of the project *"Wildly Draining Water in Urban Areas"* (WAWUR), supported by the Federal Ministery for the Environment, Nature Conservation, Nuclear Safety and Consumer Protection.

References

Peleg N., Ben-Asher M., Morin E. (2013): Radar subpixel-scale rainfall variability and uncertainty: lessons learned from observations of a dense rain-gauge network. Hydrol. Earth Syst. Sci. 17. 2195–2208.

Schleiss M., Olsson J., Berg P., Niemi T., Kokkonen T., Thorndahl S., Nielsen R., Ellerbæk Nielsen J., Bozhinova D., Pulkkinen S. (2020): The accuracy of weather radar in heavy rain: a comparative

study for Denmark. the Netherlands. Finland and Sweden. Hydrol. Earth Syst. Sci. 24. 3157–3188. https://doi.org/10.5194/hess-24-3157-2020.

van de Beek C. Z., Leijnse H., Hazenberg P., Uijlenhoet R. (2016): Close-range radar rainfall estimation and error analysis. Atmos. Meas. Tech. 9. 3837–3850. https://doi.org/10.5194/amt-9-3837-2016.

Robustness evaluation of simulated extreme floods over Switzerland: an experiment based on weather generator changes

Eleni Kritidou[1], Martina Kauzlaric[2], Marc Vis[1], Maria Staudinger[1], Jan Seibert[1], Daniel Viviroli[1]

[1] Department of Geography, University of Zurich, Switzerland
[2] Institute of Geography and Oeschger Centre for Climate Change Research, University of Bern, Switzerland

*Corresponding author: eleni.kritidou@uzh.ch

Abstract

Floods are characterized as a high-impact natural hazard in Switzerland (Hilker et al., 2009, Weingartner et al., 2003) and they are responsible for considerable damage to property values, infrastructure and agricultural land (Hilker et al., 2009). Hence, reliable estimates of flood characteristics are a critical information for damage reduction and prevention measures. Some of the most common flood estimation methods rely on statistical techniques based on historical observations such as observed hydrographs or flood peaks. Therefore, the relatively short length of observational records available is a limiting factor for such extrapolation. In case that simulation approaches are used, assumptions about antecedent conditions of an event (e.g., soil moisture, snowpack, storage levels of lakes and reservoirs) and their distribution in space are usually necessary. This limits the scope of simulated floods that can develop from a causing precipitation event.

Here we explore the robustness of an estimation framework based on continuous simulations with a hydrometeorological modeling chain (Viviroli et al., 2022). The modeling chain starts with a multi-site stochastic weather generator that can well represent the entire spectrum of precipitation amounts but was developed with particular focus on extremely high precipitation events (Evin et al., 2018). Then, the bucket-type hydrological model HBV (Hydrologiska Byråns Vattenbalansavdelning) (Seibert and Vis, 2012) is used to simulate discharge time series. Finally, the hydrological routing model RS Minerve (García Hernández et al., 2020) is employed to implement simplified representations of river channel hydraulics, floodplain inundations as well as lake regulation and retention.

To investigate the robustness of the simulated results and derived flood estimates, we select the potentially most sensitive elements of the weather generator and the hydrological model and vary them across a plausible range. For the weather generator, the chosen elements are three: precipitation distribution, precipitation lapse rates, and weather types. The first robustness experiment tackles the parameterization of the Extended Generalized Pareto Distribution (EGPD) that is used to describe precipitation intensities. Ten different EGPD parameterizations generated by a bootstrapping method serve to create 10 different 30'000 year-long realizations of the weather generator, which are in turn used as input to the hydrological modelling and routing. The second experiment aims at testing five different precipitation lapse rates ranging from 0 to 10% per 100 m elevation (0%, 2.5%, 5%, 7.5% and 10%). The third experiment tackles a parameterization of the weather generator on four weather types.

Considering a set of large (area more than ~450 km²) study catchments in Switzerland, we show how the changes to the weather generator's sensitive elements influence the simulated extreme floods and thus assess the robustness of the approach.

Further robustness experiments will concern the hydrological model: A slightly modified model structure will be tested that describes the catchment response function in a different way. Also, the

model-internal precipitation lapse rates will be varied within 0–10% per 100 m elevation. These internal lapse rates redistribute the mean catchment precipitation input from the weather generator to the different elevation zones.

The robustness experiments will shed light on the reliability of the hydrometeorological modeling chain for estimating very rare floods in Switzerland and help point out benefits and limitations of the continuous simulation approach. The findings will provide an important basis for follow-up studies related to hazard assessment, safety analyses and hydraulic engineering projects since they are expected to identify sensitive modeling decisions.

References

Evin, G., Favre, A.-C., Hingray, B. (2018). Stochastic generation of multi-site daily precipitation focusing on extreme events. *Hydrology and Earth System Sciences*, 22(1), 655–672. https://doi.org/10.5194/hess-22-655-2018

García Hernández, J., Foehn, A., Fluixá-Sanmartín, J., Roquier, B., Brauchli, T., Paredes Arquiola, J. & De Cesare, G. (2020). RS MINERVE – Technical manual, v2.25, CREALP, Sion, 156 pp. https://crealp.ch/wp-content/uploads/2021/09/rsminerve_technical_manual_v2.25.pdf (last access: 31 May 2023).

Hilker, N., Badoux, A., & Hegg, C. (2009). The Swiss flood and landslide damage database 1972–2007. *Natural Hazards and Earth System Sciences*, 9(3), 913–925. https://doi.org/10.5194/nhess-9-913-2009

Seibert, J. & Vis, M. J. P. (2012). Teaching hydrological modeling with a user-friendly catchment-runoff-model software package. *Hydrology and Earth System Sciences*, 16(9), 3315–3325. https://doi.org/10.5194/hess-16-3315-2012

Viviroli, D., Sikorska-Senoner, A. E., Evin, G., Staudinger, M., Kauzlaric, M., Chardon, J., Favre, A.-C., Hingray, B., Nicolet, G., Raynaud, D., Seibert, J., Weingartner, R. & Whealton, C. (2022). Comprehensive space-time hydrometeorological simulations for estimating very rare floods at multiple sites in a large river basin. *Natural Hazards and Earth System Sciences*, 22(9), 2891–2920, https://doi.org/10.5194/nhess-22-2891-2022

Weingartner, R., Barben, M., & Spreafico, M. (2003). Floods in mountain areas – An overview based on examples from Switzerland. *Journal of Hydrology*, 282(1–4), 10–24. https://doi.org/10.1016/S0022-1694(03)00249-X

Convective environment in ALADIN Reanalysis

R. Kvak *[1], P. Zacharov [1], M. Vokoun[1]

1 Institute of Atmospheric Physics, Prague, Czech Republic

*Corresponding author: petas@ufa.cas.cz

Abstract

In the framework of the national project PERUN (Prediction, Evaluation and Research for Understanding National sensitivity and impacts of drought and climate change for Czechia), new ALADIN (Aire Limitée, Adaptation Dynamique, Development International) reanalyses are now available for evaluation purposes. The reanalyses employ boundary conditions from the European reanalysis ERA5, the first reanalysis using an assimilation of various meteorological parameters every six hours. The reanalysis domain covers Europe with a horizontal resolution of 2.3 km. In the presented study, the area of the Czech Republic is primarily chosen as the evaluation domain.

The reanalysis contains, among other things, outputs describing convective environments in the period of 30 years (1990–2019). The aim of this work is the evaluation of CAPE (Convective Available Potential Energy), CIN (Convective INhibition) and wind shear, which can be considered key parameters for the formation of convective clouds and precipitation. The obtained data are assessed from the perspective of the most common temporal and spatial characteristics. Moreover, the study verifies the reanalysis data by sounding data, at least from the meteorological station in Prague–Libus. As an example, a fair agreement of MUCAPE (Most Unstable CAPE) values is shown in Table 1. In addition to precipitation totals, the outputs distinguish between their convective and stratiform origins, which are studied herein as well.

Tab 1: Contingency table of MUCAPE values from the Prague–Libus sounding measurement (rows) and ALADIN reanalysis (columns).

MUCAPE [J kg^{-1}]		**ALADIN/Reanalysis**		
		0–100	**100–500**	**≥500**
PRAGUE–LIBUS	**0–100**	**27579**	2618	386
	100–500	792	**2162**	1128
	≥500	61	300	**1802**
HIT = 85.6 %		**OVEREST. = 11.2 %**		**UNDEREST. = 3.1 %**

The presented results will be compared with the ALADIN climate model for the period 2025–2100. The model run employs boundary conditions from the climate model CMIP6 with the scenario SSP5-8.5, where emissions follow the worst-case pathway until 2040, among other emission scenarios.

Private sensors and crowdsourced rainfall data: accuracy and potential for modelling pluvial flooding in urban areas

K. Kyaw[1*], E.Baietti [1], C. Lussana [2], V. Luzzi[3], P. Mazzoli [3], S. Bagli [3], A. Castellarin [1]

1 DICAM, University of Bologna, Italy.
2 Norwegian Meteorological Institute, Oslo, Norway.
3 GECOsistema Srl, 47521 Cesena, Italy.

*Corresponding author: kaykhaing.kyaw2@unibo.it

Abstract

The increasing frequency of cloudbursts and extreme rainstorms combined with high population densities and soil sealing make urban areas particularly vulnerable to pluvial flooding. Pluvial flood occurs when the rainfall rate exceeds the capacity of storm water management systems and/or the infiltration capacity of the soil. This is usually associated with short-duration precipitation events (of up to three hours) and with rainfalls that exceed 20-25 mm per hour (Prokic et al. (2019)). Accurate spatial representation of these natural phenomena is crucial. Privately owned weather stations are steadily increasing, sometimes significantly higher than the number of weather services sensors, and their distribution follows population density. As a result, private rain gauging networks offer valuable crowdsourced data for high-resolution rainfall fields in urban areas.

Our contribution is twofold. First, we assess the accuracy of hourly rainfall data collected by Netatmo private sensors relative to data from the official gauging network of Norway, Sweden, Finland, and Denmark. Traditional weather stations are taken as a reference to explore the quality of the unconventional network measurements. Subsequently, we compare data collected at referenced rain gauges with the data collected at the nearest crowdsourced station within a search radius of 1000 m (red line), 3000 m (green line), and 5000 m (blue line), as illustrated in Figure 1. The comparison proved the value of crowdsourced data for correctly detecting events, and their generalized tendency to underpredict rainfall amount.

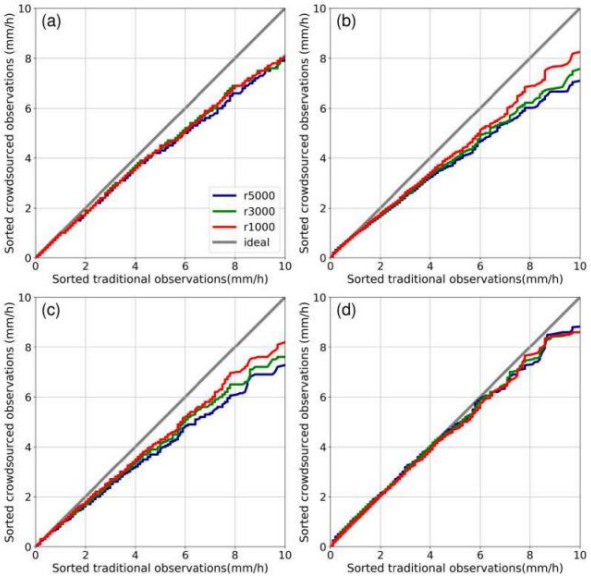

Fig 1: Comparison between the nearest neighbor and different aggregations methods estimates. a) nearest neighbor; b) mean; c) median; d) 75th percentile.

Second, we focus on two localized pluvial flood events in Oslo that occurred in June and August 2019. These events, caused by convective storms, were not predicted by weather forecasts, and there remains high spatial uncertainty for such small-scale events. Our study utilizes three rainfall data sources: official rain gauges from MET Norway's public databases, crowdsourced observations from Netatmo private sensors, and weather radar data from the Norwegian Meteorological Institute. We feed these data into simplified DEM-based and 2D physically based numerical inundation models. Safer RAIN is a simplified and fast-processing DEM-based method which is capable to map flooding in large areas and was originally proposed for pluvial flooding hazard assessment and mapping (Samela et al. (2020)). Since the Rain-on-Grid (RoG) approach is becoming popular in storm risk management and works well in HEC-RAS 2D, we chose to apply it in our research. We employed another numerical inundation model called UnTRIM. UnTRIM is a semi-implicit finite difference (or finite volume) model that is based on shallow water equations and is specifically designed to operate on grid-based systems (Casulli, V. (1990)).

Our initial finding reveals significant variability in the flooded area, depending on the models and rain data sources utilized. We focus on flood hotspot areas reported in online news, employing a 5cm threshold for flooding. Figure 2 illustrates the flood maps in one hotspot region using rainfall scenarios. Overall, our results show that (1) private sensors have very good skills in rain detection but tend to underestimate the reference value up to ~25%, (2) concerning the simulated inundation maps, rainfall fields derived from bias-corrected crowdsourced rainfall data may be significantly more accurate than those generated from official rain gauges, and as accurate as the fields resulting from the combination radar and official rain gauges data.

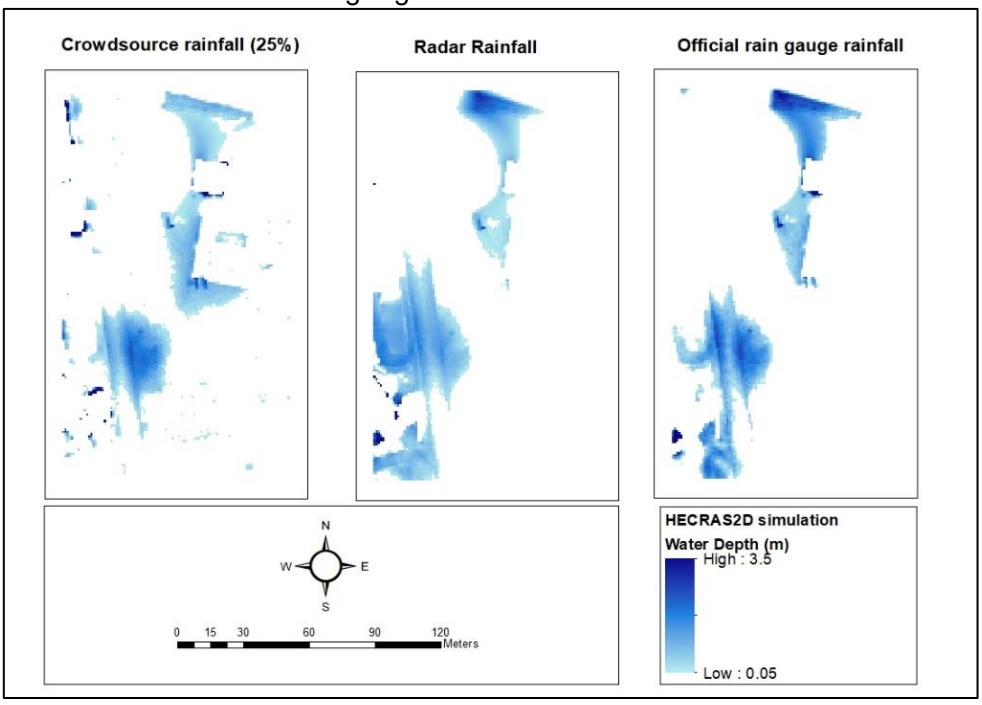

Fig 2. HECRAS 2D flood inundation maps in hotspot area (Mariedalsveien street) during the pluvial flood event on 26th June ,2019.

References

Casulli, V. (1990). Semi-implicit finite difference methods for the two-dimensional shallow water equations. Journal of Computational Physics, 86(1), 56-74

Prokic, M. N., Savić, S., & Pavić, D. (2019). Pluvial flooding in urban areas across the European continent. Geographica Pannonica, 23(4).

Samela, C., Persiano, S., Bagli, S., Luzzi, V., Mazzoli, P., Humer, G., ... & Castellarin, A. (2020). Safer_RAIN: A DEM-based hierarchical filling-&-Spilling algorithm for pluvial flood hazard assessment and mapping across large urban areas. Water, 12(6), 1514.

Streamlining the use of weather radar data for Urban run-off simulation

R. Laursen*[1], N.E. Jensen[2], M.K.S. Ahm, Y.M. Jesuloganathan[3]

1 VeVa, Denmark
2 Furuno Denmark A/S, Denmark
3 Aarhus Water, Denmark

*Corresponding author: nej@furuno.dk

Abstract

VeVa - Vejrdata i Vandsektoren is a Danish organization dedicated to providing weather data solutions for the water sector. VeVa's core activities revolve around the collection, analysis, and dissemination of weather-related data, primarily radar data, enabling water management authorities and utility companies to make informed decisions and enhance their operational practices based on easily accessible precipitation data.

Accurate estimation of precipitation is crucial for understanding the relationship between rainfall and runoff. It enables effective management and regulation of drainage systems and wastewater treatment plants during intense rainfall, mitigating flood damages and preventing water quality issues. VeVa have developed a real-time processing chain that pump real-time radar images from weather radars like the FURUNO WR-2120 to the cloud for processing (see Figure 1 VeVa processing chain)

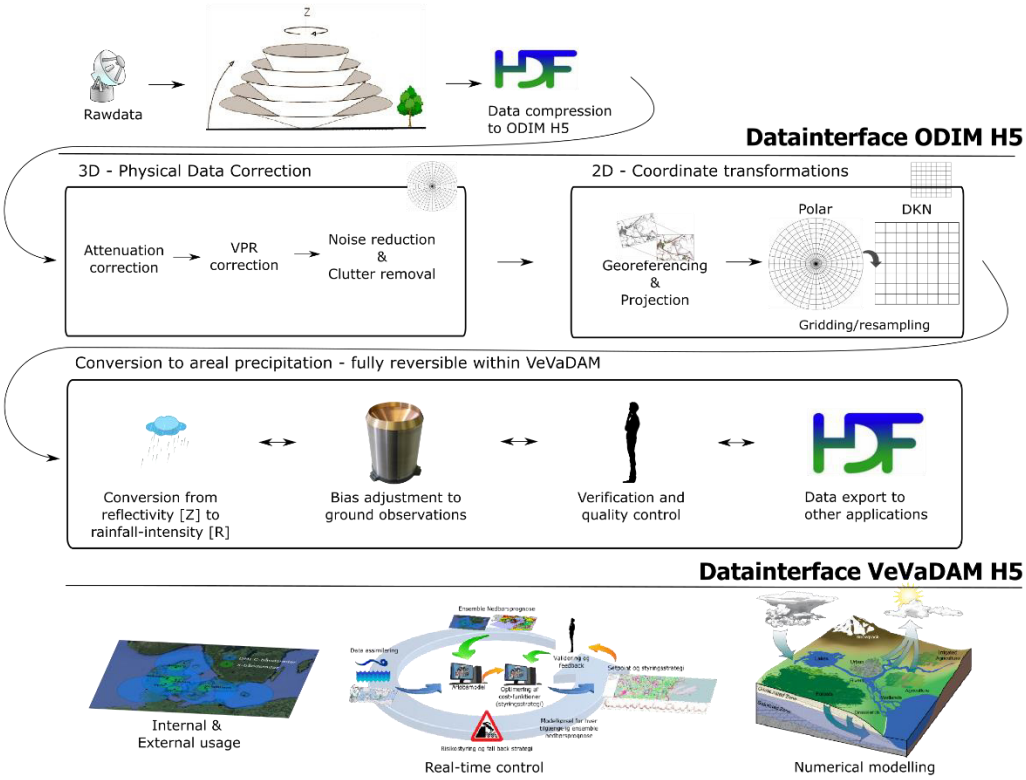

Figure 1. VeVa processing chain

The utility companies may then retrieve pCAPPI clutter reduced and bias adjusted precipitation images directly from the Amazon Cloud. The pCAPPI may then be combined with catchment shape files from the modelling tool to produce 2-D catchment rainfall in dfs2 file format useable for real-time runoff forecasting and project planning.

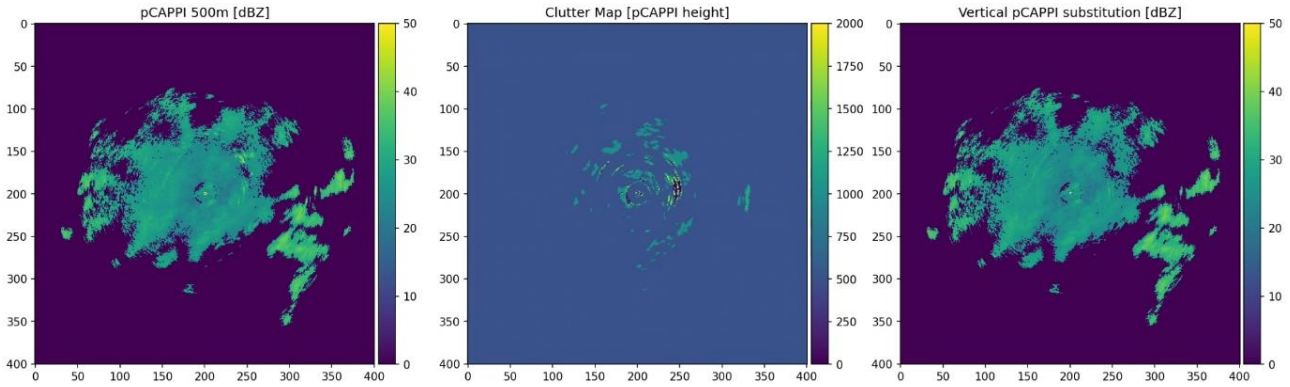

Figure.2 VeVa clutter reduction.

References

Ahm, M. Adjustment of rainfall estimates from weather radars using in-situ stormwater drainage sensors, Department of Civil Engineering, Aalborg University.

Einfalt, T., Arnbjerg-Nielsen, K., Golz, C., Jensen, N.-E., Quirmbach, M., Vaes, G., Vieux, B. (2004) Towards a roadmap for use of radar rainfall data in urban drainage. Journal of Hydrology, 299(3–4), 186–202. DOI: http://dx.doi.org/10.1016/j.jhydrol.2004.08.004.

Rasmussen, M. R., Thorndahl, S., Grum, M., Neve, S., Borup, M. (2008) Vejrradarbaseret styring af spildevandsanlæg, København.

Schilling, W. (1991) Rainfall data for urban hydrology: what do we need? Atmospheric Research, 27(1–3), 5–21. DOI: http://dx.doi.org/10.1016/0169-8095(91)90003-F.

Thorndahl, S., Rasmussen, M. R., Neve, S., Poulsen, T. S., Grum, M. (2010) Vejrradarbaseret styring af spildevandsanlæg II. DCE Technical Report, 95(95), Aalborg University, Denmark.
MIKE for developers docs (https://docs.mikepoweredbydhi.com/core_libraries/dfs/dfs-file-formats/)

A comprehensive evaluation of applicability of Poisson cluster rainfall generators for planning and operation of urban drainage system in Switzerland

Taiqi Lian[1], Dongkyun Kim[2], Jörg Rieckermann[1]*, Lauren M.Cook[1],

1 Department of Urban Water Management, Swiss Federal Institute for Aquatic Research, Dübendorf, Switzerland
2 Department of Civil Engineering, Hongik University, Seoul, South Korea

*Corresponding author: joerg.rieckermann@eawag.ch

Abstract

The performance of sewer systems, both in terms of flood safety and discharges into water bodies during rainfall, should be checked with long-term rainfall data (Bárdossy, et al., 2020). Unfortunately, in Switzerland, long and reliable rainfall data are only available at very few sites in Switzerland. One solution could be to use stochastic rainfall generators to predict synthetic precipitation time series (Egger & Maurer, 2015, Molnar and Burlando, 2005). In this contribution we present the first results from Eawag's "Future Rainfall" project, where we aim to generate synthetic rainfall for the current climate. Once successful, this should be extended for the downscaling of future climate scenarios.

To generate synthetic rainfall, we use a modern rainfall generator (Kim & Onof, 2020), which uses a stochastic Lewis-Bartlett Poisson process, i.e. a Bartlett-Lewis Rectangular Pulse (BLRP) Model, to predict the patterns of precipitation from characteristic arrival times of rain events, durations, etc. BLRP models are attractive because they can reproduce rainfall statistics over several time scales.

In this work, we modified the original BLRP generator by implementing state-of-the-art suggestions from literature and adjustments of the statistical properties (Table 1). Also, similar as in the SYNOPSE project (Bárdossy, et al., 2020), we not only evaluate the performance of the different generators on i) rainfall statistics, but also on ii) urban rainfall runoff characteristics. The latter was assessed for three typical urban drainage applications: combined sewer overflows, flooding, and blue-green infrastructures (BGI). We predict synthetic rain series with a temporal resolution of 10 minutes for 39 MeteoSwiss stations in Switzerland that have over 40 years of observation data.

Our results suggest that, in general, the generators can be adapted well to existing precipitation data, so that they can reproduce the essential characteristics of both rain (Figure 2a) and urban runoff (Figure 2b). Unfortunately, no single generator "works" well for all target variables from combined sewer overflows to assessing flood risk and the performance of BGI, because the errors for some specific performance metrics are still very large.

Table 1: Summary of modifications and candidate generators

ID	Description
Origin	Original model (Kim D. & Onof C., 2020)
SOA	Original model updated to the state-of-the-art with (1) an optimization technique, the Iteration Downhill Simplex method, (2) a sinusoidal pulse shape for rain cells, and (3) a new objective function
Mean10	Mean adjustment in calibration process
Skew25	Skewness adjustment in calibration process
Select	Select 50% wettest year as bias input data to model
P60	Introduce P factor to increase weight of skewness in calibration process
Comb	Combine the generated synthetic rainfall from the Mean10 generator and the P60 generator

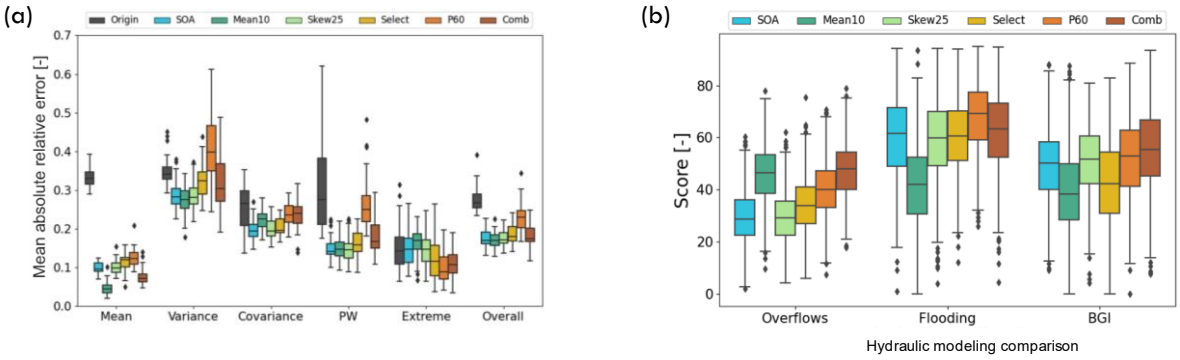

Fig 2: (a) Comparison of generators on rainfall statistics. (b) Overall results for all generators in reproducing modelled runoff regarding i) combined sewer overflows, ii) flooding and iii) BGI performance using a custom performance score (higher scores describe a better performance). The uncertainty range is generated by 1000-fold bootstrapping. Overall, it can be said that the generators adapt relatively well to existing rainfall data. Unfortunately, no single generator "works" well for all target variables from stormwater runoff management to assessing flood risk.

Specifically, the **Mean10** generator performs well in reproducing precipitation statistics and simulated combined sewer overflows but falls short in representing flooding behavior and stormwater retention. The **P60** generator excels in these areas but struggles regarding rainfall statistics. The **Comb** generator combines the advantages of the two generators regarding modelled rainfall-runoff, but still contains the disadvantages of the P60 generator. Thus, its predictions for medium durations from days to weeks are rather uncertain (not shown).

The **SOA** generator, with its functional improvements, demonstrates strong performance across all metrics for rainfall characteristics as well as for rainfall-runoff metrics. Its relative performance compared to modified candidate generators highlights that optimizing performance in one area often is only possible at the expense of another. In our view, this emphasizes the need to assess our rain generators based on their suitability for rainwater management and hydraulic performance in urban water management applications, rather than solely relying on their ability to describe observed rain.

As expected, the BLRP models are structurally extremely flexible and often estimate substantially different parameters for similar rainfall series. Therefore, future work should focus, among other things, on reliable inference. This could possibly be achieved through regularization, e.g. by accounting for spatial dependencies. The long-term goal of this work would be to downscale future predictions of climate models to provide the best available knowledge to urban drainage practitioners.

References

Bárdossy, A., Birkholz, P., Eisele, M., Fangmann, A., Fuchs, L., Haberlandt, U., Sympher, K.-J. (2020). Synthetische Niederschlagszeitreihen für die optimale Planung und den Betrieb von Stadtentwässerungssystemen II. Hannover: Leibniz Universität Hannover.

Egger, C., & Maurer, M. (2015). Importance of anthropogenic climate impact, sampling error and urban development in sewer system design. Water Research(Volume 73), S. 78-97. doi:https://doi.org/10.1016/j.watres.2014.12.050

Heim, C., Hentgen, L., Ban, N., & Schär, C. (2020). Simulation of subtropical marine stratocumulus clouds in convection-resolving models. EGU General Assembly. doi:https://doi.org/10.5194/egusphere-egu2020-9123

Kim, D., & Onof, C. (2020). A stochastic rainfall model that can reproduce important rainfall properties across the timescales from several minutes to a decade. Journal of Hydrology(Volume 589). doi:https://doi.org/10.1016/j.jhydrol.2020.125150
Molnar, P., Burlando, P., 2005. Preservation of rainfall properties in stochastic disaggregation by a simple random cascade model. Atmospheric Research, Precipitation in Urban Areas 77, 137–151. https://doi.org/10.1016/j.atmosres.2004.10.024
Sideris, I. V., Gabella, M., Erdin, R., & Germann, U. (2014). Real-time radar–rain-gauge merging using spatio-temporal co-kriging with external drift in the alpine terrain of Switzerland. Quarterly Journal of the Royal Meteorological Societ, S. 1097-1111. doi:https://doi.org/10.1002/qj.2188

Sub-grid peaks in localized intense rain events using high-resolution operational radar data in Switzerland

Adrien Liernur*[1,2]; Marco Gabella[2]; Urs Germann[2], Alexis Berne[1]

1 Environmental Remote Sensing Laboratory, École Polytechnique Fédérale de Lausanne, Switzerland
2 MeteoSwiss, Locarno-Monti, Switzerland

*Corresponding author: adrien.liernur@epfl.ch

Abstract

Localized intense rain events can cause significant societal and economic damages. Their accurate identification is key in order to best mitigate their impacts on people and infrastructures. By collecting distributed space-time observations, weather radars can provide useful information for the analysis and forecasting of such events. In Switzerland, five operational dual-polarization C-band radars are scanning the atmosphere with a half-power beam-width of 1 degree up to a height of 18 km, using 20 interleaved sweeps that are updated every 5 minutes. Data are generated at a native radial resolution of 83 m (Germann et al., 2022). This information is then integrated at 500 m combining all clutter-free 83-m gates and quality-checked before being used in subsequent product chains. This integration may smooth out peaks of those localized intense rain events and, the information from high-resolution radar data might become valuable as complementary information to existing products. Small-scale spatial variability can indeed be quite significant in the context of extreme rainfall (e.g. Peleg et al., 2018).

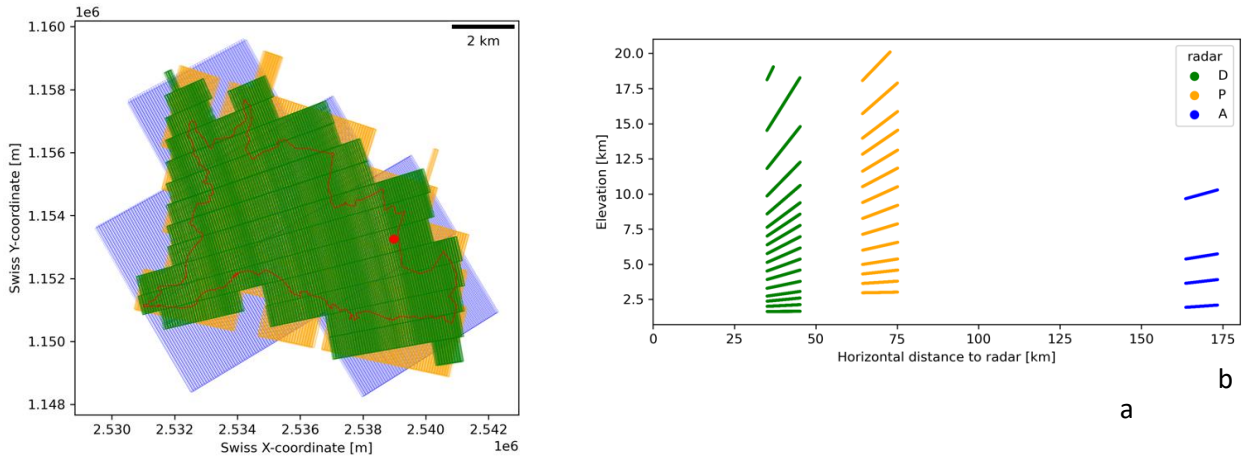

Fig 1: Top view (a) and side view (b) of the selected gates at high-resolution (83 m) from the three closest radars – La Dôle (D), Plaine Morte (P) and Albis (A) – spatially overlapping with the Lausanne catchment (red polygon). In (a), the Lausanne rain gauge is also displayed (red dot).

In this study, we analyze how the spatial integration of the native radar data at coarser polar radial resolutions of 500 m and 1000 m influences the captured spatial variability of rainfall peaks. We investigate the potential added information that would result from the use of high-resolution data for the analysis of such localized intense rain events. We focus on a case-study from June 11, 2018 when a localized intense rain event hit the city of Lausanne causing significant damages and leading to the largest 10-min rainfall accumulation ever recorded by the Swiss rain gauge network (41 mm) and was associated with reflectivity values up to 60 dBz at 83 m. The analyses are conducted in the 3D space by selecting the radar gates at the native resolution that spatially

overlap with the catchment of interest. Fig 1 displays the selected gates overlapping with the catchment of Lausanne for the three closest radars and highlights the spatial distribution of the native data across the horizontal (Fig 1a) and vertical (Fig 1b) dimensions. We quantify the impact of the spatial integration by successively averaging all selected clutter-free high-resolution native data to the coarser 500 m and 1000 m radial resolutions, and then downscaling the integrated data back to the same 83 m resolution. We compare the native data with the integrated-downscaled ones at different timesteps and elevations, and we apply a single Z-R relationship ($Z=316R^{1.5}$) to derive a corresponding "equivalent" rain rate at the gate level for the different spatial resolutions.

Preliminary results indicate that the difference between the rain estimates at the native resolution and after integration to 500 m and 1000 m exhibits a strong spatial and temporal variability. By selecting gates with high reflectivity values (i.e. native reflectivity > 50 dBz), about 2% of the gates show differences of more than 50 mm/h between the "equivalent" rain rate estimated at 83 m and at 500 m resolution. Looking at the ratio between the "equivalent" rain rate at 83 m and at 500 m, about 19%, 5% and 0.3% of the selected gates have a rain rate at 83 m that is respectively 1.25, 1.5 and 2 times larger than the integrated one at 500 m. These values vary over the different 5-min timesteps as a function of the event intensity. Looking at the most intense 5-min timestep of the event (i.e. 21:00 UTC), Fig 2 displays the equivalent rain rate difference (y-axis) and the equivalent rain rate ratio (x-axis) together with the equivalent rain rate as computed from the native data. It can be seen that the largest differences (y-axis) are generally observed at gates with the highest intensity values. A similar but amplified behavior is observed at the 1000 m resolution, due to the largest number of gates being averaged. Despite the limitations associated to the application of a Z-R relationship independently of the drop size distribution and hydrometeor types, these differences already provide initial indications on the added value of high-resolution radar data for the analysis of those localized intense rain events. Given the non-linearity of many hydrological processes and runoff generation mechanisms across space, such differences in rainfall peaks and spatial variability can play a key role on flooding processes and related damages.

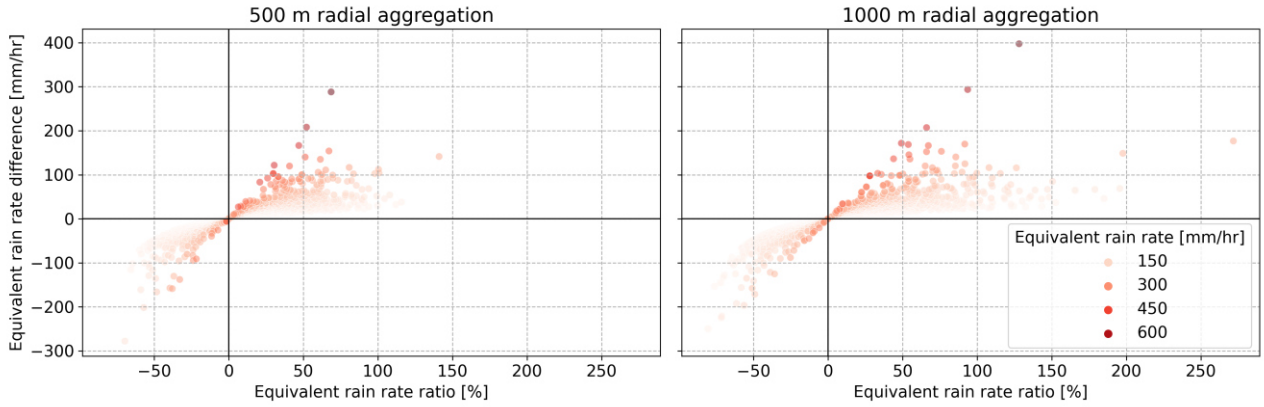

Fig 2: Equivalent rain rate difference and equivalent rain rate ratio between the native data and the integrated-downscaled data over the most intense 5-min timestep (i.e. 21:00 UTC) of the Lausanne event for both 500 m (right) and 1000 m (right) radial aggregations. The data points correspond to the gates displayed in Fig 1a filtered for clutter removal and with reflectivity larger than 50 dBz. The color scale corresponds to the equivalent rain rate as estimated from the native data.

References

Germann, U., Boscacci, M., Clementi, L., Gabella, M., Hering, A., Sartori, M., Sideris, I. V., and Calpini, B. (2022). Weather Radar in Complex Orography. Remote Sensing, 14(3), 503.

Peleg, N., Marra, F., Fatichi, S., Paschalis, A., Molnar, P., & Burlando, P. (2018). Spatial variability of extreme rainfall at radar subpixel scale. Journal of Hydrology, 556, 922–933.

Mean Areal Precipitation simulation with GWEX-MRC, a hybrid WGEN combining daily generation and disaggregation with a Multiplicative Random Cascade

K. Maloku*[1], G. Evin[1], B. Hingray[1]

1 Univ Grenoble Alpes, CNRS, INRAE, IRD, Grenoble INP, IGE, 38000 Grenoble, France

*Corresponding author: kaltrina.maloku@univ-grenoble-alpes.fr

Abstract

Continuous hydrometeorological simulation is a powerful approach to estimating design discharges for ungauged catchments. For small catchments mean areal precipitation (MAP) scenarios with a high temporal resolution, e.g. hourly, are usually required.

For the stochastic generation of long time series of such scenarios, one approach consists on nesting stochastic weather generators (WGENs) that perform well at different temporal scales, i.e. a daily WGEN for the generation of daily time series with a stochastic disaggregation method for their disaggregation to high temporal resolution (e.g. Paschalis et al., 2014).

For the generation of daily scenarios, we use a single-site simplification of GWEX, a multi-site stochastic WGEN able to generate daily scenarios of precipitation focused on the reproduction of extreme events (Evin et al., 2018; Viviroli et al., 2022). Occurrences and precipitation depths are modelled independently. At-site occurrences are modelled with Markov chains of order 2 to 4 and the spatial structure of occurrences is represented by an unobserved Gaussian process. The E-GPD distribution, Naveau et al., 2016, is used to model daily precipitation amounts. This distribution has been found successful in reproducing intensities of any range, including extreme ones.

Then, high-resolution MAP are obtained by disaggregating daily amounts through a Multiplicative Random Cascade (MRC) model. We consider an analytical approach to model the distribution of the cascade generator. It offers an important parsimony in comparison to empirical MRC models, while still providing the possibility to model the dependency of the cascade generator on different factors, Maloku et al., 2023. In our work, the MRC model accounts for the dependency of the cascade generator on the season, precipitation intensity and asymmetry. To model the dependency to asymmetry, we introduce a precipitation asymmetry index which allows the characterization of the local asymmetry of precipitation, i.e. of the $\{R_{t-1}, R_t, R_{t+1}\}$ sequence of precipitation amounts around the precipitation to disaggregate, R_t. Accounting for the precipitation asymmetry enables an essential improvement in reproducing all statistics related to precipitation persistency, a well-known challenge of MRC models.

In this work, we evaluate the possibility of using this hybrid WGEN, combining GWEX+MRC, to simulate hourly MAP time series at different spatial scales, ranging from 10 to 1000 km^2, for small catchments in Switzerland. For this, we use the gridded precipitation dataset CombiPrecip, a reanalysis product of radar measurements and at-site records, covering the whole of Switzerland with a spatial resolution of 1 km^2 and a temporal resolution of an hour.

This work is part of the EXCH Swiss project " Extreme discharge scenarios for small catchments in Switzerland", funded by the Swiss Federal Office of Energy and Water (Viviroli et al., 2022).

References

Evin, G., Favre, A.-C., and Hingray, B.: Stochastic generation of multi-site daily precipitation focusing on extreme events, Hydrol. Earth Syst. Sci., 22, 655–672, https://doi.org/10.5194/hess-22-655-2018, 2018.

Maloku, K., Hingray, B., and Evin, G.: Accounting for Precipitation Asymmetry in a Multiplicative Random Cascades Disaggregation Model, EGUsphere [preprint], https://doi.org/10.5194/egusphere-2023-544, 2023.

Naveau, P., Huser, R., Ribereau, P., and Hannart, A. (2016), Modeling jointly low, moderate, and heavy rainfall intensities without a threshold selection, *Water Resour. Res.*, 52, 2753– 2769, doi:10.1002/2015WR018552.

Paschalis, A., Molnar, P., Fatichi, S., Burlando, P., 2014. On temporal stochastic modeling of precipitation, nesting models across scales. Advances in Water Resources 63, 152–166. https://doi.org/10.1016/j.advwatres.2013.11.006.

Viviroli, D., Sikorska-Senoner, A. E., Evin, G., Staudinger, M., Kauzlaric, M., Chardon, J., Favre, A.-C., Hingray, B., Nicolet, G., Raynaud, D., Seibert, J., Weingartner, R., and Whealton, C.: Comprehensive space–time hydrometeorological simulations for estimating very rare floods at multiple sites in a large river basin, Nat. Hazards Earth Syst. Sci., 22, 2891–2920, https://doi.org/10.5194/nhess-22-2891-2022, 2022.

Hershfield rainfall sampling adjustment factors: A review of existing methods and a unified proposal for engineering practice

Claudio I. Meier[1*], Patricio Muñoz-Proboste[1], Apeksha Marasini[1], Nischal Kafle[1], and Francesco Dell'Aira[1]

1 Department of Civil Engineering, The University of Memphis, Memphis, Tennessee, USA

*Corresponding author: cimeier@memphis.edu

Abstract

The well-known precipitation Intensity-Duration-Frequency (IDF) or Depth-Duration-Frequency (DDF) values are used by engineers and scientists to understand extreme rainfall at a point-scale location. For any duration of interest, they represent the value of rainfall (intensity or depth) that can be expected to be equalled or exceeded with a certain frequency. The latter is typically given as some type of average interarrival time, which can be either a return period T, if the frequency analysis is performed for annual maxima, or else an average recurrence interval ARI, when using partial-duration (also known as peaks-over-threshold) series. The literature contains many studies on how to perform such procedures, either for specific stations or else as regional frequency analyses.

For the storm durations of interest to engineers designing urban stormwater infrastructure, which range from a few minutes to a few hours, it is clear that the IDF-DDF values must be derived analyzing rainfall maxima obtained from data collected with "continuously measuring" raingages. However, there is an issue with such data: due either to the technology of different types of raingages, or else to considerations of data storage, most rainfall records are not truly continuous, but are instead totalized or aggregated. This means that they only contain information about the rain depths that fell over fixed (also called clock, or constrained) time durations, e.g., between 9:00 and 9:10, from 9:10 to 9:20, and so on. Because of this, when we are interested in short rainfall durations, in the same order of magnitude as the raingage or datalogger resolution (say, we want to determine how much it can rain in the 20 minutes that it rains the most, with data that are themselves totalized every 10 minutes), we cannot know the actual maxima in continuous time, i.e., for sliding or unconstrained time windows, but must instead use fixed, clock, or constrained windows.

It is evident that this issue always introduces a negative bias or underestimation, as information about the actual maxima is lost due to totalization. It is only recently, within the last 10 to 15 years at most, that the meteorological agencies of some developed countries have installed modern raingages, typically at a high resolution of 1 min, which can be basically considered to be continuous. This means in turn that most of the rainfall maxima that were used to compute the IDF-DDF that we use at present actually came from totalized rainfall data. How were these biased, "fixed maxima" converted into rainfall values that are closer to the actual, unconstrained maxima?

The traditional engineering solution to this problem has been to use the so-called rainfall sampling adjustment factors (SAFs), also referred to as Hershfield factors, as he was the first person to propose their use in the 1950s. These correction factors can only be derived at locations which have raingages with a higher temporal resolution, so that rainfall maxima can be extracted using sliding time windows which are closer to continuous, allowing then to compare with maxima extracted from the same data, but totalized. Typically, SAFs are then assumed to be applicable at other locations, or even universally. SAFs are multiplicative correction factors: The clock or constrained maxima extracted from totalized data are simply multiplied by a constant number, larger than 1, in order to obtain their corresponding sliding or unconstrained equivalents, which are

then considered to be the actual maxima in continuous time, that are then used to determine IDF-DDF values. The most well-known SAFs are the 60-min rainfall (actual maximum, in continuous time) to 1-hr rainfall (fixed maximum, for clock durations), as well as the 24-hr rainfall to daily rainfall, which have been both found to be about 1.13 at many locations on Earth. Note that both these SAFs are for a sampling ratio of one, i.e., the duration of interest is equal to the totalization time. The previous example using 10-min data to determine the 20-min maximum would correspond to a sampling ratio of 2, as in that case the duration of interest was twice the raingage resolution or totalization period.

A detailed literature review reveals that there are several important issues and research gaps with the way we determine and apply SAFs in current engineering practice: (i) different authors have used varied procedures to compute them, without performing comparative analyses, (ii) no one has looked at the uncertainty or variability of SAFs at a given location, (iii) as currently used, SAFs are determined as a mean or central tendency value, and across multiple locations, without considering their spatial variability, and (iv) nobody has considered how the uncertainty of SAFs affects the resulting predictions of extreme rainfall.

In this work, we use more than 800 German stations with basically continuous rainfall data (gage resolution of 1 min), to perform a detailed analysis of rainfall sampling adjustment factors. Our aims are to compare SAFs determined using all of the different procedures that have been proposed in the past (except those that are fully theoretical, not based on actual rainfall data), to study SAF variability both at a station and in space, and then to propose a unified engineering methodology for dealing with the effects of rainfall totalization on the estimation of extreme precipitation. Given that these 1-min records are short (between 10 and 15 years), we use partial duration series to compute the rainfall quantiles and restrict our work to low and intermediate (< 25 years) average recurrence intervals, to avoid estimation issues.

Our results suggest that: (i) there is a preferred procedure for computing SAFs that should be adhered to, (ii) the mean SAF for a sampling ratio of one is indeed very close to the widely reported 1,13 value, but at-a-station variability of SAFs is large enough to be relevant for engineering design considerations, (iii) SAFs display spatial structure, and (iv) all of these findings should be studied in different regions or countries, and incorporated into engineering practice.

Is the antecedent precipitation before precipitation extremes average on average?

M. Müller*[1,2], M. Kašpar[1], M. Laco[1,2], L. Crhová[3]

1 Institute of Atmospheric Physics, CAS, Prague, Czech Republic
2 Charles University, Faculty of Science, Prague, Czech Republic
3 Czech Hydrometeorological Institute, Prague, Czech Republic

*Corresponding author: mullerr@ufa.cas.cz

Abstract

The hydrological response to heavy rainfall is significantly influenced by not only the precipitation totals and precipitation intensity distribution in time and space but also by the soil moisture within the catchment. The main factor determining the soil moisture at the beginning of a precipitation event is the antecedent precipitation, usually evaluated by the Antecedent Precipitation Index (API) introduced by Kohler and Linsley (1951).

From the climatological point of view, the annual course of API mean values corresponds to the annual precipitation regime, with maxima in summer at most Central-European stations. However, because precipitation is unequally distributed in time, API values seriously fluctuate. If precipitation extremes were randomly distributed, API would be average before them on average. Actually, soil moisture before a precipitation extreme is usually considered average when designing anti-erosion or flood protection measures in small, ungauged catchments. However, is it correct? Is it right that an extreme precipitation total and previous weather are independent of each other? Or is there a statistically significant API deviation (positive or negative) from its normal values before precipitation extremes at least in some regions and when considering extreme precipitation totals of some duration?

To answer the questions, we analysed two different datasets of annual precipitation maxima of daily and sub-daily (from 12 hours to 30 minutes) precipitation totals from the Czech Republic: (i) 59 years (1961–2019) of maxima reached at 60 rain gauge stations; (ii) 20 years (2002–2021) of maxima determined in individual 1x1 km pixels from 10-min radar-derived precipitation intensities, adjusted by daily precipitation totals from more than 700 rain gauge stations (Bližňák et al., 2018). Longer series of station data enabled us to distinguish several return levels within the sets of annual maxima, while detailed radar-derived data could be used for classifying the annual maxima of 6-hour totals into six types with respect to the time structure of rainfall (Kašpar et al., 2021).

First, we normalized API values by their seasonal mean values. For sub-daily totals, we also corrected the API values with respect to possible precipitation which was recorded between the morning measurement of the previous daily precipitation total and the beginning of the time window when precipitation reached its annual maximum at the given station / in the given pixel. Each normalized API value (NAPI) was than expressed as the respective quantile of the empirical cumulative distribution function of the whole data series (qNAPI). Finally, mean qNAPI values were determined for each considered set of precipitation maxima.

With increasing time window of the precipitation accumulation, uniformity of precipitation intensity, and the return period of the precipitation total, the probability of abnormally high antecedent precipitation increases mainly in mountain areas. This fact is demonstrated in Figure 1 and Table 1 where qNAPI values before precipitation maxima at a mountain station (Lysá hora, 1322 m a.s.l.) are presented. In lowlands, however, the signal is much less significant. Thus, we can conclude that on average, antecedent precipitation is average or can be even below average before precipitation extremes within time windows up to 3 hours, while it is usually above average before longer

precipitation extremes in mountains. The explanation is different circulation conditions conducive to precipitation extremes of different duration. If 6-hour or longer time window is considered, it is usually only a part of a much longer, up to several days lasting precipitation event, which increases the probability of abnormally high antecedent saturation at the beginning of the time window.

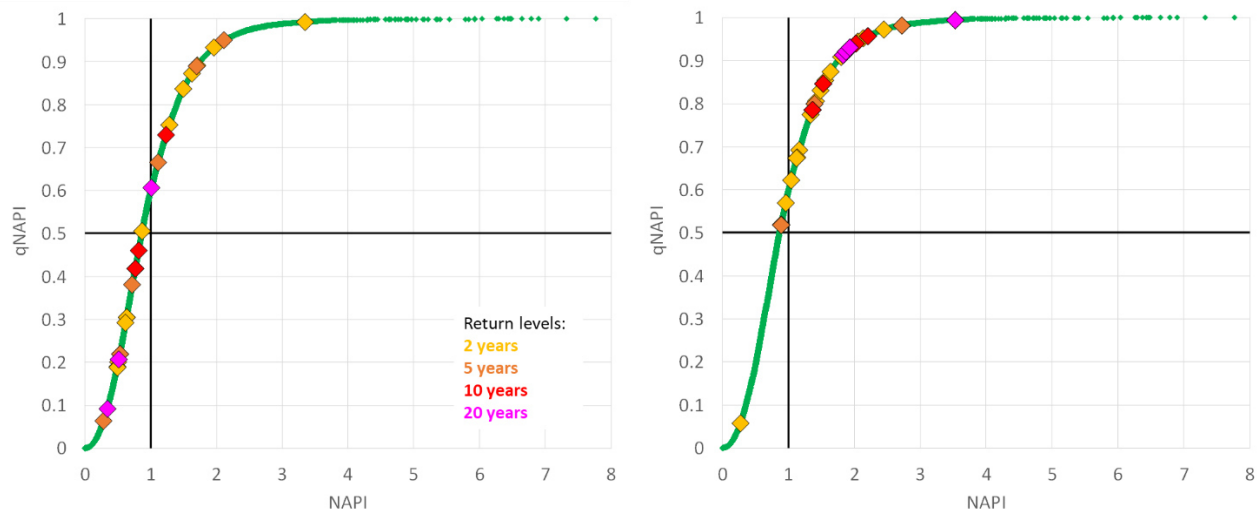

Fig 1: Statistical distribution of normalized API values at the station Lysá hora Mt.; the values before 1-hour and 1-day precipitation annual maxima at four return levels are highlighted in the left and the right graph, respectively.

Tab 1: Mean quantiles of normalized API values before precipitation annual maxima of different duration and return levels at the station Lysá hora Mt. Values corresponding with Figure 1 are highlighted with the same colours as in the figure.

	Return levels			
Duration	1 year	2 years	5 years	10 years
30 minutes	0.516	0.473	0.493	0.463
1 hour	0.483	**0.474**	**0.474**	**0.419**
3 hours	0.565	0.624	0.501	0.224
6 hours	0.666	0.697	0.803	0.725
12 hours	0.654	0.778	0.798	0.865
1 day	0.659	**0.781**	**0.879**	**0.914**

References

Bližňák, V., Kašpar, M., and Müller, M. (2018), Radar-based summer precipitation climatology of the Czech Republic, Int. J. Climatol., 38, 677-691.

Kašpar, M., Bližňák, V., Hulec, F., and Müller, M. (2021), High-resolution spatial analysis of the variability in the subdaily rainfall time structure, Atmos. Res., 248, 105202.

Kohler, M. A., Linsley, R. K. (1951), Predicting the runoff from storm rainfall, Washington, Weather Bureau, US Department of Commerce, Research Paper No.34.

Linking climate change to urban water infrastructure design: recent advances and shortcomings in modeling of extreme rainfall processes

V-T-V. Nguyen*[1]

1 Department of Civil Engineering, McGill University, Montreal, Quebec, Canada

*Corresponding author: van.tv.nguyen@mcgill.ca

Abstract

Most countries in the world have significant investments in urban water infrastructures. Every day, people rely on these systems to protect lives, property, and natural water environment. These infrastructures have reduced the vulnerability of the cities, but at the same time could make them more vulnerable to climate extremes, due to the lack of consideration of what might occur when the design criteria are exceeded. Furthermore, recent climate change assessment reports have indicated a worldwide increase in the frequency of extreme weather events because of global warming. Consequently, research on developing innovative approaches for limiting and adapting climate change impacts on urban water infrastructures is highly critical due to the substantial investments involved. However, it has been widely recognized that the main difficulty in dealing with climate change impacts for urban water infrastructure design is "how to estimate accurately the changes in the extreme rainfall processes at the urban basin scale projected by global/regional climate models because these models do not contain an adequate description of the governing physical processes at relevant high temporal and spatial resolutions as required by the impact and adaptation studies". This necessitates some form of downscaling of climate model simulations from a coarse spatial resolution down to much finer spatial grids, and even point values. In addition, the required time scales for these climate change impact studies are usually less than one day. Therefore, the overall objective of this paper is to provide an overview of some recent advances and shortcomings in the downscaling of extreme rainfall processes in the climate change context. In particular, another focus of this work is on the development of a technical guide to provide some guidance to water professionals in Canada on how to consider the climate change information in the urban water infrastructures design (CSA, 2019).

More specifically, the design of various urban infrastructures often requires the estimation of the "design storm" that is computed from the "intensity-duration-frequency" (IDF) relations at a given location (CSA, 2019). In engineering practice, these IDF relations are developed based on statistical frequency analyses of available annual maximum (AM) rainfall series for different durations. However, these AM rainfall records for sub-daily time scales are often limited or unavailable at the location of interest while those for the daily scale are widely available. Hence, it is necessary to develop new methods for modeling extreme rainfall processes over a wide range of time scales such that information related to sub-daily rainfalls could be inferred from the available daily rainfalls in the context of a changing climate. In Canada, Environment and Climate Change Canada (ECC) provides short-duration extreme rainfall data for different rainfall durations (from 5 minutes to one day) and the IDF relations for approximately 650 stations across Canada with at least 10-year rainfall record. Traditionally, the extreme rainfalls for different return periods were computed by fitting the two-parameter Gumbel distribution to the AM series for each rainfall duration independently using the method of moments (MOM). However, it has been widely known that this Gumbel/MOM-based traditional approach may not produce accurate and robust extreme rainfall estimates as compared to those given by, for instance, the Generalized Extreme Value (GEV)/L-Moment method (Nguyen et al. 2017). Consequently, there are several recently developed IDF products in Canada. The key differences between these products are: (i) the different probability models that were selected for describing the distribution of extreme rainfalls; (ii) the different estimation methods that were used for estimating the probability model parameters; (iii) the different regression models that were

chosen to represent the IDF curves; (iv) the different estimation methods that were used for estimating the regression model parameters; (v) the different spatial interpolation techniques that were used for transferring IDF information from gaged sites to the ungaged location; and (vi) the different considerations of the scale-invariance property of the extreme rainfall processes for different rainfall durations. Hence, a detailed comparative study was carried out to assess the performance of the traditional and newly developed rainfall estimation methods to identify the best approach for use in practice for deriving the IDF relations in Canada. In general, the traditional methods were based on the relationships between the extreme rainfall quantiles with the rainfall durations while the new approaches were relied on the scale-invariance relationships between the statistical moments of extreme rainfalls and the rainfall durations. It has been demonstrated that the traditional methods were less accurate than the new scale-invariance approaches. Hence, the new scale-invariance methods can be used for the development of IDF relations in the context of a changing climate (Nguyen and Nguyen, 2020).

In addition, the IDF curves for different locations in Canada have displayed different patterns that can be linked to the scale-invariance (or scaling) behaviour of the extreme AM processes. These different scaling behaviours can be identified based on the relations between the first-order empirical statistical moments of rainfall amounts and the rainfall durations. Figure 1 shows the ratios of the slopes of these relations for two different scaling regimes for all available IDF stations (approximately 650 stations) in Canada. In general, it can be seen that there are distinct IDF patterns for different regions representing diverse climatic conditions across Canada, including convex, linear, and concave patterns. However, for a large number of stations in the Pacific region the convex pattern (i.e., the slop ratio value is less than one) occurs more frequent. This could be due to the orographic effect in this region which causes a very different behaviour of short-duration extreme rainfall processes.

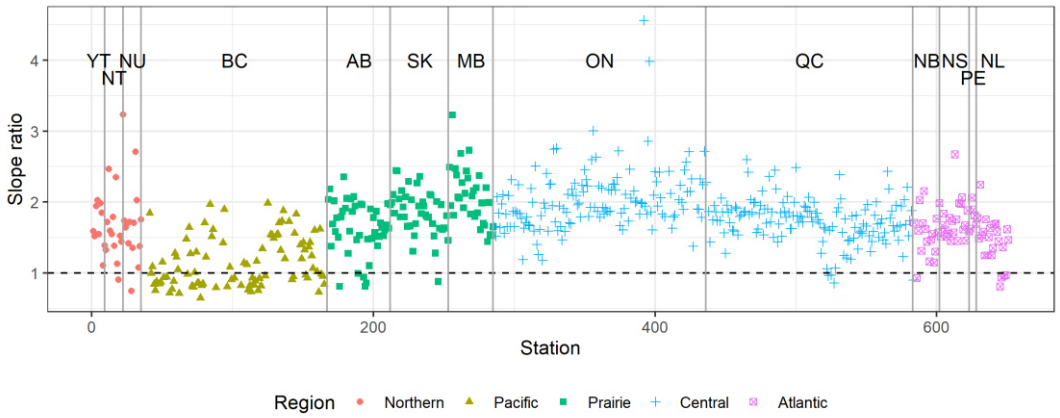

Fig 1: The slope ratios of two different scaling regimes given by the relations between the first-order rainfall statistical moments and durations for different regions of Canada

References

CSA (Canadian Standards Association) (2019). Technical guide: Development, interpretation, and use of rainfall intensity-duration-frequency (IDF) information: Guideline for Canadian water resources practitioners. CSA PLUS 4013:19, 126 pages.

Nguyen, T.-H., El Outayek, S., Lim, S.H., Nguyen, V.-T.-V., (2017). A systematic approach to selecting the best probability models for annual maximum rainfalls – A case study using data in Ontario (Canada). *Journal of Hydrology*, 553: 49-58.

Nguyen, T.-H., Nguyen, V.-T.-V., (2020). Linking climate change to urban storm drainage system design: An innovative approach to modeling of extreme rainfall processes over different spatial and temporal scales. *Journal of Hydro-environment Research*, 29: 80-95.

Forecast verification analysis of the CombiPrecip ensemble

Athanasios Ntoumos*[1,2], Ioannis V. Sideris[1], Alexis Berne[2], Marco Gabella[1], Urs Germann[1]

1 MeteoSwiss, Locarno, Switzerland
2 Environmental Remote Sensing Laboratory, EPFL, Lausanne, Switzerland

*Corresponding author: Athanasios.Ntoumos@meteoswiss.ch

Abstract

CombiPrecip is a real-time application developed by MeteoSwiss since 2012, which combines point raingauge measurements with radar-derived spatial estimations of precipitation over a vast 710x640km domain, extending beyond the Swiss borders. It relies on the geostatistics-based kriging with external drift as an interpolation technique. This method is probabilistic by nature, yielding both a mean value and an associated variance for every estimation. The purpose of our study is two-fold: (i) validate that the variance provided by the underlying geostatistical method of CombiPrecip can properly represent the true uncertainty of the CombiPrecip product and (ii) devise a numerical method to build an ensemble of realistic-looking members based on this geostatistical variance. For this, we employ widely used probabilistic verification measures (reliability diagrams, rank histograms, ROC curves) for a large set of cross – validation results over the period 2016 – 2022. In addition, based on established methods developed within the nowcasting community, we produce ensembles of N realistic precipitation members that not only mimic the spatial autocorrelation of the mean-value CombiPrecip but also replicate its pixel-scale variance. Overall, our results indicate that observations fall reasonably well in the uncertainty range provided by the CombiPrecip ensemble.

References

Sideris I.V., M. Gabella, R. Erdin and U. Germann, (2014) Real-time radar-raingauge merging using spatiotemporal co-kriging with external drift in the alpine terrain of Switzerland, Q. J. Roy. Meteor. Soc., 140 (680), 1097-1111.

Sideris I.V., M. Gabella, M. Sassi and U. Germann (2014) The CombiPrecip experience: development and operation of a real-time radar-raingauge combination scheme in Switzerland, Proceedings, 2014 International Symposium Weather Radar and Hydrology, Washington DC, USA.

Sideris, I.V., Foresti, L., Nerini, D. and Germann, U., 2020. NowPrecip: Localized precipitation nowcasting in the complex terrain of Switzerland. Quarterly Journal of the Royal Meteorological Society, 146(729), pp.1768-1800.

Towards understanding the impact of future rainfall upon urban drainage

Christian Onof*[1], Yuting Chen[2], Athanios Paschalis[1], Barnaby Dobson[1], Lipen Wang[3]

1. Imperial College London, United Kingdom
2. McKinsey & Co.
3. National Taiwan University

* Corresponding author: c.onof@imperial.ac.uk

Abstract

How can we estimate the impact of changing rainfall patterns upon the high flows generated in urban drainage networks? The immediate port-of-call to answer such a question must be climate models. Regional Circulation Models (RCMs) precipitation projections have recently improved through the development of convection-permitting models (CPMs). There are however three reasons for which such models, even on the assumption that they provide reliable estimates of future precipitation, are not, on their own, sufficient to address this question.
First, the computational cost of runs of CPMs is prohibitive. As a result, only a small number of runs are feasible, so that it is unlikely that the actual range of natural variability is thereby represented. Second, while the spatial scales are getting finer, they are often too coarse for urban applications. Third, the temporal sampling frequency of one hour is certainly insufficient.
This leaves us with the option of stochastic downscaling of the CPM projections, and here, a range of possible approaches are available. Amongst others, we have:

- Poisson-cluster based models focussing upon structures at certain scales.
- Multifractal models focussing upon the scale-invariance of precipitation features.
- Alternating renewal process for the event-no event structure and the event's global features, with conditional simulation for the spatial structure in the event

Although all have their own pros and cons, in this paper we focus upon the third approach famously pioneered by, among others, Geoff Pegram. As we will see this choice is motivated by its enabling us to distinguish between different aspects of the precipitation, i.e. the process of event arrivals and the internal structure of these events, in their role in urban runoff generation. The chosen model, STREAP (Paschalis 2013), now part of weather generator AWE-GEN-2D (Peleg 2017), has a tri-partite structure:

1. The *storm arrival* process and the event's global features
2. The structure of the *time-series* (WAR_t, IMF_t), i.e. wet area ratios and mean intensities throughout the event
3. The temporal evolution of the *space-time structure* inside the event.

Calibrating STREAP to radar rainfall over an area of 10^4 km^2, we see that it reproduces well various precipitation statistics at scales ranging from 5 mins to 24 hrs. Figure 1 shows the marginal distribution and the extreme behaviour of mean areal rainfall (compared with a Poisson-cluster approach). After debiasing the CPM outputs and downscaling to 5 mins, STREAP is also calibrated to future precipitation projections and several scenarios are considered (Table 1).
Drawing upon recent work by Dobson et al. (2022), drainage flows and storage contents are obtained from a complex network covering an area of about 850 km^2: for instance the impact of the change in the precipitation overall as compared with that in the internal structure of events, i.e. respectively the change from blue to pink and that between pink and red in Figure 3.

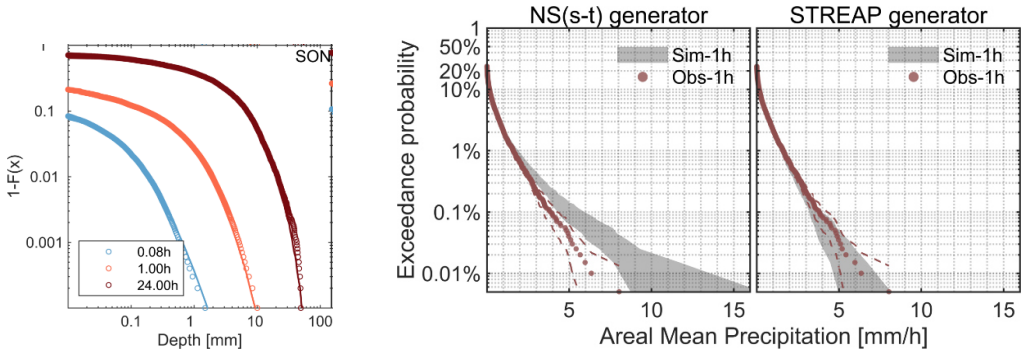

Figure 1: Validation of STREAP

STREAP-CC model setting		***Rainfall input resolution in CWSD modelling***
Modelled Period	*Spatial variability consistent with the modelled period?*	*Spatial-temporal resolution*
Current	Y	5min in time, blanket in space
Current	Y	5min in time, spatially varying
Future	Y	5min in time, blanket in space
Future	Y	5min in time, spatially varying
Future	N	5min in time, spatially varying

Table 1: Scenarios for STREAP

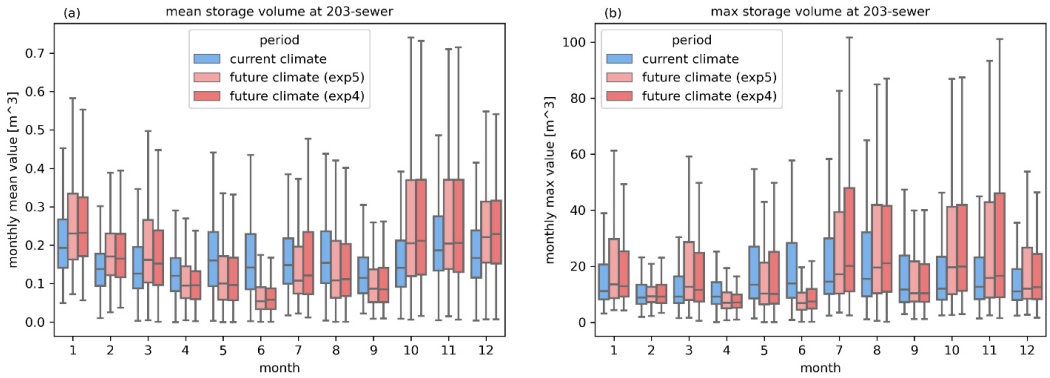

Figure 3: Impact upon storage volume of changing climate and changing internal event structure

References

Dobson, B. et al. (2022) A reduced complexity model with graph partitioning for rapid hydraulic assessment of sewer networks. *Water Resources Research*, *58*(1)

Paschalis, A. et al. (2013). A stochastic model for high-resolution space-time precipitation simulation. *Water Resources Research*, *49*(12), 8400-8417

Peleg, N. et al. 2017) An advanced stochastic weather generator for simulating 2-D high-resolution climate variables, *J. Adv. Model. Earth Syst.*, 9

Evaluation of subkilometer scale NWP for short-term predictions of convective rainfall events

J.W. Pedersen*[1,2], O.H. Fjellander[2], X. Yang[1], P.S. Mikkelsen[2]

1 Weather Research, Danish Meteorological Institute, Copenhagen, Denmark
2 DTU Sustain, Kgs. Lyngby, Denmark

*Corresponding author: jope@dmi.dk

Abstract

The extreme rainfall intensities associated with deep convective events in the atmosphere often overwhelm local urban drainage infrastructure and cause pluvial flooding in cities. Being able to predict these events in advance can provide valuable lead-time for emergency preparedness and real-time control mechanisms in drainage systems below and above ground. The genesis and evolution of convective rainfall events are often fast, sometimes even below hourly time scales. These fast dynamics severely limits the accuracy and timeliness of forecasts based on extrapolation of weather radar observations (called “radar nowcasts”). Instead, one of the main alternatives are numerical weather predictions (NWP) that are performed by large, computationally expensive models based on detailed physical descriptions of atmospheric processes. Many different aspects of the weather models influence the ability of NWPs to adequately predict convective events, such as the choice of convective schemes, data assimilation for good initial conditions, etc. This study focuses on the effect of the spatial grid resolution of NWPs, especially what happens once the model grid cells get down into the subkilometer scale, which allows for better simulations of convective processes (Clark et al., 2016). Emphasis is put on the ability to accurate locate extreme rainfall cells as well as the properties of the simulated rainfall fields such as scale, shape and peak intensity.

This study investigates NWP models based on the HARMONIE software, which is used for operational models at national weather services in many European countries (Bengtsson et al., 2017). Two NWP setups are compared: The 2.5km resolution NWP that runs operationally at the Danish Meteorological Institute (called “NEA2500”) and an experimental high-resolution setup at 0.75km (called “DK750”). See Table 1 for characteristics of the two NWPs. The rainfall predictions are here compared for the full convective season of the summer period in 2021, and forecast verification is performed with rainfall observations from DMI’s national C-band weather network over Denmark. Verification is based on the fractions skill score (FSS) and “structure, amplitude, location” (SAL) frameworks as quantitative metrics alongside subjective, visual comparisons.

The 2.5km model overestimates the structure and amplitude components of SAL, which means that rainfall fields are too smooth and contain too much rainfall (see Figure 1). On the other hand, the high-resolution model actually tends to underestimate both structure and amplitude, which is mainly caused by simulated rain cells being a bit too small and too “peaky” in shape. Subjective visual verification shows that both NWP’s tend to underestimate the peak intensity of extreme cells, but that there is a clear improvement in the high-resolution model’s simulated peak intensities.

Subjective visual comparison of predictions and verifying radar observations shows that the high-resolution model is better at spatially locating extreme rainfall cells. The quantitative metrics also show that the high-resolution setup improves FSS values at small spatial scales, which is mainly due to a better representation of small and distributed showers. These showers are often entirely missing in the coarser 2.5km model setup. In the SAL framework, both models produce good scores on the L-components with the high-resolution NWP being slightly better, which again highlights improved spatial localization accuracy.

For some events, the initial conditions of the high-resolution setup are markedly better than in the 2.5km model. We speculate that this might be because the increased grid resolution improves the data assimilation scheme by being able to better integrate the weather radar observations, which are produced at 0.5km resolution. Looking at FSS scores across different lead times within the forecast horizon shows that the improvements from using the higher resolution model are mainly seen at short lead times (< 6 hours), whereas improvements diminish for longer lead times. This is likely due to the small domain size of the high-resolution model as the influence boundary conditions, which come from the 2.5km model, become more pronounced at longer lead times.

We conclude that increasing the grid resolution of the operational NWP setup (1) addresses the well-known issue with too smooth rainfall fields in NWP outputs, but perhaps too aggressively, (2) leads to slight improvements in spatial accuracy of extremes, and (3) for some events provide markedly better initial conditions.

Tab 1: Characteristics of the high-resolution NWP ("DK750") and the current operational NWP ("NEA2500").

Characteristics	**DK750**	**NEA2500**
Horizontal resolution	0.007° (~750m)	0.022° (~2500m)
Vertical resolution	65 levels	65 levels
Temporal resolution	1 h	1 h
Forecast horizon	9 h	54 h
Forecast frequency	1 h	3 h
Domain size	630x700 cells (only covers Denmark)	1280x1080 cells (covers Northern Europe)
Lateral boundary conditions	NEA2500	ECMWF's "HRES" setup

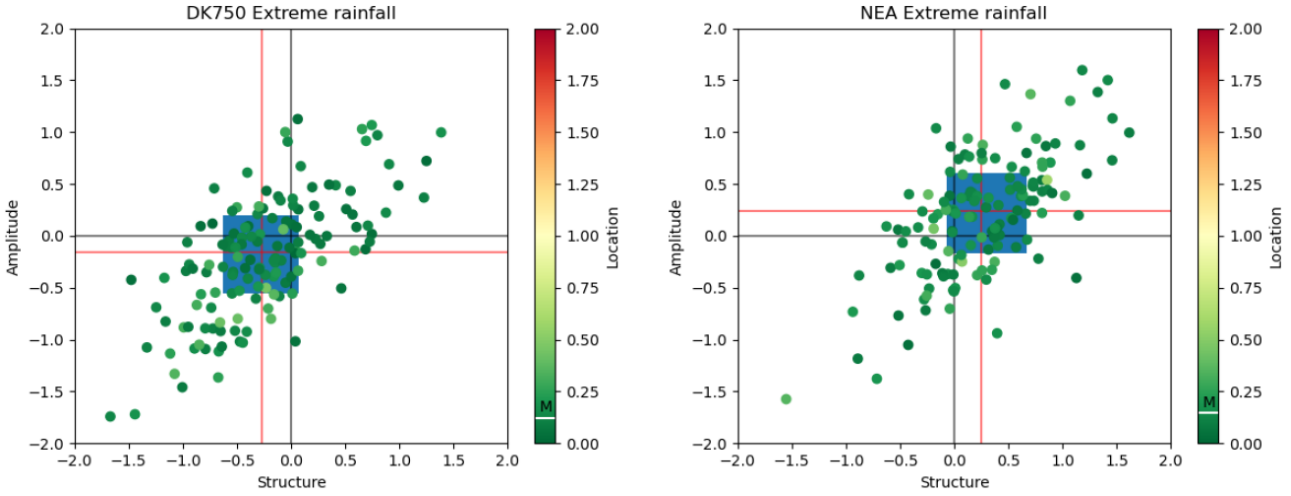

Fig 1: SAL scores for the two operational NWP setups with each dot representing an individual NWP run. The large red cross indicates the median score across all model runs, while the blue box shows the area between 25th and 75th percentiles on S and A components. The black cross indicates the axes that intersect at the point (0,0).

References

Bengtsson, L., Andrae, U., Aspelien, T., Batrak, Y., Calvo, J., de Rooy, W., ... & Køltzow, M. Ø. (2017). The HARMONIE–AROME model configuration in the ALADIN–HIRLAM NWP system. Monthly Weather Review, 145(5), 1919-1935.

Clark, P., Roberts, N., Lean, H., Ballard, S. P., & Charlton-Perez, C. (2016). Convection-permitting models: a step-change in rainfall forecasting. Meteorological Applications, 23(2), 165-181.

On the integration of a probabilistic seamless prediction model and a hydrological model for flooding prediction

R. Reinoso-Rondinel*[1,2], D. Buekenhout[1], M. van Ginderachter[2], R. O. Imhoff[3], L. De Cruz[2,4], P. Willems[1]

1 Department of Civil Engineering, KU Leuven, Leuven, Belgium
2 Observations, Royal Meteorological Institute of Belgium, Brussels, Belgium
3 Operational Water Management & Early Warning, Deltares, Delft, The Netherlands
4 Electronics and Informatics Department (ETRO), Vrije Universiteit Brussel, Brussels, Belgium

*Corresponding author: ricardo.reinoso-rondinel@kuleuven.be

Abstract

In recent years, heavy precipitation and flooding events have taken a heavy socio-economic toll and the impact of these events is expected to increase due to climate change (Spano et al., 2021). Impact-based warnings increase preparedness and inform effective and timely measures such as the evacuation of neighborhoods. However, such warnings require accurate precipitation forecasts, which is challenging due to the low predictability of rainfall, and its high spatiotemporal variability and uncertainty. Furthermore, modeling the hydrological processes associated with water flow in urban areas and valleys is particularly complex due to their non-linear nature. In addition, hydrological models for flooding prediction heavily depend on the accuracy, resolution, and lead time of the forecasted precipitation. This makes it a challenging task for weather and hydrological models to produce reliable predictions of flooding occurrences.

In this study, we present a forecasting framework that integrates 1) a probabilistic seamless prediction model of precipitation up to 12 h by blending the ensembles from radar-based nowcasting and numerical weather prediction (NWP) models and 2) a distributed hydrodynamic model for urban flood prediction. Figure 1 shows a representation of the framework. The objective of this study is to assess the effectiveness of the framework in predicting the response of the urban catchment, considering the inherent uncertainties associated with the models. Specifically, the aim is to evaluate the performance of a hydrodynamic flood model by utilizing different types of precipitation inputs, including deterministic and probabilistic forecasts with short-term (0-3h) and long-term (0-12h) lead times.

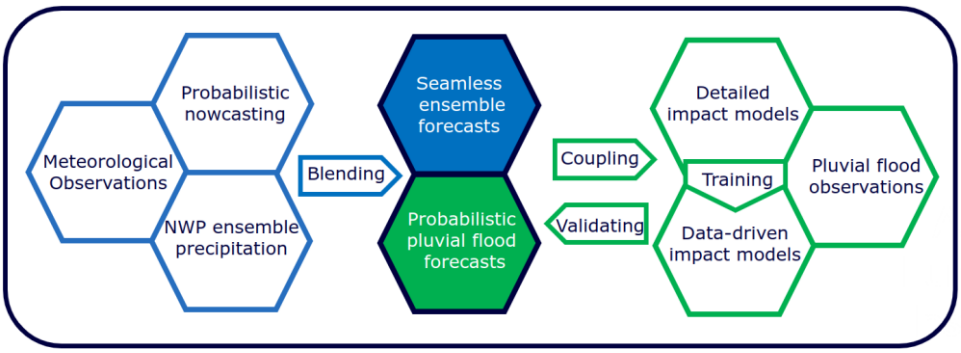

Fig 1: A schematic representation of the integrated hydro-meteorological framework for flood forecasting

For demonstration purposes, observations of precipitation fields, i.e., estimated rainfall rates, will be given by the radar-gauge adjusted product (Goudenhoofdt and Delobbe, 2016), which is operated by the Royal Meteorological Institute of Belgium (RMI). The blended forecast system will be obtained from the open-source pysteps community (Pulkkinen et al., 2019 and Imhoff et al., 2023) and adapted by the RMI (De Cruz et al., 2022) for its implementation towards an operational seamless prediction product. The hydrodynamic model for flooding prediction will be implemented using the InfoWorks ICM software (Innovyze, 2017) and configured to simulate the hydrological and hydraulic characteristics of the city of Antwerpen (Li and Willems, 2020). The event of 30 May 2016, which caused floods in the main cities of Flanders area (VMM, 2016), will be our case study.

The result of this analysis is expected to highlight the benefits and limitations of having such an integrated approach for flooding prediction in urban areas as well as the necessary compatibilities among the rainfall products and their representation of uncertainties. This study will be extended to include and validate a set of surrogate urban flood modeling such as physically informed data driven models for real-time pluvial flood forecasting.

References

De Cruz, L., Deckmyn, A., Degrauwe, D., Dehmous, I., Delobbe, L., Dewettinck, W., et al. (2022), Project IMA : building the Belgian seamless prediction system. EGU General Assembly 2022, Abstracts. Presented at the EGU General Assembly 2022, Vienna, Austria & Online. https://doi.org/10.5194/egusphere-egu22-12529.

Goudenhoofdt, E., and L. Delobbe (2016), Generation and Verification of Rainfall Estimates from 10-Yr Volumetric Weather Radar Measurements. J. Hydrometeor., 17, 1223–1242, https://doi.org/10.1175/JHM-D-15-0166.1.

Imhoff, R.O., De Cruz, L., Dewettinck, W., Brauer, C.C., Uijlenhoet, R., van Heeringen, K.-J., et al. (2023), Scale-dependent blending of ensemble rainfall nowcasts and numerical weather prediction in the open-source pysteps library. Quarterly Journal of the Royal Meteorological Society, 1– 30, Available from: https://doi.org/10.1002/qj.4461.

Innovyze (2017). InfoWorks ICM help v8.5, https://help.innovyze.com.

Li, X., and Willems P. (2020), A hybrid model for fast and probabilistic urban pluvial flood prediction. Water Resources Res, 56, e2019WR025128, https://doi.org/10.1029/2019WR025128.

Pulkkinen, S., D. Nerini, A. Perez Hortal, C. Velasco-Forero, U. Germann, A. Seed, and L. Foresti (2019), Pysteps: an open-source Python library for probabilistic precipitation nowcasting (v1.0). Geosci. Model Dev., 12 (10), 4185–4219, https://doi.org/10.5194/gmd-12-4185-2019.

Spano D., Armiento M., Aslam M.F., Bacciu V., Bigano A., Bosello F., Breil M., et al. (2021), “G20 Climate Risk Atlas. Impacts, policy and economics in the G20”, https://doi.org:10.25424/cmcc/g20_climaterisk.

VMM (2016), 12 dagen wateroverlast en overstromingen in Vlaanderen [Web log post]. Retrieved May 2023, from: https://www.vmm.be/nieuwsbrief/juni-2016/12-dagen-wateroverlast-en-overstromingen-in-vlaanderen.

Measured and perceived urban heat island: cross-measurements and lived paradoxes

F. Renard*[1], L. Alonso[2]

1 University of Lyon, University Jean Moulin Lyon 3, France
2 L&F Enviroconsulting, France

*Corresponding author: florent.renard@univ-lyon3.fr

Abstract

Current climate change is increasing the frequency and intensity of extreme events. This is particularly the case for heat waves, the severity of which has increased over Europe in recent decades. In addition, the rise in temperatures due to global climate change is amplified by the urban heat island (UHI) effect. The UHI is characterized by a temperature difference between an urban area and rural environments. The study of the UHI can be complemented by the study of the surface UHI (SUHI) which is based on the measurement of Land Surface Temperatures (LST). These UHI can be quantified in different ways. Regarding the measurement of air temperature, fixed measurements are most often used. However, measurement networks in urban areas are generally not dense enough to finely characterize the processes (Keeratikasikorn and Bonafoni, 2018): mobile measurement can then be used. LST are most often measured by remote sensing (Alonso and Renard, 2020). Finally, more qualitative measurements can be used by asking users about their thermal feelings and their practice of the places, through questionnaires, interviews or mental maps for example. Thus, the aim of this study is to compare three different means of data acquisition in Lyon (France). The first is the setting up of mind maps with volunteers who then participate in a measurement campaign using continuous temperature recorders coupled to GPS, which is the second means of information retrieval. Finally, these data will be compared to Landsat LST.

Methodology

Participatory or citizen measurements represent a democratization of science and an opening of the public to environmental issues. Volunteers, recruited through student associations, were equipped with two air temp. sensors (EL-USB-1-RGC-JM, accuracy +/-1°C, Log 32 accuracy +/-0.5°C) and GPS. This has several advantages. The first is to be able to deploy campaigns synchronous to the Landsat overpass. In this study, 20 measurement campaigns were carried out over 18 days (Fig. 1).

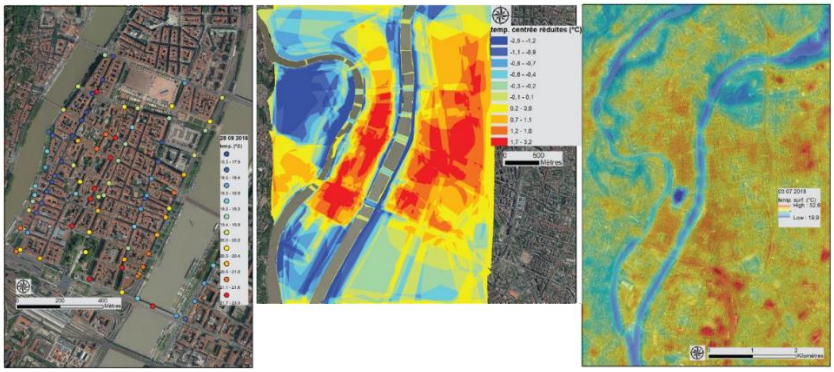

Figure 1: 28th September 2016 participatory measurements (left), synthetic mind map (center) and 03rd July 2018 surface temperatures (right).

As a complement to the measurements, the volunteers were asked to make thermal mental maps before the measurement campaigns. The objective of using mental maps is to compare the

perception of the thermal environment on the territory of Lyon with the quantitative measurements carried out in parallel on the study site and by remote sensing. Thus, a map synthesizing the perception of the temperature distribution during a hot day in Lyon from the mental maps issued by the participants is obtained (fig. 1), after georeferencing, digitizing, quantifying and standardizing.

Surface temperatures (fig. 1) were calculated from the Landsat 8 satellite (30 m). The single channel method was selected (Renard et al., 2019). This involves calculating spectral radiance, brightness temperature, emissivity using NDVI thresholds and removing atmospheric effects occurring between the Earth's surface and the satellite sensor using appropriate functions. Then, the three methods of temperature assessment are compared spatially with each other using GIS. In the end, the Pearson correlation coefficient (r), the mean square error (MCE), and the root mean square error (RMCE) are used to assess the adequacy of the measurements.

Results and discussion

Compared to the surface temperature data, the measurements from the two continuous loggers provide similar results (r=0.509 for EL and r=0.510 for Log32). It then appears that the fit between mobile measurements and surface temperatures is highly variable. Some campaigns such as May 25, 2018 have an r of 0.02 while that of June 25, 2018 have an r of 0.68. Thus, we obtain a range of results from measurement campaigns with no correlation to very strong correlations. These differences can be explained by the weather context during the campaign. Indeed, when the r's are confronted by linear regression to the average temperature of the day, relative humidity, pressure and wind (speed and direction), it appears that the type of weather with the best correlation between mobile measurements and surface temperatures lies during a campaign with high heat, low humidity, pressure and wind. The comparison of thermal mental maps of a warm agglomeration with surface temperatures also reveals a wide range of r from 0.05 to 0.83. Finally, the comparison of mobile measurements and thermal mental maps reflect the same trends: some campaigns show a strong match (e.g., June 26, 2018; r = 0.70) and others a complete lack of correlation (e.g., April 20, 2017; r = 0.07) or even a negative correlation (e.g., May 39, 2017; r = -0.24). These results are not really surprising because from our field experiments, thermal gradients can be much more changeable than imagined with consistently warm or cold sectors in a rather uniform manner, depending on time of day and weather type.

Conclusion

The confrontation of the three different sources of apprehension of the thermal gradients reflects understandable disparities according to the days, but also strong correlations. These dissimilarities are essentially related to the type of weather of the measurement campaign or to an idealized perception of thermal gradients which evolve in the imagination less rapidly than those measured in the field, which can be very changeable from one day to another. This demonstrates that the characterization of UHIs must involve a variety of measurement techniques, both qualitative and quantitative, in order to improve the knowledge of thermal comfort and adapt urban areas in a climate change context.

References

Alonso L. and Renard F. (2020), A new approach for understanding urban microclimate by integrating complementary predictors at different scales in regression and machine learning models, Remote sensing. 2020, 12, 2434, 2020

Keeratikasikorn C. and S. Bonafoni (2018), Urban heat island analysis over the land use zoning plan of Bangkok by means of landsat 8 imagery, Remote sensing, 10(3)

Renard F., Alonso L., Fitts Y., Hadjiosif A. and Comby J.,(2019), Evaluation of the effect of urban redevelopment on surface urban heat islands. Remote sensing, 11(3)

Measuring diameters and velocities of artificial raindrops with a neuromorphic dynamic vision sensor disdrometer

Jan Steiner[1], Kire Micev[1], Asude Aydin[2], Jörg Rieckermann[3*], Tobi Delbruck[2]

[1]Department of Mechanical and Process Engineering, ETH Zurich, Zurich, Switzerland
[2]Institute of Neuroinformatics (INI), University of Zurich and ETH Zurich (UZH-ETH), Zurich, Switzerland
[3]EAWAG, Swiss Federal Institute of Aquatic Science and Technology, Dübendorf, Switzerland

*Corresponding author: joerg.rieckermann@eawag.ch

Abstract

There's a growing number of optical disdrometers that measure hydrometeor diameter and speed at ground level. These measurements can be combined with weather radars or microwave links to predict the Drop Size Distribution (DSD) over a larger area (Kruger and Krajewski, 2002). The leading scientific instrument in this field is the 2-Dimensional Video Disdrometer. However, both 2DVD and competing PARSIVEL laser-sheet disdrometers have limitations, such as underestimating rainfall volume and drifting over time (Jaffrain and Berne, 2011). Different types of disdrometers also produce significantly different measured DSDs for small droplets. These instruments are expensive and power-hungry, making them impractical for widespread deployment and solar-powered weather monitoring. Therefore, an ideal disdrometer should be precise, low-cost, and consume less power when measuring fewer droplets.

This paper proposes, first, a novel approach using a Dynamic Vision Sensor (DVS) event camera to analyze brightness changes caused by droplets. The DVS camera reports asynchronous changes in brightness (Figure 1A) and has been successfully used in robotics and machine vision applications, but not yet in environmental or atmospheric monitoring (Gallego et al., 2020). Second, we generate high-quality ground-truth data for the droplets by modifying the Hard Disk Droplet Generator (HDDG) (Kosch and Ashgriz, 2015).

The proposed DVSD (Droplet Velocity and Size Detection) method is depicted in Figure 1 and explained in detail in (Steiner et al., 2023). The method utilizes a DVS (Dynamic Vision Sensor) camera that asynchronously detects brightness change events caused by droplets passing through a thin depth of field (DoF) at the Plane of Focus Rectangle. The camera is positioned at a steep angle to capture rainfall from above. Each droplet generates a cluster of DVS brightness change events, which can be analyzed to determine the size and speed of the droplet. The DVS camera records an illuminated falling water droplet (Figure 1B and 1C). The method relies on two key principles: First, the camera is angled downward with respect to the vertical direction. Second, the diameters of the droplets passing through the shallow DoF at the Plane of Focus (PoF) are measured unambiguously. By locating the PoF at a fixed working distance from the lens, the 3D position of the droplet can be inferred by measuring the droplet diameter at the waist of the hourglass shape, enabling the determination of the absolute size based on the image size.

To generate reproducible drops of small diameters, we modified the Hard Disk Droplet Generator (HDDG) by Kosch and Ashgriz (2015), who employed a computer hard disk arm as an actuator to break a steady stream of water into small droplets (Figure 1D). For large diameter drops, we used an IV drip kit (IVDG). We used measurements with a scale as ground truth.

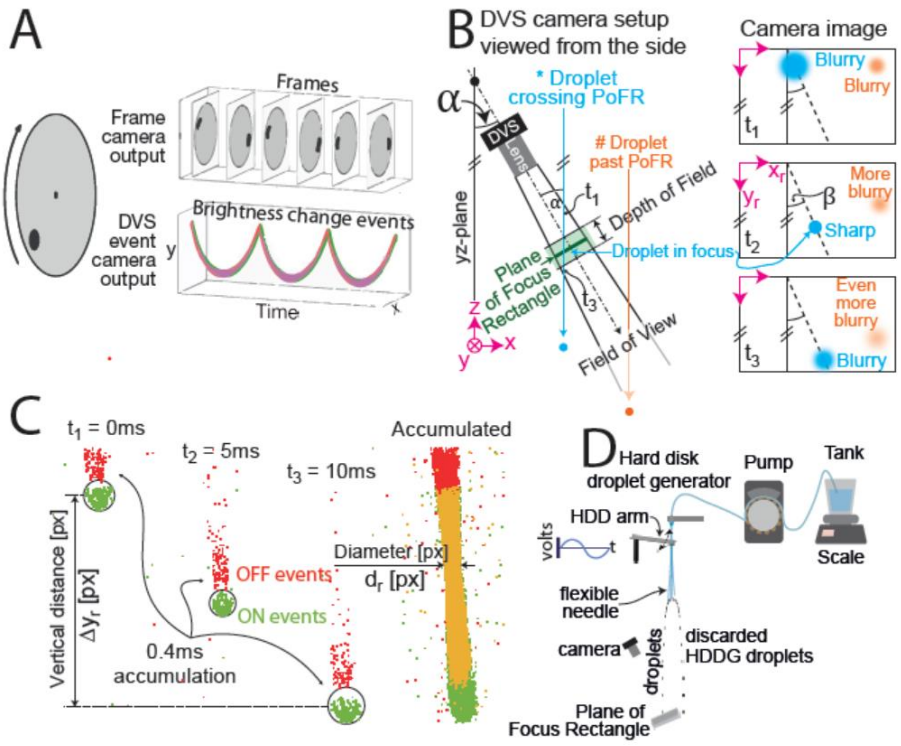

Fig 1: Summary of Dynamic Vision Sensor Disdrometer (DVSD) methods. **A**: Comparison between a conventional frame camera and a DVS capturing a rotating disk with a black dot. The frame camera outputs frames with finite exposure duration at discrete time intervals, whereas the event camera continuously outputs brightness change events, which results in a helix of discrete events in the space time plot (green: increase in brightness, red: decrease in brightness). **B**: Side view of the DVS camera setup in experiments and three illustrations of DVS recordings. The cyan droplet enters and exits the Field of view (FoV), which is tilted at a small angle from the vertical yz-plane. In the corresponding recording, first, the cyan droplet enters the FoV and is blurry. Second, it becomes sharp when crossing the plane of focus (PoF), and, thirds, is blurred again when exiting the FoV. The orange droplet never crosses the PoF and only grows increasingly blurry. **C**: Sample DVS recording of a droplet crossing the PoF, which is demonstrated in three frames with 5 ms time differences between each frame. Green points correspond to ON events, red points show OFF, and yellow points show overlapping of ON and OFF events. The rightmost frame shows all accumulated events over 10 ms. Each droplet creates several hundred to several thousand events, depending on its size. We estimate the falling speed *vr* by measuring the focal plane speed of the droplet. The diameter *dr* of the droplet is measured at the waist of the hourglass when the droplet is in focus.

We conducted two series of experiments, one with the HDDG and one with the IVDG (Figure 2). We used different lenses to make it easier to capture droplets crossing the PoF. The droplets created by the HDDG ranged from 0.3mm to 0.6mm (10 to 20 pixel diameter on the image), while the droplets created by the IVDG were 2.5mm (17-18 pixel diameter). In both experiments, the height of the fall was sufficient for the droplets to reach within 97% of the terminal speed.

The results show excellent linearity over the entire measurement range for both size and speed (Figure 2); the dashed line in each plot has a slope of one and passes through the origin; it lies close to both small and large droplet measurements. Size measurements slightly overestimate small droplet diameters, and speed measurements slightly underestimate large droplet speeds. The quantization of the data arises from the quantized droplet size generation and the pixel discretization. Horizontal quantization is caused by the quantized HDDG droplet creation frequencies, which control the diameters of the droplets. Vertical quantization is caused by the low pixel count of the diameter of the droplets in the DVS recording. The speed measurements do not have any significant vertical quantization effects, due to large pixel displacements (~100 pixels) and the fine DVS event timestamp resolution of 1 µs.

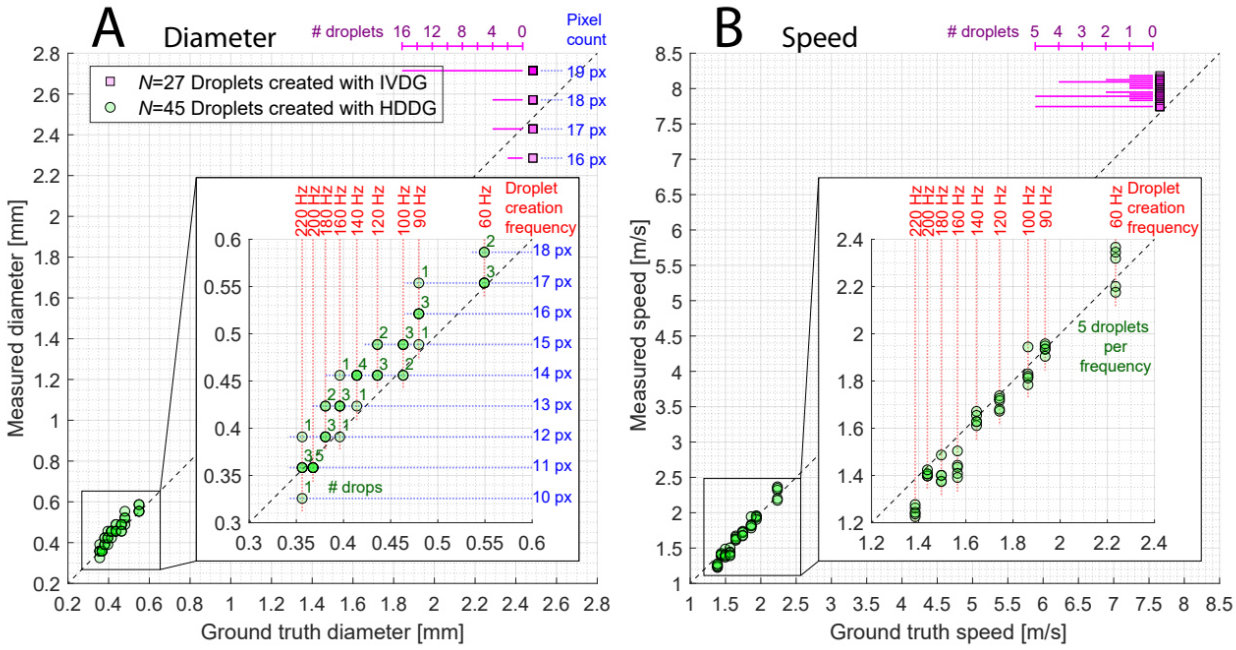

Figure 2: This is the figure caption. DVSD measurement results of droplets compared to Ground truth reference values, where A shows the diameter and B shows the velocity. The dashed black line represents a 45°-line passing through the origin. Both drop creation methods are included in the plots. The zoomed plots show droplets created with the HDDG for improved visibility. Numbers adjacent to the points on the left zoomed plot indicate overlaps whereas the zoomed plot on the right has 5 droplets per frequency. The IVDG droplets are shown in purple with a histogram for number of overlapping points. Quantization effects caused by the pixel count or frequency are illustrated as a grid pattern in the plots where the effect is significant.

To assess the uncertainty of the DVS measurements we used the Mean Absolute Percentage Error (MAPE) and found that the MAPE remains below 7% for the drop size diameter and below 4% for the velocity, which is very encouraging (Steiner et al., 2023).

Limitations arise from the fact that our experiments were only carried out with generated water drops in a controlled environment. First, unlike real rainfall conditions, there were no strong winds, which will disturb the trajectory of the drops. Moreover, the drop jets were localized and did not occlude each other. We do not believe that occlusion would be a fundamental problem due to the optical arrangement, but the droplet tracks could merge or overlap and the droplets in front or behind the PoF could disturb the measurements. Future studies should therefore investigate the performance under natural conditions, which probably also requires more advanced data analysis methods, such as tracking algorithms, to identify the trajectories of individual rain drops.

References

Gallego, G., Delbrück, T., Orchard, G., Bartolozzi, C., Taba, B., Censi, A., Leutenegger, S., Davison, A.J., Conradt, J., Daniilidis, K., 2020. Event-based vision: A survey. IEEE Trans. Pattern Anal. Mach. Intell. 44, 154–180.

Jaffrain, J., Berne, A., 2011. Experimental quantification of the sampling uncertainty associated with measurements from Parsivel disdrometers. J Hydrometeor 12. https://doi.org/10.1175/2010JHM1244.1

Kosch, S., Ashgriz, N., 2015. Note: A simple vibrating orifice monodisperse droplet generator using a hard drive actuator arm. Rev. Sci. Instrum. 86, 046101. https://doi.org/10.1063/1.4916703

Kruger, A., Krajewski, W.F., 2002. Two-dimensional video disdrometer: a description. J Atmos Ocean. Technol 19, 602–617.

Steiner, J., Micev, K., Aydin, A., Rieckermann, J., Delbruck, T., 2023. Measuring diameters and velocities of artificial raindrops with a neuromorphic dynamic vision sensor disdrometer. EGUsphere 1–8. https://doi.org/10.5194/egusphere-2023-215

WMO Guide to Operational Weather Radar Best Practices – progress and plans

Pekka Rossi[1], Daniel Michelson[2], Mark Curtis[3], Tom Kane[4], Hiroshi Yamauchi[5], Thomas Einfalt[6], Martin Hagen[7], Michael Istok[8], Wai Kong[9], Donald Rinderknecht[10], Benjamin Rohrdantz[11], Annakaisa von Lerber[12]

1 World Meteorological Organization, Geneva, Switzerland
2 Environment Canada, Toronto, Canada
3 Bureau of Meteorology, Melbourne, Australia
4 Bureau of Meteorology, Melbourne, Australia
5 Japan Meteorological Agency, Tokyo, Japan
6 hydro & meteo GmbH, Germany
7 German Aerospace Center (DLR), Oberpfaffenhofen, Germany
8 NOAA National Weather Service, Washington DC, USA
9 Hong Kong Observatory, Hong Kong, China
10 NOAA National Weather Service, Radar Operations Center, Oklahoma, USA
11 DWD, Offenbach, Germany
12 Finnish Meteorological Institute, Helsinki, Finland

*Corresponding author: prossi@wmo.int

Abstract

The Joint Expert Team on Operational Weather Radar (JET-OWR) of the World Meteorological Organization (WMO) is preparing an eight-volume Operational Guide to Weather Radar Best Practices (BPG). The scope addresses the end-to-end of a complete weather radar system starting with the planning and sustainable resourcing of a national weather radar program, and ending with a radar-based quantitative precipitation estimate (QPE). Included in this scope are the representation (formatting) of sweep and volume data in polar (spherical) coordinates (FM301-CfRadial2, see separate presentation), and methods of data exchange. The respective BPG parts are guides to weather radar

I. Network Program Design
II. Technology
III. Procurement
IV. Siting, Configuration and Scan Strategies
V. Calibration, Monitoring and Maintenance
VI. Data Processing
VII. Data Representation and International Exchange
VIII. Operational Weather Radar Glossary of Terminology

The BPG identifies typical challenges associated with each of these topics, and offers solutions for each, including essential literature references. Target audiences are managers (decision-makers) of weather radar networks and practitioners like engineers and software developers, of WMO's Members that are National Meteorological and Hydrological Services and supporting organizations, both those embarking on the establishment of a national weather radar network and those that already have.

In early 2023, Volumes I, II, III, and VII were officially approved for publication. Pre-production versions of these Volumes are available online at the WMO's community website while official typeset versions are being prepared. The BPG's WMO Guide number is yet to be assigned, but is expected be as part of production.

Volumes IV, V and VI are being prepared for submission to, and endorsement by, the third session of WMO's Infrastructure Commission in early 2024. Volume VIII is still at the thought stage, and could either contribute to or complement the AMS Glossary of Meteorology, recognizing that the WMO has recently taken the initiative to create a standard vocabulary that may also serve this purpose.

The BPG is expected to complement existing material such as the chapter on weather radar in the WMO Guide on Instruments and Methods of Observation (GIMO, WMO Publication No. 8, Volume III, Chapter 7), the International Standards Organization's "Meteorology — Weather radar — Part 1: System performance and operation" (ISO 19926-1:2019), and WMO Integrated Global Observing System (WIGOS) Manual and Guide (WMO Publications No. 1160 and 1165, respectively).

Using personal weather station data for improving precipitation estimates and gauge adjustment of radar data

J. Seidel*[1], T. Einfalt[2], M. Jessen[2], A. Bárdossy[1], A. El Hachem[1], A. Treis[3]

1 Institute for Modelling Hydraulic and Environmental Systems, University of Stuttgart, Germany
2 hydro & meteo GmbH, Luebeck, Germany
3 Emschergenossenschaft/Lippeverband, Essen, Germany

*Corresponding author: jochen.seidel@iws.uni-stuttgart.de

Abstract

Personal Weather Stations (PWS) are simple, low cost meteorological instruments that can be set up by private persons or companies. A detailed technical description of the most common PWS is provided by de Vos et al. (2019). In Central Europe, the number of PWS has increased significantly over the last years, in the meantime clearly outnumbering the number of rain gauges operated by national weather services and other authorities. However, the data from PWS suffer from many drawbacks since these stations are not set up and maintained according to professional standards. Apart from this, there are additional sources of errors and uncertainty originating from data transmission errors and incorrect information about the location of a PWS. Hence, the precipitation data from PWS has to be filtered and corrected before this information can be used e.g. for improving precipitation interpolation. Such algorithms have been developed by de Vos et al. (2019) and Bárdossy et al. (2021).

In the area of the water boards Emschergenossenschaft and Lippeverband (EGLV), investigations were carried out to determine whether data from private weather stations (PWS) can improve the interpolation of rainfall fields and if PWS can be used for the gauge-based adjustment of radar data. The area of the EGLV is located in a densely populated area in the federal state of Northrhine-Westfalia, where there is also a high density of PWS. Furthermore, the EGLV operate a dense rain gauge network which is required for the quality control (QC) algorithm by Bárdossy et al. (2021) which was used in this study.

The results show that the additional information from PWS can capture the spatial structures of precipitation better than a standard measurement network alone. An example is shown in Figure 1, which shows a 1-hourly rainfall field from different sources. Panel a) is interpolated using only the standard rain gauges from the EGLV and the German Weather Service DWD. Panel b) shows the result using the additional data from PWS. The reference from a gauge-adjusted rain radar is depicted in panel c). The improvement in interpolating rainfall fields with additional PWS data is also shown in the higher areal precipitation for smaller catchment within the study area and various other metrics which were evaluated in this study. However, the spatial resolution and the maxima of the radar data are not achieved, especially in areas with low PWS density. Overall, the improvement of interpolated rainfall fields is fundamentally dependent on the PWS station density and the quality of these data.

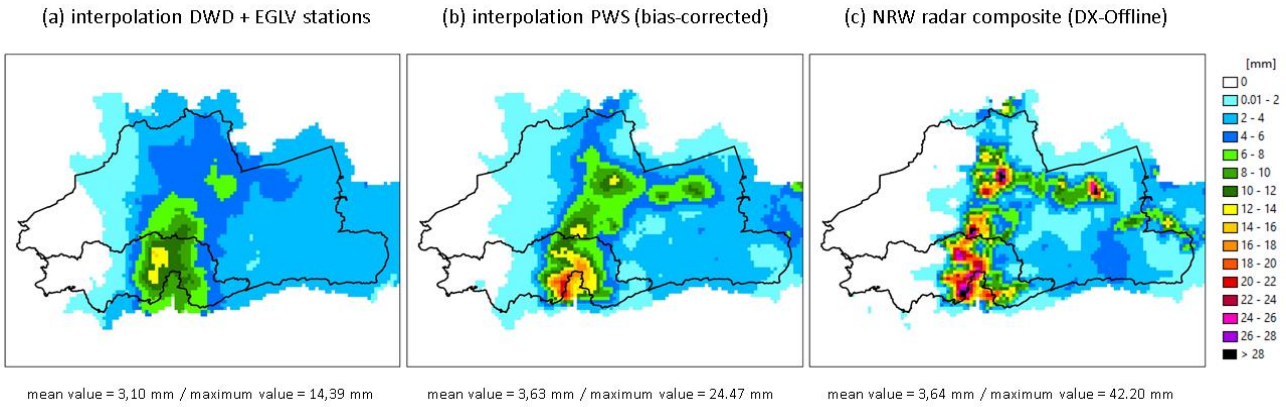

Fig 1: Event 14.08.2020 20:00 – 21:00 MEZ.

Another aspect that was investigated it the question whether individual PWS can be used for the gauge adjustment of radar data. In principal, individual quality controlled PWS can be used for this purpose, there are however issues due to data gaps and the underestimation of hourly precipitation maxima, which limit the use of PWS for commonly used gauge-adjustment procedures which require reliable precipitation measurements at specific sites.

In conclusion, the results of this study have highlighted the potential of PWS data to capture the spatio-temporal variability of precipitation and thus to improve the interpolation of rainfall fields. When using PWS for such purposes, data gaps of individual stations during one or more time steps are not so crucial. On the other hand, the results have shown that currently PWS cannot be treated as adequate alternative for standard precipitation measurements, e.g. for the gauge-adjustment of radar data. This requires further research in the quality control, especially with respect to filling data gaps and improving the bias correction.

References

Bárdossy, A., Seidel, J., and El Hachem, A. (2021), The use of personal weather station observations to improve precipitation estimation and interpolation. Hydrol. Earth Syst. Sci., 25, 583–601.

de Vos, L., Leijnse, H.,Overeem, A., and Uijlenhoet, R. (2019), Quality control for crowdsourced personal weather stations to enable operational rainfall monitoring. Geophysical Research Letters,46,8820–8829.

A Flood Monitoring System for the City of Reutlingen in South-West Germany

J. Seidel*[1], T. Müller[1], A. Schüller[2], T. Kiess[3]

1 Institute for Modelling Hydraulic and Environmental Systems, University of Stuttgart, Germany
2 Stadtentwässerung Reutlingen, Germany
3 KWMSys GmbH, Remseck, Germany

*Corresponding author: jochen.seidel@iws.uni-stuttgart.de

Abstract

The city of Reutlingen and neighbouring municipalities in the Echaz river basin have been repeatedly affected by flooding events and flash floods in recent years, sometimes even several times in one year. As a result, these municipalities forged a partnership at the end of 2016 and have since been working to refine an efficient flood risk management system. One key component is mapping and interpreting precipitation and runoff data for the river basin. Together with a private company, the partnership has thus launched a new monitoring strategy in order to increase lead times for heavy rain and flood events in the future. Due to the fast hydrological response times in case of a heavy rain events in the study area, an essential goal of the partnership is to record and evaluate the relevant meteorological and hydrological parameters in real time and to derive warning thresholds, which enable a fast and targeted deployment of rescue forces in case of heavy rainfall or flash floods.

Rainfall Monitoring

A total of 12 weighing rain gauges (OTT Pluvio²) have already been installed. However, these are all located in the urban area of Reutlingen in the lower part of the Echaz catchment. In order to capture precipitation in the upper parts of the catchments additional 6 tipping buckets rains gauges have been installed recently. Via the Flood Information and Warning System (FLIWAS 3) radar data are available online as so called “virtual rainfall gauges”. These data are available in real-time with 5-minute temporal resolution and provided 5 minutes after each measurement with a spatial resolution of 250m.

Water Level Monitoring

The Echaz has a total of nine tributaries, but there is only one gauging station in the lowest part of the river itself. For water level measurements, ultrasonic gauges were chosen and installed at different sites in the Echaz and its tributaries. The location of the gauges was chosen strategically, usually at tributaries as close as possible to the inflow into the Echaz or within the Echaz itself downstream of tributaries.
Furthermore, water level gauges were installed at critical points of the urban water infrastructure such as inflows of flood retention basins. These points were also equipped with cameras to monitor the status of these structures which are prone to clogging from debris during flood events.
Currently there are 44 gauges installed for monitoring the water levels of rivers and 43 gauges as well as 86 cameras for monitoring the inflows of urban drainage system structures.

The water level gauges are ultrasonic gauges which transmit the data via LoRaWAN were installed by KWMSys GmbH. This company also set up a dashboard to visualize all hydrometeorological data in real time. The following requirements were taken into consideration:

- Monitoring of the level changes with measurement/transmission rate every 4 minutes or faster
- Highest possible monitoring network density in the catchment (main river and tributaries)
- No infrastructure (power, data connection) available at the potential measuring site

- Online display of water level values in real time
- Cost-optimisation of the overall system including set-up and maintenance
- Possibility of transmitting the measurement data to third-party systems e.g. flood information and warning system (FLIWAS 3)

Data Processing and Visualisation

The data from water level and rain gauges are transmitted to a cloud server, where the data are checked, processes and forwarded to the user-backend (dashboard). In addition, individual warning threshold levels are defined for each site. These warning levels are displayed alongside with the data for each site as shown in Figure 1.

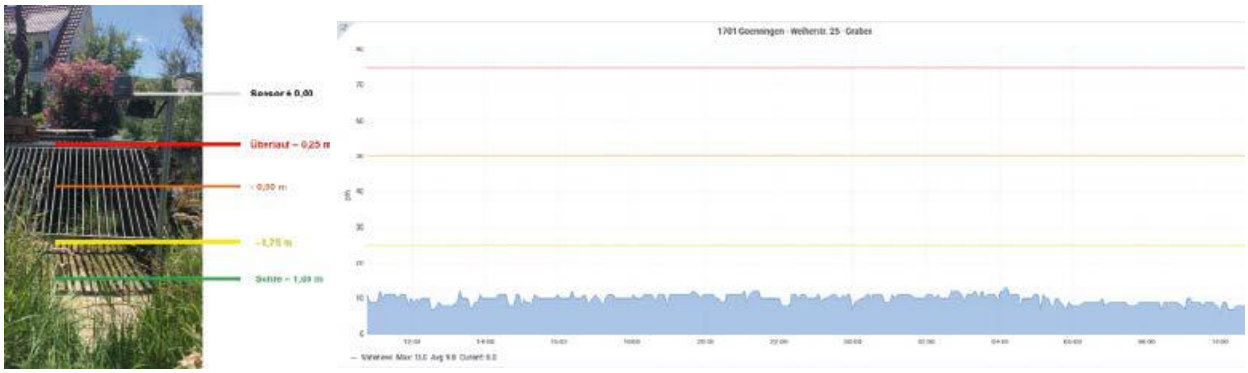

Fig 1: Specific warning levels for an inflow of a flood retention basin (left) and implementation of these warning levels in the dashboard (right).

In general, the monitoring system implemented in the City of Reutlingen and the neighbouring municipalities in the Echaz catchment can be assessed as positive. The experiences in the summer of 2020 have shown that the sensors provide a good representation of the water level during a rain event. In particular, the high transmission rate of 4 minutes on average in real time is profitable during heavy rainfall. At some sites where the water level exceeded a warning threshold during the rain events (e.g. by clogging from debris) rapid cleaning of the inflows could be arranged and thus damage prevented. It was possible to act in a demand-oriented manner and thus to use manpower could be deployed efficiently.

NowPrecip version 2: Precipitation nowcasting within the complex terrain of Switzerland

Ioannis V. Sideris*[1], Athanasios Ntoumos[1,2], Marco Boscacci[1], Lorenzo Clementi[1], Urs Germann[1]

1 MeteoSwiss, Locarno, Switzerland
2 Environmental Remote Sensing Laboratory, EPFL, Lausanne, Switzerland

*Corresponding author: ioannis.sideris@meteoswiss.ch

Abstract

A number of upcoming improvements for NowPrecip, the currently operational application of MeteoSwiss for precipitation nowcasting, will be presented. The very first version of NowPrecip (2020) was based on a localization architecture, necessary to reproduce important processes within the complex terrain of Switzerland, e.g. orographic precipitation. The next version is expanding on that design, introducing several new elements, such as, a new motion-field computation module, computation of intensity-based growth and decay profiles, methods to take advantage of information that can be extracted by the NWP ensembles, temporal disaggregation algorithms of the nowcasting sequence, and utilization of ensembles of initial conditions for the nowcast. Apart from improving the skill, one of the ultimate goals of the new version is the operational production of a multi-member NowPrecip ensemble, which is expected to assist considerably with the accuracy of rainfall-related severe weather warnings within Switzerland (project OWARNA2@MCH).

References

Sideris, I.V., Foresti, L., Nerini, D. and Germann, U., 2020. NowPrecip: Localized precipitation nowcasting in the complex terrain of Switzerland. Quarterly Journal of the Royal Meteorological Society, 146(729), pp.1768-1800.

Sideris, I., Foresti, L., Germann, U. and Nerini, D., 2018, July. Nowprecip: an algorithm for localized probabilistic precipitation nowcasting in the complex terrain of Switzerland. In Proceedings of the 10th European Conference on Radar in Meteorology and Hydrology (ERAD), Ede-Wageningen, The Netherlands.

Compound flood risk in small, ungauged catchments using LSTMs

F. Simon*[1], A. Hotzel[1], C. Mudersbach[1],

1 Department of Civil and Environmental Engineering, Bochum University of Applied Sciences, Germany

*Corresponding author: felix.simon@hs-bochum.de

Abstract

Heavy rainfall events and urban flash floods pose a high risk potential for humans and the environment, as a specific prediction of the regional impacts is difficult. The consequences of these events depend on various factors, including land use, soil type, topography, and pre-rainfall conditions. River floods also pose a significant risk, although they can be predicted more accurately, as a significantly larger data set is available, enabling more targeted flood risk management, particularly in larger river systems. When heavy rainfall and river floods coincide, such as in the July 2021 flood disaster in Rhineland-Palatinate and North Rhine-Westphalia in Germany, the hazards and risks to people and the environment increase substantially. According to Bevacqua et al. (2019) and Zscheischler et al. (2018), the likelihood of combined flooding will increase in the future due to anthropogenic climate change.

In this study, the occurrence of compound river floods and heavy rainfall events in small and medium-sized catchments are investigated using discharge data from multiple gauges in North Rhine-Westphalia, along with precipitation data from radar data of the German Weather Service and the ERA5-Land reanalysis data. The analysis involves identifying and analysing individual events based on different statistical parameters. Then, compound events that coincide in time and space are examined by creating simultaneous series from time series data. But the problem with these small and medium-sized catchments is, that there are often no or only few gauging stations and thus discharge time series. In order to perform a compound risk analysis for these smaller catchments, a solution with AI methods is used. By means of a regionalization approach using LSTMs and catchment characteristics, these time series are simulated for small and medium-sized catchments (Arsenault et al., 2023). LSTMs are well suited to process sequences and simulate long-term dependencies. In this study, different catchment characteristics are used for training the LSTM to support runoff pattern recognition. A more comprehensive compound analysis is then conducted with the additional simulated data.

Furthermore, the joint occurrence probability of river floods and heavy rainfall is determined (see Fig. 1). This is done with archimedean copula functions. A statement on the joint probability of occurrence of river floods and heavy rainfall has not yet been included in practice or in standards but should be adopted for the correct determination of hazards and risks.

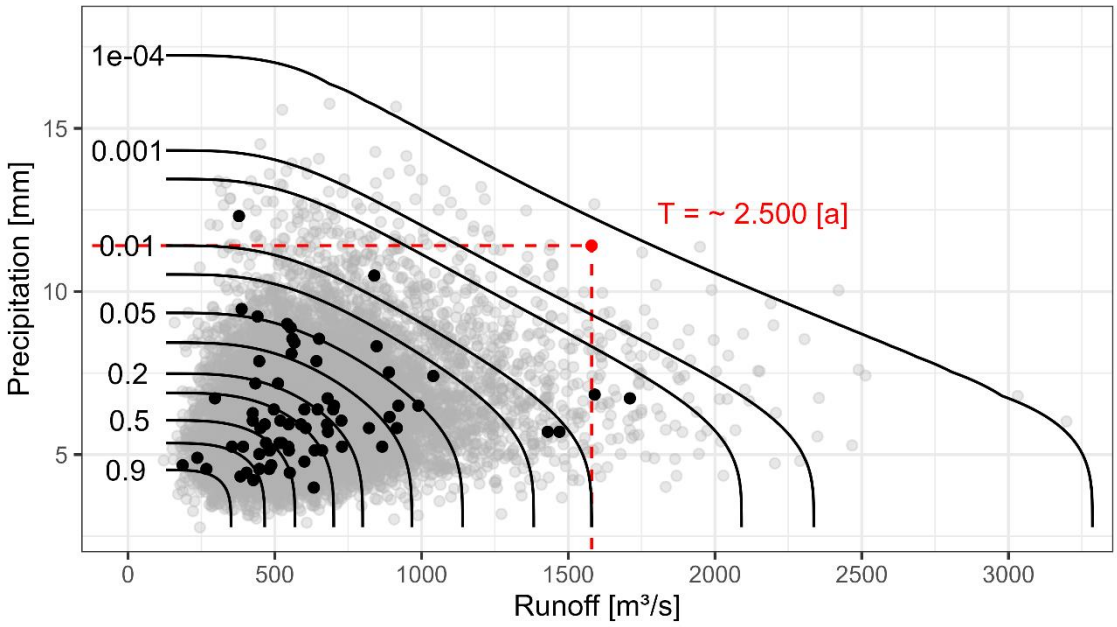

Fig 1: Multivariate extreme value analysis for the combination of precipitation and runoff with copula functions. The red dashed lines represent 100-year return period related to the single events whereas the red dot represents the combined return period.

References

Arsenault, R., Martel, J.-L., Brunet, F., Brissette, F. & Mai, J. (2023) Continuous streamflow prediction in ungauged basins: long short-term memory neural networks clearly outperform traditional hydrological models 1 [Online]. https://hess.copernicus.org/articles/27/139/2023/.

Bevacqua, E., Maraun, D., Vousdoukas, M. I., Voukouvalas, E., Vrac, M., Mentaschi, L., Widmann, M. (2019): Higher probability of compound flooding from precipitation and storm surge in Europe under anthropogenic climate change. In: Science advances 5 (9), eaaw5531. DOI: 10.1126/sciadv.aaw5531.

Zscheischler, J., Westra, S., van den Hurk, B., Seneviratne, S., Ward, P., Pitman, A., AghaKouchak, A., Bresch, D., Leonard, M., Wahl, T., Zhang, X. (2018): Future climate risk from compound events. In: Nature Clim Change 8 (6), S. 469–477. DOI: 10.1038/s41558-018-0156-3.

Identifying predictors within information theory framework for uncertainty reduction in commercial microwave links quantitative precipitation estimates

A. Špačková*[1], M. Fencl[1], V. Bareš[1]

1 Dept. of Hydraulics and Hydrology, Czech Technical University in Prague, the Czech Republic

*Corresponding author: anna.spackova@cvut.cz

Abstract

Commercial microwave links (CMLs) are point-to-point radio connections commonly used in telecommunication networks having a dense spatial coverage especially in urbanized areas. The CMLs have the great potential as opportunistic rainfall sensors as their transmitted signal is sensitive to droplets and attenuated along the link path. Even though the signal attenuation is related to rainfall intensity by simple power law, the quantitative precipitation estimates using microwave links are obscured by uncertainty.

This study proposes to use information theory methods to reduce uncertainty in CML quantitative rainfall estimates. This method enables evaluation of the strength of relationships between different variables using discrete probability distributions in target-predictor model and, alongside, it expresses the related estimation uncertainty. The virtue of the method is in its ability to employ any type of data without conceptualizations of its relationships.

The method is attracting interest also in the field of hydrology. Neuper and Ehret (2019) evaluated potential of different hydrometeorological predictors such as weather radar, micro rain radar, or disdrometers for quantitative precipitation estimates. Similarly, we can use different predictors related to CMLs data, characteristics, and other predictors to investigate and appraise the information content of the predictors and their combinations. Besides, Thiesen et al. (2019) identified rainfall-runoff periods in discharge timeseries using information theory, which is a similar challenge as an identification of wet and dry periods in CML signal attenuation data, thus, it could be addressed with this approach.

The analysis employs data from Prague CML network at a temporal resolution of 15 min from non-winter periods of the years 2014 to 2016. The target data are the rain gauge adjusted radar observation extracted as weighted mean of rain rates of pixels intersected by the link path. The CML data (signal attenuation and processed rainfall intensity) and the characteristics of CML hardware are used as predictors. Furthermore, additional hydrometeorological predictors are incorporated, e.g., seasonality and synoptic types.

The ability of selected predictor(s) to estimate the target variable can be compared using a measure of conditional entropy in units of bits. First, the models without knowledge of any predictor can serve as benchmark. The assumption, that all states in the range of the target distribution have equal probability, maximizes the uncertainty (no. 1 in Table 1). The prior knowledge of real target distribution reduces the uncertainty (no. 2 in Table 1). Further, the information content of the predictors to the target is measured (no. 3 to 7 in Table 1). The results show that the specific attenuation as predictor is less informative to the target than the rainfall intensity. However, combination of the specific attenuation with CML frequency is close to the case of rainfall intensity as single predictor. Additional predictors of seasonality and synoptic type bring useful information for rainfall estimation.

Moreover, the dependence of uncertainty reduction on the size of the data set can be tested using the measure of cross entropy (Figure 1). Different sizes of random samples of the dataset are

subset and their information content for the target is quantified as model robustness. The more predictors the model has, the greater the dataset needs to be. The model with rainfall intensity as predictor and model with specific attenuation and CML frequency perform similarly with full dataset, but sampling makes the model with more predictors less robust.

The ongoing experiments aim to employ information theory to identify precipitation episodes (separation of dry and wet periods) in time series of signal attenuation measurements of CML and to evaluate which predictors and their combinations are effective for separation of wet and dry periods.

Tab 1: Entropy of the benchmark (no. 1 and 2). Conditional entropies of the target with one or more predictors (no. 3-7).

no.		(Conditional) entropy [bit]	Relative (conditional) entropy [%]
1	Rainfall intensity Radar (uniform dist.)	3.70	162.7
2	Rainfall intensity Radar (actual dist.)	2.27	100.0
	Predictor/s		
3	CML (rainfall intensity)	1.87	82.3
4	CML (specific attenuation)	1.94	85.3
5	CML (rainfall intensity), synoptic type	1.75	76.8
6	CML (specific attenuation), CML (frequency)	1.86	81.9
7	CML (rainfall intensity), synoptic type, seasonality	1.65	72.5

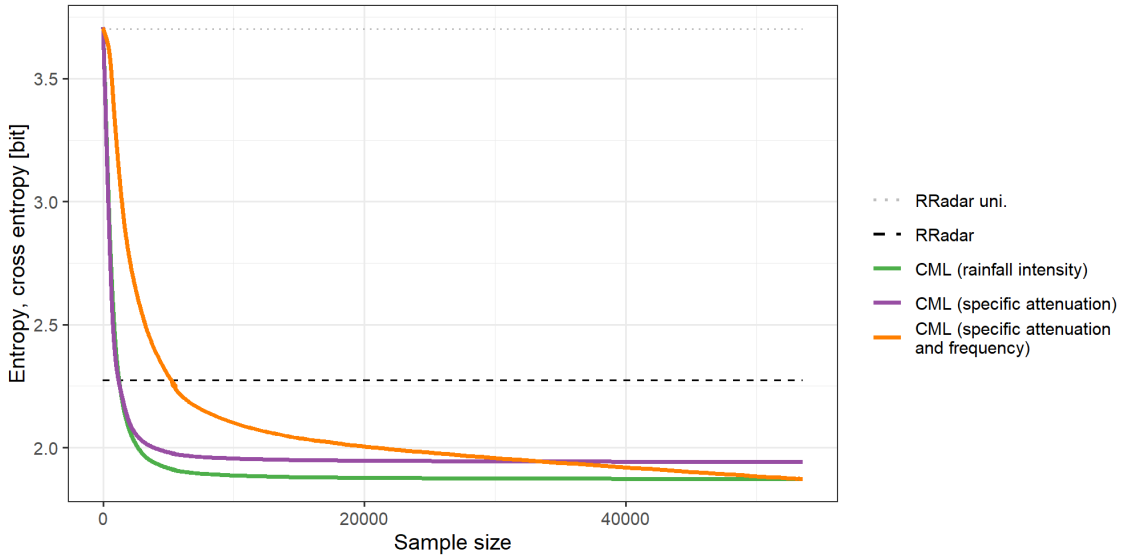

Fig 1: The effect of sample size on entropy reduction measured as cross entropy. Entropy of the benchmark (dotted line) and of the target (dashed line). Cross entropy with CML rainfall intensity (green), CML specific attenuation (purple), and CML specific attenuation with CML frequency (orange) as predictors across different sample sizes.

References

Neuper, M. and Ehret, U. (2019), Quantitative precipitation estimation with weather radar using a data- and information-based approach, Hydrol. Earth Syst. Sci., 23, 3711–3733, https://doi.org/10.5194/hess-23-3711-2019.

Thiesen, S., Darscheid, P., a Ehret, U. (2019), Identifying rainfall-runoff events in discharge time series: a data-driven method based on information theory, Hydrol. Earth Syst. Sci., 23, 1015–1034, https://doi.org/10.5194/hess-23-1015-2019.

The impact of sub-kilometre resolution climate model simulations on extreme rainfall events

E.D. Thomassen*[1], K. Arnbjerg-Nielsen[2], H.J.D. Sørup[2], P.L. Langen[3], J. Olsson[4], R.A. Pedersen[5], O.B. Christensen[5]

1 Weather Research, Danish Meteorological Institute, Copenhagen, Denmark
2 Department of Environment and Resource Engineering, Technical University of Denmark, Kgs. Lyngby, Denmark
3 iClimate, Department of Environmental Engineering, Aarhus University, Roskilde, Denmark
4 Hydrology Research, Swedish Meteorological and Hydrological Institute, Norrköping, Sweden
5 National Centre for Climate Research, Danish Meteorological Institute, Copenhagen, Denmark

*Corresponding author: emt@dmi.dk

Abstract

The impact of climate change on extreme precipitation event are of high interest. However, climate models are well-known to have difficulties in representing the small spatial and temporal scales of extreme convective rainfall events. Convection-permitting climate model (CPM) simulations have shown clear improvements in description of convective events. Here CPMs are understood as climate models with a grid cell size typical below 4 km and with no parameterisation of deep convection. Despite a better representation of convective events in CPMs, literature have also shown that these simulations still struggle in the representation of convective events. This study aims to analyse if the representation of convective extreme events improve with sub-kilometer scale climate model simulations.

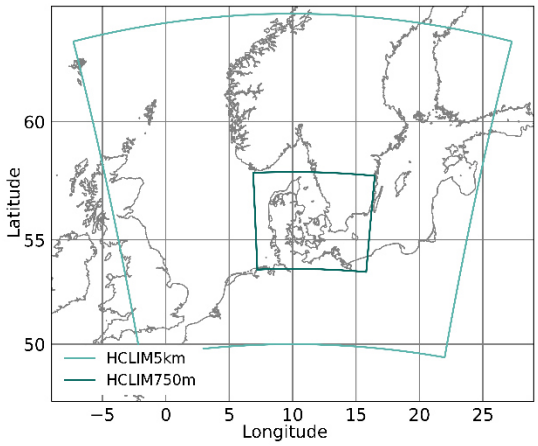

Fig 1: Domain of HCLIM simulation in 750 m resolution over Denmark (HCLIM750m) nested within a 5 km simulation with a larger domain (HCLIM5km). Figure from Thomassen et al. (2023).

This study utilise a new 750 m climate model simulations over Denmark (Thomassen et al. 2023, see Fig. 1), to analyse the added benefit of higher resolution. The study uses four simulations with HARMONIE Climate (HCLIM) at different grid cell sizes (750 m, 3 km, 5 km & 12 km), two reanalysis products (ERA5 and ERA-Interim) and a dense rain gauge dataset (POINT). The 750 m simulations consists of data from April to October, where cloudburst are most likely to happen in Denmark, for five selected years. The years are selected based on observed extreme convective events, and hence not representative for climatology. The HCLIM750m downscales ERA5 with an

intermediate HCLIM5km simulation, while HCLIM3km downscales ERAI with an intermediate HCLIM12km simulation.

We apply a wide range of metrics to quantify the added benefit of sub-kilometre resolution climate model simulations. These metrics are applied across the seven datasets to analyse the representation of extreme events with respect to diurnal cycle, intensity levels and spatial structure. The analyses are performed at both hourly and sub-hourly scales. The spatial correlation of the extreme events shows an improvement in the spatial extent of climate model simulations with higher resolution (see Fig. 2). HCLIM750m shows the best performance, but with limited differences between the CPM simulations (HCLIM750, HCLIM3km and HCLIM5km).

Across the applied metrics the 750 m climate model performs better for most of them. However, CPMs with coarser resolution (3 and 5 km grid spacing) also perform well. The sub-kilometre resolution simulations only shows a limited added benefit in the current setup and the model setup including parameterisation of shallow convection must be further evaluated. Results shows that the model performance varies between different temporal scales. The CPMs, in general, represent hourly convective precipitation much better than sub-hourly extremes. Further analyses on sub-hourly scale is, therefore, essential to assess the model performance of convective events.

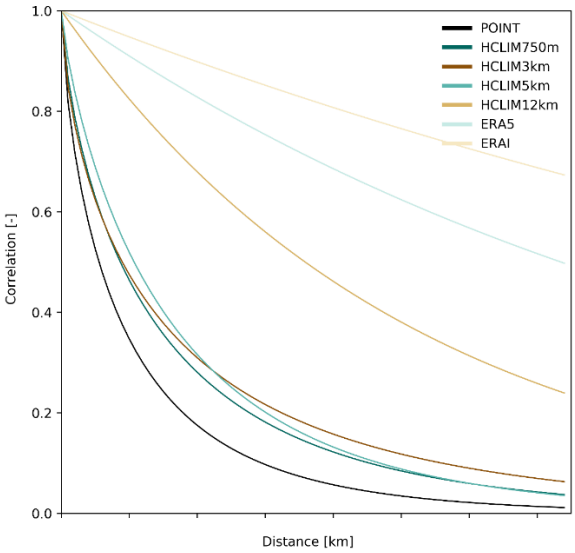

Fig 2: Spatial correlation of extreme events sampled with Peak Over Threshold method, with an average of 3 events per year and a duration of 3 hours. Modified figure from Thomassen et al. (2023).

References

Thomassen ED, Arnbjerg-Nielsen K, D Sørup HJ, Langen PL, Olsson J, Pedersen RA, Christensen OB (2023) Spatial and temporal characteristics of extreme rainfall: Added benefits with sub-kilometre resolution climate model simulations? Q J R Meteorol Soc. https://doi.org/10.1002/QJ.4488

Spatial extreme value rainfall statistics from weather radar and rain gauges

S. Thorndahl*[1], C.B. Andersen[1], H.J.D Sørup[2]

1 Department of the Built Environment, Aalborg University, Denmark
2 DTU Sustain, Technical University of Denmark

*Corresponding author: st@build.aau.dk

Abstract

Historically, point rainfall statistics have played a crucial role in the design of urban hydrological systems by providing information on rainfall intensities over specific durations and return periods. However, when dealing with the design of systems that drain large urban catchments, it becomes necessary to account for the spatial variability of rainfall. To incorporate this aspect, an additional statistical framework, including the spatial component, must be introduced. In this case, a dense network of rain gauges or weather radar data can provide valuable information.

Previously, long-term statistics relied alone on rain gauge records. However, the accessibility of radar data spanning decades enables a more comprehensive examination of rainfall variability across space and time. For radar-based statistical analyses to serve as a reliable alternative to rain gauge statistics, high-quality, error-free, and consistent data is important. Although technological advancements, such as dual polarimetric estimation, have enhanced our capacity to quantify radar-based rainfall intensities, it remains crucial to incorporate "ground truth" data from rain gauges in adjusting radar data (Thorndahl et al. 2017).

In Denmark, the first statistical regional rainfall model was developed in the late 1990'ies (Mikkelsen et al. 1996). The statistical database for this model has been updated several times since then, following the same methodology. Recently, the model has been updated to its 5th version by The Water Pollution Committee of The Society of Danish Engineers (Arnbjerg-Nielsen et al., 2023). The extreme rainfall statistics procedure is based on a peak-over-threshold approach from which a generalized Pareto distribution (GDP) is fitted. Regionalization is obtained by relating GPD-parameters to e.g., yearly precipitation.

In this study, we do not change this method of extreme value statistics but extend the database to also include a 20-year radar data series from a single radar covering parts of Denmark.

The objectives of this study are to:

1. Compare extreme value statistics derived from point rain gauges and single radar pixels.
2. Compare spatial correlation structures obtained from rain gauge and radar data following the method presented in Thomassen et al. (2022).
3. Compare GPD parameters obtained from fitting probability distributions to the two data sources.
4. Derive statistical point-area relationships from obtained probability distribution functions.

Figure 1 shows an example of IDF-curves obtained from rain gauges and radar data in the locations of rain gauges. Figure 2 shows the number of annual exceedances (λ) of hourly peak-over-threshold for radar and rain gauge data respectively.

Results show significant regional variability in the extreme value statistics and statistical differences in rain gauge and radar data due to differences in ground observations and areal observations in the atmosphere from radar data.

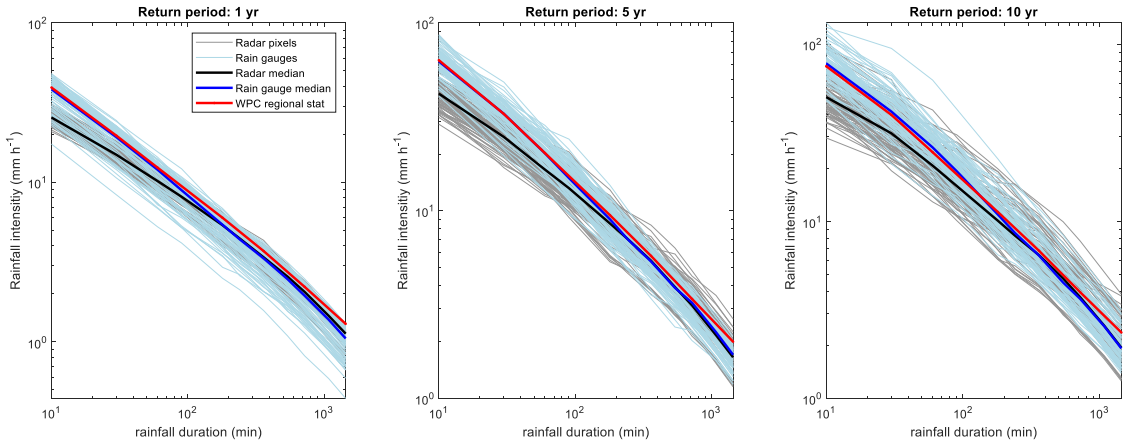

Fig. 1. Example of derived IDF-curves from rain gauges and radar respectively.

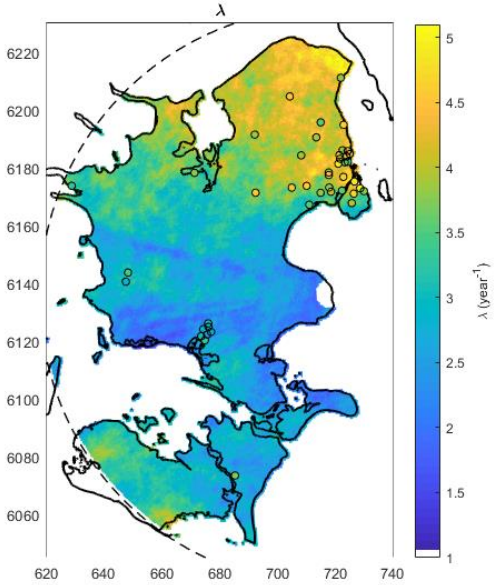

Fig. 2: Spatial representation of the number of annual exceedances (λ) of hourly maxima larger than 6.7 mm h^{-1} based on radar data. Circles represent the corresponding rain gauge values.

References

Arnbjerg-Nielsen, K., Gregersen, I.B., Madsen, H., Sørup, H.J.D. (2023) Skrift nr. 32 Regional variation af ekstremregn i Danmark (1979-2019) inkl. korrektion for klimaændringer (In Danish). The Water Pollution Committee of The Society of Danish Engineers, Copenhagen, Denmark.

Mikkelsen, P.S., Madsen, H., Rosbjerg, D., Harremöes, P. (1996). Properties of extreme point rainfall III: Identification of spatial inter-site correlation structure. Atmos. Res. 40, 77–98. https://doi.org/10.1016/0169-8095(95)00026-7.

Thomassen, E.D., Thorndahl, S., Andersen, B.A. Gregersen, I.B, Arnbjerg-Nielsen, K., Sørup, HJD (2022) Comparing spatial metrics of extreme precipitation between data from rain gauges, weather radar and high-resolution climate model re-analyses. https://doi.org/10.1016/j.jhydrol.2022.127915

Thorndahl, S., Einfalt, T., Willems, P., Nielsen, J. E., ten Veldhuis, M.-C., Arnbjerg-Nielsen, K., Rasmussen, M. R., Molnar, P. (2017) Weather radar rainfall data in urban hydrology. Hydrology and Earth System Sciences, 21(3), 1359–1380. http://dx.doi.org/10.5194/hess-21-1359-2017

Changing spatial patterns of convective rainfall across urban areas

H. Torelló-Sentelles*[1], F. Marra[2], M. Koukoula[1], N. Peleg[1]

1 Institute of Earth Surface Dynamics (IDYST), University of Lausanne, Switzerland
2 Department of Geosciences, University of Padova, Italy

*Corresponding author: herminia.torello@unil.ch

Abstract

Urban areas have been shown to impact rainfall both by altering its intensity and spatial structure on small scales (i.e., at sub-hourly and sub-kilometer resolutions). However, there is currently not a clear understanding of how the spatial structure of rainfall fields is changing in different urban areas and the mechanisms that drive these changes. The hydrological response in urban areas is highly sensitive to such space-time changes therefore, it is important to understand the precise pattern of change to nowcast rainfall and assess flood risk. We used high-resolution C-band weather radar data (5 min and 1 km) to analyze changes in patterns of intensity, structure, and storm motion of rain cells across 7 cities in Europe and the US. We tracked convective rain cells using a storm tracking algorithm (in a Lagrangian perspective) and assessed changes in rainfall properties in the upwind and downwind regions of each urban area. We also investigated changes in the frequency of the cell's life cycle, namely initiations, terminations, splitting, and merging. Our results show that rainfall is intensified mostly over the urban areas but the effect sometimes continued downwind. Overall, larger cities and daytime storms tended to show larger rainfall enhancements. We also found altered rain cell spatial structures over some of the cities: either a decreased area and increased heterogeneity (Milan, Italy; Phoenix, US, and Atlanta, US) or the opposite (Charlotte, US, and Indianapolis, US). Additionally, we observed increased storm initiations over or downwind of most urban areas. It also seems that some cities might be acting as "barriers", by increasing storm terminations upwind and over them (Milan, Italy, and Birmingham, UK).

How to deal with uncertainties in flood forecast

A. Treis*[1], D. Falk[1], B. Teichgräber[1], A. Pfister[1]

[1] Emschergenossenschaft, Essen, Germany

*Corresponding author: treis.adrian@eglv.de

Abstract

The Emscher region is one of the most densely populated industrial regions in Europe. In particular, the high percentage of impervious area and the influence of mining exacerbate the risk of flooding. The runoff concentration time of the Emscher River ranges between two and six hours, while flood waves from tributaries emerge in less than two hours. In addition to continuous winter rainfall, convective heavy rainfall events can also trigger flood situations in the Emscher river and its tributaries, often accompanied by local flooding of the sewer system. Particularly during these summer convective situations, flood forecasting faces the challenge of dealing with the uncertainties of the forecasts.

There are several factors contributing to uncertainties in flood forecasting. These factors include uncertainties in the measurement and data assimilation of weather models, as well as precipitation and river gauge measurements. Additionally, model uncertainties exist both within the rainfall-runoff model and the weather forecast itself. Another source of uncertainty relates to the watershed itself. Construction sites along watercourses, technical malfunctions, or deviations from regular operation can lead to developments that are not represented in the hydrological models. Furthermore, climate change introduces an additional layer of complexity, as it gives rise to weather phenomena that have not yet been accounted for in existing hydrological models.
The Emschergenossenschaft (EG) utilizes deterministic weather models, namely ICON, ICON-EU and ICON-D2 of the German Weather Service (DWD, 2022), as inputs for their modeling. Various products have been tested for nowcasting purposes. Ensemble forecast systems, which provide probabilistic forecasts, offer an estimate of uncertainty levels but can be are more intricate to interpret and communicate effectively. Regarding flood forecasting specifically for the Emscher river, the DWD models ICON-D2 (EPS) and ICON-EU (EPS), along with the ECMWF model (COSMO-LEPS), are employed (ECMWF 2022). In the past, assessment of the situation relied solely on deterministic weather model data from the German Weather Service. Although this approach yielded unambiguous interpretations of water levels and discharges, it failed to capture the rapid dynamics of weather events adequately. With the introduction of ensemble-based weather forecasts, it has become possible to assess uncertainties and potential developments. However, this also presents challenges in deriving specific actions since all members of the model run represent the same probability. Close consultation with operational departments regarding potential consequences is crucial, as is the establishment of pre-established actions, responsibilities, and agreements. The experiences, conclusions and actions based on the flood event of July 2021 will be described.

The July 2021 flood serves as a prime example that encompasses the entire spectrum of uncertainty (Fig. 1). On July 14th, 2021, at 06:00 CEST, the forecasts indicated an exceptionally severe flood event with the potential for surpassing the design discharge thresholds and resulting in overflows of the dykes. The predicted precipitation accumulation for the Emscher area, as indicated by the 24-hour forecast of ICON-D2 (EPS), exhibits a range of 65 mm to 140 mm. At specific locations, approx. 30 mm of precipitation had already been recorded by that point. The green line indicates the deterministic model run. This was the starting point for the initiation of our flood control centre.

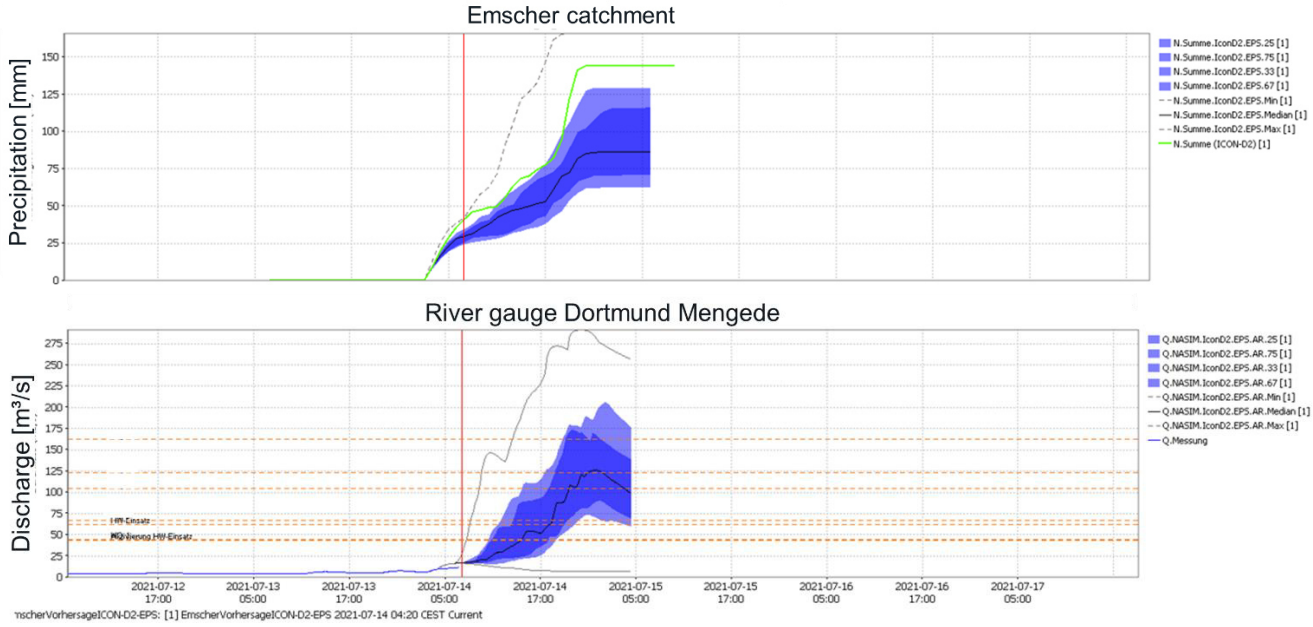

Fig 1: Simulated precipitation amount for the Emscher region and resulting discharges at river gauge Dortmund-Mengede on 14.07.2021 at 06:00 a.m. CEST (model run from 03:00 a.m.)

Following a period of reduced rainfall and significant downward corrections of the afternoon forecasts, the predicted discharge levels in the Emscher river reached a magnitude equivalent to a HQ-25 event. This became the final opportunity to coordinate additional actions such as evacuations or reinforcing dykes in collaboration with local authorities. However, from 6 p.m. onwards, heavy rainfall occurred in the eastern Emscher area, which was not accounted for in the forecast models. As a result, the eastern Emscher Area experienced a HQ-100 event and even a HQ-200 in the middle Emscher area was measured. Thus, the extreme values initially forecasted in the morning were at least reached in some areas. Precipitation measurements in the Dortmund area ranged from 110 mm to 120 mm, serving as a reliable benchmark for the forecast situation at 6 a.m.

Drawing from the lessons learned during the July flood event, the EG has developed a Crisis Flood Roadmap, which outlines measures across various areas of focus in relation to flood forecasting. One of the initial measures implemented was to initiate new model runs every 15 minutes, as the previous update schedule of 30 minutes proved inadequate for capturing such dynamic developments. Additional action items related to flood forecasting include the implementation of online hydrologic models for tributaries, establishment of new river gauges, automation of risk assessments for potential pumping station failures, and the development of a communication platform for both internal and external information dissemination. Central to these efforts is the clear and concise presentation of uncertainties and their impacts on water bodies. Emphasizing the comprehensibility of these uncertainties, as well as their implications, is vital. Furthermore, it is crucial to enhance the management and understanding of uncertainties through exercises conducted with internal and external partners. Several examples will be provided on this subject. Moving forward, a joint workshop with the Regional Weather Advisory Service of the German Weather Service will be prepared focusing on these matters.

References

Deutscher Wetterdienst (2022): DWD Database Reference for the Global and Regional ICON and ICON-EPS Forecasting System.
<https://www.dwd.de/SharedDocs/downloads/DE/modelldokumentationen/nwv/icon/icon_dbbeschr

_aktuell.pdf;jsessionid=F167135DC50EE3B44FFFBD062D821D37.live31092?view=nasPublication&nn=13934> last access: 25.05.2023
ECMWF (2022): Limited Area Ensemble Prediction System (COSMO-LEPS). https://www.ecmwf.int/en/forecasts/dataset/limited-area-ensemble-prediction-system. Last access 30.5.2023

Evaluation and integration of professional and opportunistic high-resolution rainfall observations in the Öresund region

R. van de Beek*[1], J. Mosekær Nielsen[2], S. Liedtke Thorndahl[2], J. Olsson[1], J.C.M. Andersson[1], J. Ellerbæk Nielsen[2], M.R. Rasmussen[2]

1 Hydrology Research, Swedish Meteorological and Hydrological Institute (SMHI), Sweden
2 Department of the Built Environment, Aalborg University (AAU), Denmark

*Corresponding author: remco.vandebeek@smhi.se

Abstract

The Öresund region (western Scania (Sweden) and eastern Zealand (Denmark); a.k.a. greater Copenhagen) has been hit by a few notable extreme rainfall events during the 2000s. In 2011, 135 mm of rainfall in 24 h, with most of it in a few hours, flooded Copenhagen leading to severe pluvial flooding and damages totaling more than 650 MEUR. In 2014, parts of Malmö city were hit by some 100 mm in 6 h, leading to the worst and most expensive pluvial flooding on record in Sweden (~80 MEUR). These events have spawned a lot of R&D related to observations and forecasts of heavy rainfall in both countries.

In this work, the Öresund region is often used as a case study area. This is largely owing to the excellent availability to high-resolution rainfall observations from different sensors (Table 1):

- Professional rainfall gauges: On the Danish side there is a particularly dense network operated by SVK, with some 70 gauges in the region. On the Swedish side there are some 30 gauges from the national network of automatic stations as well as a similar number of gauges operated by water utilities.
- Weather radar: The areas on both sides of Öresund are covered by C-band radars in the national networks as well as X-band radars (2 in Sweden, 1 in Denmark). Furthermore, a vertically pointing Micro Rain Radar (MRR) is explored on the Swedish side.
- Commercial microwave links (CML): Data are available from selected link networks on both sides of Öresund, mainly covering urban areas.
- Private weather stations (PWS): In this collaboration, we have access to observations from extensive networks of Netatmo gauges on both sides of Öresund.

Within the framework of the COST Action OPENSENSE, a collaboration between SMHI and AAU has been initiated in spring 2023. The overall focus of the collaboration is to explore how to make best use of this multitude of available high-resolution rainfall observations from different sensors, ultimately for (urban) flood risk assessment as well as other urban hydrological applications. The collaboration has a range of sub-objectives, including e.g.:

- Correction of C-band radar based on opportunistic data (i.e. CML and PWS data). This has recently been explored on the Danish side, e.g. by implementing the quality control procedure of de Vos et al. (2019).
- Multi-scale sensor fusion for tailored applications. This is being developed and tested on the Swedish side, aiming at quantifying performance at different scales, to aid subsequent use of the fused rainfall product (see e.g. van de Beek et al., 2020).
- Accuracy of PWS data. This is being evaluated on both sides of Öresund, as a key component of the use of PWS data in the above applications.

In this presentation, we will show and discuss updated results from the different components of the collaboration. One example is the relevance of merging different types of opportunistic data to obtain an improved rainfall product from opportunistic rainfall sensors, as well the importance of appropriate filtering (Figure 1). Furthermore, we will elaborate on subsequent applications of the

Tab 1: Overview of high-resolution rainfall observations in the Öresund region.

Sensor	Swedish side	Danish side
Professional rainfall gauges	~60	70
Weather radars	2 C / 2 X	1 C / 1 X
Commercial microwave links	286 sublinks	373 sublinks
Private weather stations	many	>1000

improved rainfall products generated, e.g. for nowcasting or for hydrological and hydraulic modelling. We hope and believe our efforts will help to make the region more “water wise” and “climate proof”.

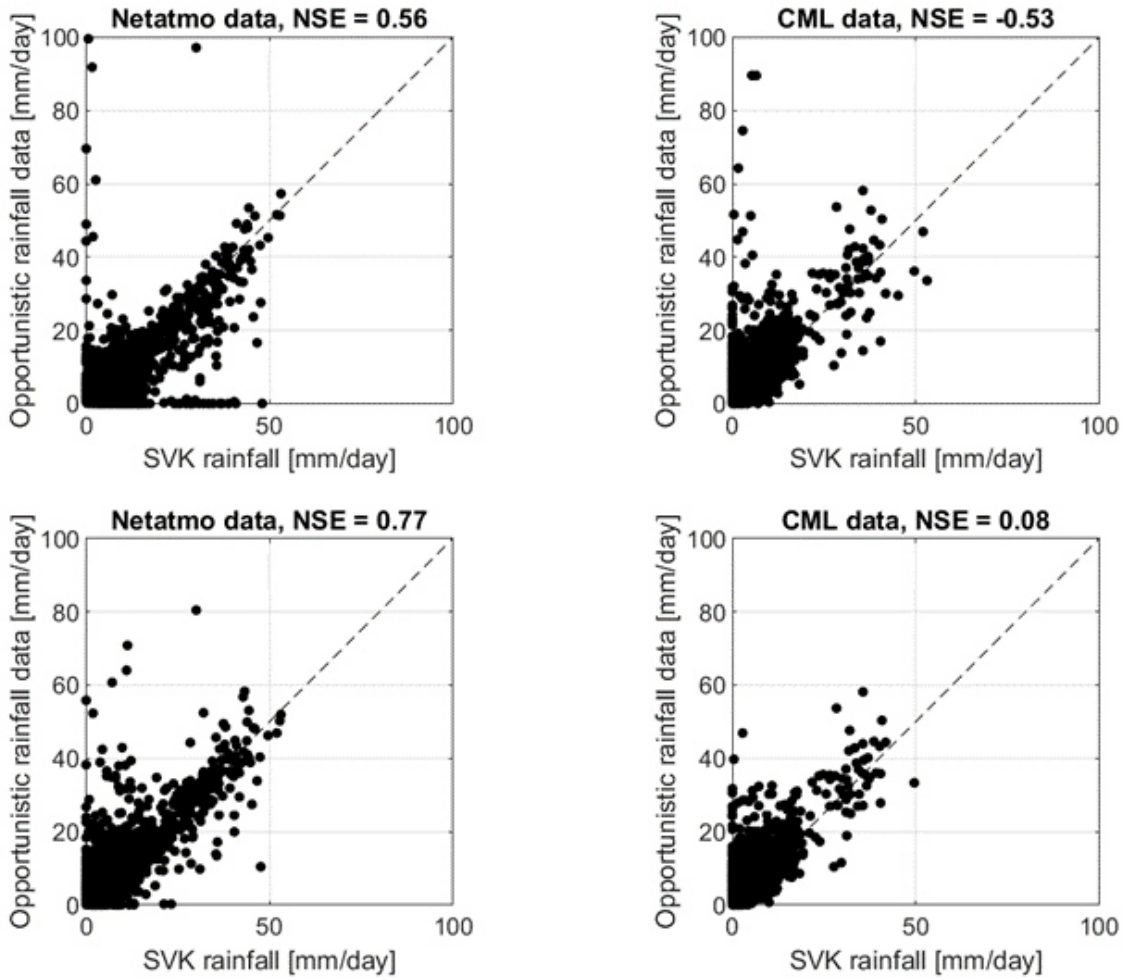

Fig 1: Unfiltered opportunistic data (topmost figures) and filtered opportunistic data (bottommost figures) after applying the method of de Vos et al. (2019) compared to official gauges within a range of 1 km from the opportunistic sensor.

References

van de Beek, R. (C.Z.)., Olsson, J., and Andersson, J. (2020), Optimal grid resolution for precipitation maps from commercial microwave link networks, Adv. Sci. Res., 17, 79-85, https://doi.org/10.5194/asr-17-79-2020.

de Vos, L. W., Leijnse, H., Overeem, A., and Uijlenhoet, R. (2019), Quality control for crowdsourced personal weather stations to enable operational rainfall monitoring, Geophys. Res. Letters, 46, 8820-8829, https://doi.org/10.1029/2019GL083731.

Soil-pipe system as an element of climate-adapted urban drainage (BoRSiS)

H. Walther*[1], M. Quirmbach[1]

1 Institute of Civil Engineering, University of applied sciences Ruhr West, Germany

*Corresponding author: henrike.walther@hs-ruhrwest.de

Abstract

The “soil-pipe system as an innovative element of climate-adapted urban drainage” (BoRSiS) research project addresses adaptation strategies to climate change. The project combines tree pit systems with existing street pipe trenches and rainwater storage elements. It provides a storage space for rainwater and, thus, helps to relieve the stormwater sewer system during heavy rain events and to prevent flooding in cities. In addition, some of the absorbed water can percolate and is used to water the trees in the tree pits (Rockwool 2021)The pipe trenches provide previously unused space for water storage and for the root zone of the trees without requiring additional space on the surface. As a result, the root space of the trees can be increased and the trees can continue to grow. The retarded release of water from the water reservoir implies that the trees can be watered for a longer period of time. These factors ensure better vitality and longevity of the trees at the tree pits. The vital and large trees have, in turn, a positive effect on the urban micro-climate by helping to minimize urban heat island effects through the evaporation of water and the provision of shade (Back et al. 2022).

In order to be able to employ the previously unused line trench as storage for rainwater and root space, a change in current practice is necessary. Currently, pipe trenches are heavily compacted to ensure a stable bedding of the pipes. Roots should be kept away from the pipe trench as much as possible. Pipes made of ductile cast iron, as manufactured by the members of the industry partner EADIPS®/FGR® e. V., can be bedded in pore-rich, coarse-grained material and are root-resistant. Tree roots can grow into the trench of this soil-pipe system without damaging the pipe (EADIPS FGR 2022). Industry partner Rockflow is supplying the storage element for this project. The Rockflow material, which was developed from rock wool and has a higher storage capacity (93 percent in volume) than gravel bodies, will be installed in the pipe trenches and directly below the tree pits. The material is currently used for decentralized infiltration and finds a new function as a storage body in this project. The overall system can be seen in Figures 1 and 2. Figure 1 shows an overview of the system in a top view. Figure 2 shows the functioning of the system in more detail through a cross-section.

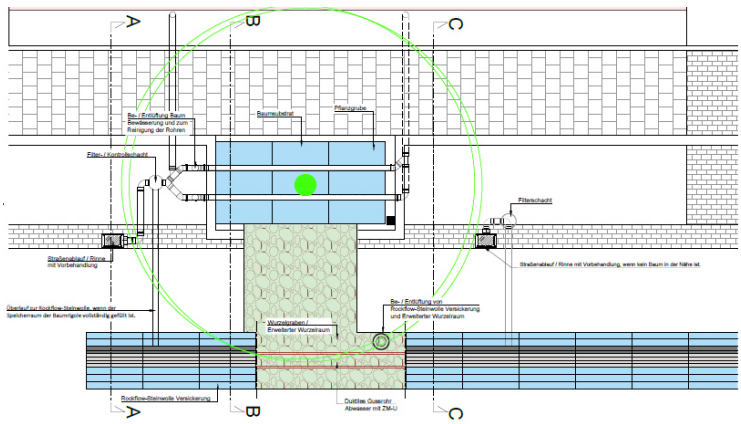

Figure 1: Site plan of the soil-pipe system

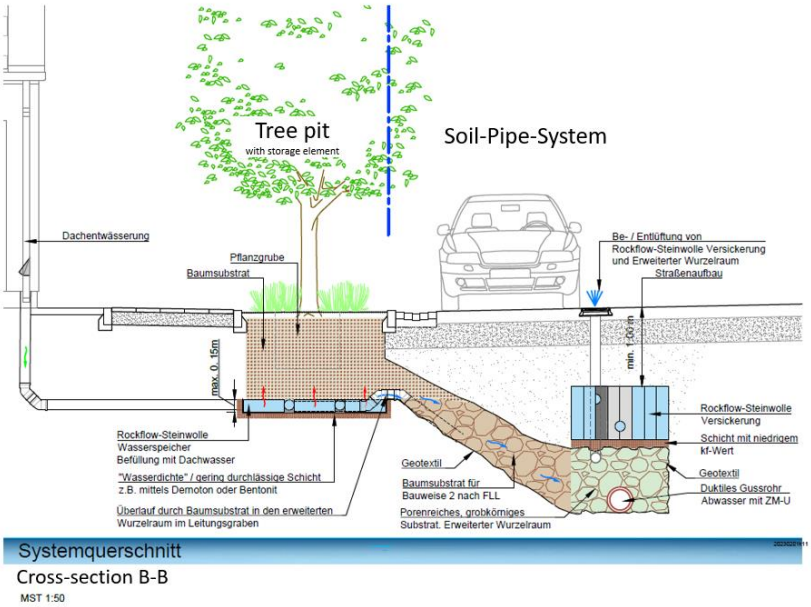

Figure 2: Cross-section B-B through the soil-pipe system

As part of the project, an assessment of different urban climate change adaptation measures was completed through a newly created assessment matrix. This shows possible synergies with other measures and helps to place the soil-tube system in the overall context of the sponge city concept.

Moreover, an analysis of air temperature and precipitation time series has been undertaken to estimate the frequency of heavy rainfall events followed by dry periods. The aim of the analysis is to estimate for which types of event combination can the system thrive or be overcharged. This information is essential for the development of a holistic heavy rainfall and climate adaption concept. To ensure that the system performs properly, initial evaporation tests are being implemented out with rock wool and a test stand is being set up to model the root trench. With this test facility, the hydraulic properties of different soil materials and their interactions are investigated. For the same materials, grading curve tests and load tests are being carried out in the geotechnical laboratory. Furthermore, a cost and a cost-benefit analysis are currently being conducted for all the proposed products, so that a cost overview can be produced.

The project is scheduled to be completed by September 2024. Within the project time frame, all elementary tests should be performed and the project will be implemented in several cities. In the cities, the project can be installed in new construction sites, as shown so far. However, it is also possible to implement parts of the project in existing structures.

References

Back, Y.; Bach, P.; Jasper-Tönnies, A.; Rauch, W.; Kleidorfer, M.; (2022): Mapping ecological and human systems responses to land-atmosphere interactions altered by climate change, EGU General Assembly 2022, Vienna, Austria, 23-27 May 2022, https://doi.org/10.5194/egusphere-egu22-3411

EADIPS FGR (2022): Rohre, Formstücke & Armaturen aus duktilem Gusseisen. https://eadips.org/ (last accessed on 22.04.2023)

Rockwool (2021): Rockflow, Städtische Klimaanpassung mit Sickerlösung aus Steinwolle. https://www.rockwool.com/de/produkte/rockflow/ (last accessed on 24.04.2023)

Exploring the use of 3D radar measurements for predicting the lifespans of single-core convective rain cells

L.-P. Wang*[1], Y.-S. Cheng[1]

1 Department of Civil Engineering, National Taiwan University, Taipei, Taiwan

*Corresponding author: lpwang@ntu.edu.tw

Abstract

Object-based radar rainfall nowcasting is a widely-used technique for convective storm prediction. Due to the data and algorithmic limitations, most existing object-based nowcasting methods focus on predicting the movements of each rain object (or cell). The evolution of rain cells' properties (e.g. cell size, shape and intensity) themselves is often neglected or assumed to be unchanged. It is however critical to account for the temporal changes in cells' properties in order to improve the predictability for convective storms (Radhakrishna et al., 2012).

In the literature, three-dimensional (3D) radar images have been used for observing the vertical feature changes through the formation process of convective rain cells. This shows the potential of extracting useful information from 3D images to facilitate characterising the life cycle of rain cells. Most of these works however focused on analysing or reconstructing the life cycles of individual convective rain cells or storm events. It remains an open challenge to incorporate 3D radar rainfall information into object-based radar rainfall nowcasting.

In this research, we explored the use of deep learning techniques to predict the evolution of single-core convective rain cells. The proposed work comprises two main parts. The first part is rain cell data preparation. An enhanced TITAN storm tracking algorithm proposed by Muñoz et al. (2018) is employed to identify 2D rain cells and their temporal associations (or tracks) across successive time steps. The information of 2D cells are then used to extract cell properties from 3D radar images. These include mean reflectivity, area, major and minor axis lengths and the convective core altitude of each rain cell. In the second part of the work, a LSTM-Encoder-Decoder model is developed, which uses cells' properties from the past 10-15 min to predict the evolution of these properties in the next 15 min.

A total of 4708 lifespans of rain cells extracted from high-resolution (5-min, 1 km, 24 levels) 3D radar images provided by the UK Met Office are used to train the model, and a total of 1177 extracted lifespans are used to validate the prediction result. The result suggests that the proposed LSTM-Encoder-Decoder model can well predict the evolution of cells' properties at various life stages (i.e. developing, mature and dissipating; see Figure 1), and, with the employed 3D information (convective core altitude), the prediction errors of mean reflectivity can be effectively reduced by 20-25% at 15-min forecast lead time (see Figure 2). In addition, two innovative methods are proposed to estimate the prediction uncertainty. The first one is based upon the statistical analysis of the errors between the observed and the predicted estimates of the cell properties. The second one is inspired by the widely-used weather analog methods. That is, we search for the historical rain cells whose properties are sufficiently close to those of the predicted cell at each forecasting lead time. The properties of these 'similar' cells then constitute the estimation uncertainty. Our results suggest that both methods can well represent the prediction uncertainty (i.e. the percentage of predictions falling within the uncertainty range is >80% at 15-min lead time).

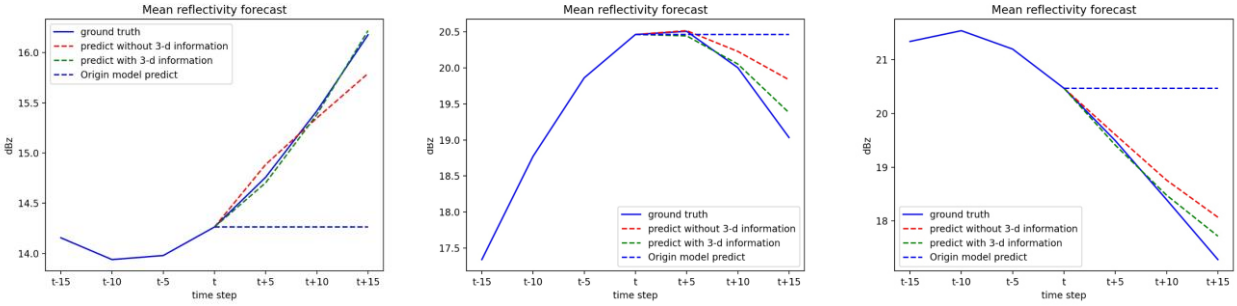

Developing Mature Dissipating

Fig 1: The proposed LSTM-Encoder-Decoder model can well predict the evolution of the mean intensities of a single-core convective cell at different life stages with the help of 3D radar measurements (from left to right, developing, mature and dissipating).

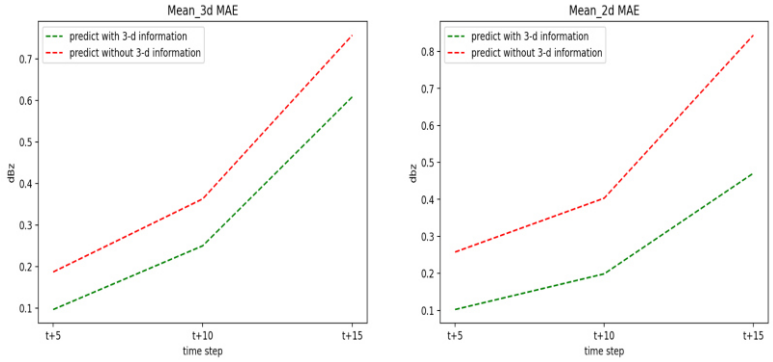

Fig 2: MAE estimates for predicting both 2D and 3D mean intensities are largely reduced with the help of 3D radar measurements.

References

Muñoz, C., Wang, L.-P., and Willems, P. (2018), Enhanced object-based tracking algorithm for convective rain storms and cells, Atmospheric Research, 201, 144-158, https://doi.org/10.1016/j.atmosres.2017.10.027

Radhakrishna, B., Zawadzki, I., and Fabry, F. (2012), Predictability of Precipitation from Continental Radar Images. Part V: Growth and Decay, J. Atmos. Sci., 69, 3336-3349, https://doi.org/10.1175/JAS-D-12-029.1.

HoWa-Pro: A project setting up a flood risk warning system using radar-, rain gauge- and opportunistic data from telecommunications network

M. Wenzel*[1], C. Vogel[1], A. Stefanova[2], J. Sallwey[2], A. Philipp[2], J. Grundmann[3], M. Wagner[3], M. Müller[4], M. Graf[5], C. Chwala[6], T. Winterrath[1]

1 Deutscher Wetterdienst - Hydrometeorologie, Offenbach am Main, Germany
2 LHWZ Saxony, Dresden, Germany
3 Institute of Hydrology and Meteorology - University of Dresden, Dresden, Germany
4 PIKOBYTES GmbH, Dresden, Germany
5 Institute of Geography - University of Augsburg, Augsburg, Germany
6 Institute of Meteorology and Climate Research - Karlsruhe Institute of Technology, Garmisch-Partenkirchen, Germany

*Corresponding author: Malte.Wenzel@dwd.de

Abstract

Especially heavy rainfall can cause damage to public and private infrastructure, e.g. by overflowing drainage systems in urban areas. To reduce the risk reliable and precise flood risk warning systems are essential. In the project HoWa-Pro [1] radar, rain gauge and data from opportunistic sensors from a telecommunication network are combined to set up a flood risk warning system. We contribute the software framework, which processes these different data.

Rainfall leads to attenuation of the signal level along a commercial microwave link (*CML*). Chwala and Kunstmann [2] have shown, that applying the k-R-relation (with k = specific attenuation and R = rain rate) to the CML attenuation results in additional quantitative precipitation estimations (*QPEs*). We use CML-QPEs in addition to the observation network of the DWD consisting of weather radars and rain gauges to generate new precipitation products.

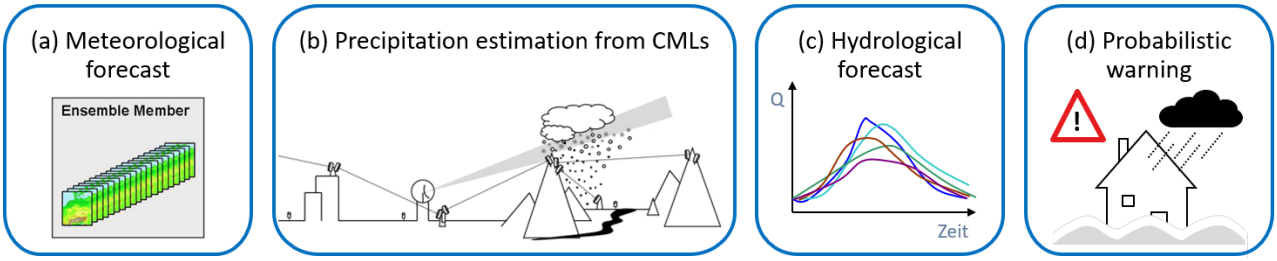

Fig 1: Processing steps of the HoWa-Pro flood risk management system

These new products and meteorological forecast products (e.g. ICON-D2) build the starting point to generate hydrological 48 hours forecasts once an hour like shown in Fig 1. The results of actual and former hydrological forecasts are presented in an interactive dashboard to optimize disaster management.

One of the key parts in the system is the radar QPE from DWDs radar composite. An algorithm called RADOLAN [3] produces the composite of radar QPE with high spatial resolution from 17 locations in Germany (Fig 2 (a)) every 5 minutes. To improve the quality of the radar QPE the data are adjusted with precipitation measurements from ~1500 rain gauges (Fig 2 (b)) with a time resolution down to one minute and a delivery time of ~20 minutes. This adjustment process runs every ten minutes with an accumulation time of one hour in operational mode at DWD.

We redesigned the adjustment algorithm of RADOLAN [3] and increased the time resolution by reducing the accumulation time down to the smallest possible time interval depending on the data

types. For example, rain gauge data are delivered in ten minutes intervals, but can yield a measurement resolution down to one minute.
To obtain a more frequent availability of products we included CML data with low latency from Germany's telecommunications network. For this purpose, a continuous data flow from Ericsson of roughly 10000 CML signals (Fig 2 (c)) to DWD has successfully been implemented. All specifications of the data used in the new adjustment process are listed in Tab 1.

(a) (b) (c)

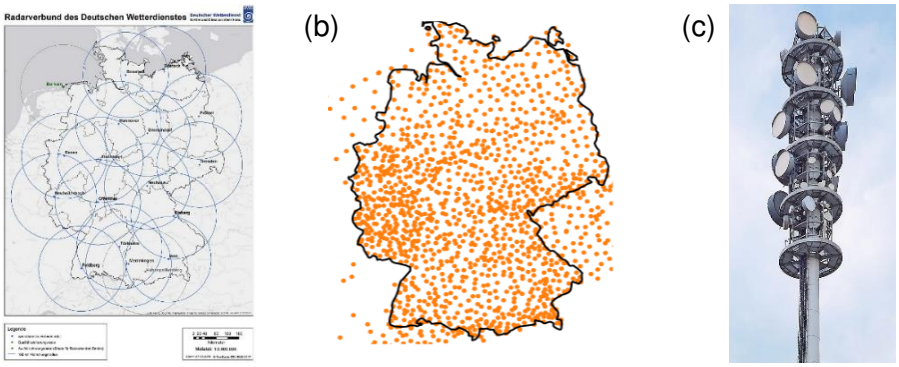

Fig 2: (a) DWDs radar network, (b) ~1500 rain gauges covering Germany, (c) Photo (© Cynthia Ruf) of a CML antenna

Tab 1: Summary of data specifications used in the adjustment process.

Data type	Format	Locations	Time interval of delivery	Time resolution of measurement	Delay of file delivery
Radars	Binary	17	5min	5min	~3min
Rain gauges	BUFR	~1500	10min, 60min	1min, 10min, 60min	5-20min
CML antennas	JSON	~10000	1-5min	10sec	~2min

First, we've implemented software modules to combine the different data individually. Based on this we are developing new adjustment procedures to potentially further improve the QPE compared to RADOLAN [3].
This framework will be part of the flood risk warning system according to Fig 1 (b). Especially the time resolution of ten seconds and availability with a delay of only about two minutes makes CML data suitable for use in fast flood risk warning. Another advantage of data from opportunistic sensors is that the amount of CML antennas exceeds the amount of rain gauges by far as described in Tab 1.

At DWD we set up a modular and flexible software to process and combine all data in routine mode. We introduce the system and show the potential of using opportunistic data in flood risk warning systems.

References

[1] https://www.wasser.sachsen.de/howa-pro.html, accessed in June 2023

[2] Chwala, Christian and Harald Kunstmann. "Commercial microwave link networks for rainfall observation: Assessment of the current status and future challenges." *Wiley Interdisciplinary Reviews: Water* 6.2 (2019): e1337

[3] https://www.dwd.de/DE/leistungen/radolan/radolan.html, accessed in June 2023

A new member of the DWD radar product palette

T. Wilke*[1], K. Lengfeld[1]

1 Deutscher Wetterdienst, Offenbach am Main, Germany

*Corresponding author: tabea.wilke@dwd.de

Abstract

Rainfall data are essential for weather forecasting, hydrological modeling, and climate research. Especially after the flood catastrophe in western Germany in July 2021, heavy rainfall events are more and more in the focus of public attention.

For climatological analysis long and homogeneous time series play an important role, allowing e.g. much more precise evaluation of return periods. The German gauge network can give some of those long time series already combined on a grid (Junghänel, Dr. Ostermöller, & Dr. Deutschländer, 2022). However, as a precipitation event can evolve rapidly in space and time, many of the short and mostly small-scale events are missed by station measurements. In order to still be able to account for these events, we make use of radar data that provide a complete spatial coverage of Germany. Using the RADOLAN (Radar Online Adjustment) (Bartels, et al., 2004; Winterrath, Rosenow, & Weigl, 2012) approach, we adjust the precipitation estimates from the radar data with the station data to get the best of both datasets.

The German radar network consists of 17 C-band radars. Of these, 16 are equipped with dual-polarization technology since 2015. In 2021, the last remaining radar (on the Borkum island in North-West Germany) was also upgraded with the new technology. Each radar produces ten volume scans and one terrain-following low-elevation scan every five minutes. After local quality control algorithms, the local data are combined to a composite.

The goal of radar-based climatologies is to assess the spatio-temporal distribution of precipitation events, their possible hotspots, and regions at high risk of heavy precipitation. In Germany, we can benefit at the moment from a high spatial resolution of grids with at least 1 km² and a high temporal resolution of up to 5 minutes. The existing radar climatology RADKLIM covering 2001 until now by the Deutscher Wetterdienst (Winterrath, et al., 2017) focuses on homogeneity. This limits the possibility of using improvements, which have been available in the meantime, especially those, which could be applied only to individual radar sites.

The idea for the new member of the radar product palette is to use the best possible product at all times. As a result, the climatology cannot be homogeneous. Where possible, the new product uses the new radar range where possible of 150 km with 250 m resolution, as opposed to RADKLIM's 128 km with 1 km resolution. Another improvement is the use of dual-polarization moments. In recent years, all radar sites have been upgraded with this technology, which makes it easier to detect echoes that do not belong to precipitation, and improves the hydrometeor classification and thus the precipitation estimates. Furthermore, we can make use of the currently operational quality assurance that have been developed in recent years. RADKLIM uses its own correction methods, which cannot be directly mapped to those currently used.

This work presents the first results of the new radar climatology and compares it to the RADKLIM. We attempt to provide an overview of the benefits of using improved technology and algorithms, and the limitations imposed by inhomogeneity, starting with simple differences and then going to a deeper statistical level.

References

Bartels, H., Weigl, E., Dr. Reich, T., Lang, P., Wagner, A., Kohler, O., & Gerlach, N. (2004). *Projekt RADOLAN-Routineverfahren zur Online-Aneichung der Radarniederschlagsdaten mit Hilfe von automatischen Bodenniederschlasstationenen (Ombrometer): zusammenfassender Abschlussbericht für die Projektlaufzeit von 1997 bis 2004.*

Junghänel, T., Dr. Ostermöller, J., & Dr. Deutschländer, T. (2022). KOSTRA-DWD-Datensatz Version 2020. *https://opendata.dwd.de/climate_environment/CDC/grids_germany/return_periods/precipitation/KOSTRA/KOSTRA_DWD_2020/*.

Winterrath, T., Brendel, C., Hafer, M., Junghänel, T., Klameth, A., Walawender, E., . . . Becker, A. (2017). *Erstellung einer radargestützten Niederschlagsklimatologie.* Berichte des Deutschen Wetterdienstes Nr. 251.

Winterrath, T., Rosenow, W., & Weigl, E. (2012). On the DWD quantitative precipitation analysis and nowcasting system for real-time application in German flood risk management. *IAHS-AISH publication*(351), S. 323-329.

The DWD Catalogue of Radar-based heavy Rainfall Events (CatRaRE) and its application in hazard and risk analysis

T. Winterrath*[1], K. Lengfeld[1], E. Walawender[1], E. Weigl[1], S. Hänsel[1]

1 Department of Hydrometeorology, Deutscher Wetterdienst, Germany

*Corresponding author: tanja.winterrath@dwd.de

Abstract

Heavy precipitation events, especially convective storms, often occur on a local scale and are therefore hard to detect by traditional ombrometer networks. Additionally, the meteorological and hydrological impacts depend on the areal extent of the rain event with large areas with high intensity rainfalls leading to potentially extreme responses. Radar-based areal precipitation monitoring is therefore necessary to study and characterize heavy rainfall events. DWD has developed the **Cat**alogue of **Ra**dar-based heavy **R**ainfall **E**vents (CatRaRE; Lengfeld et al., 2021) that lists all extreme precipitation events in Germany since 2001. The catalogue is based on the radar-based precipitation climatology RADKLIM (Winterrath et al., 2018) that has been presented at the Urban Rain conference in 2018.

In CatRaRE precipitation events are defined by several attributes describing the place and time of the event, event-specific meteorological characteristics, as well as external features of the surrounding, e.g. topographic position index and population density. An event is defined by specific criteria applied in the following steps:

- detection of adjacent pixels with duration-specific intensities above a defined threshold (e.g. DWD's warning level 3) under the constraint of a defined minimum size resulting in so-called objects,
- checking independence in space and time of the detected objects of different durations between 1 and 72 hours,
- selection of the one object with the highest extremity according to the concept of the Weather Extremity Index (WEI) by Müller and Kaspar (2014) as representative resulting in so-called events.

The catalogue can be downloaded from DWD's open data server. For an easy access an online WebGIS visualization is provided (Fig 1).

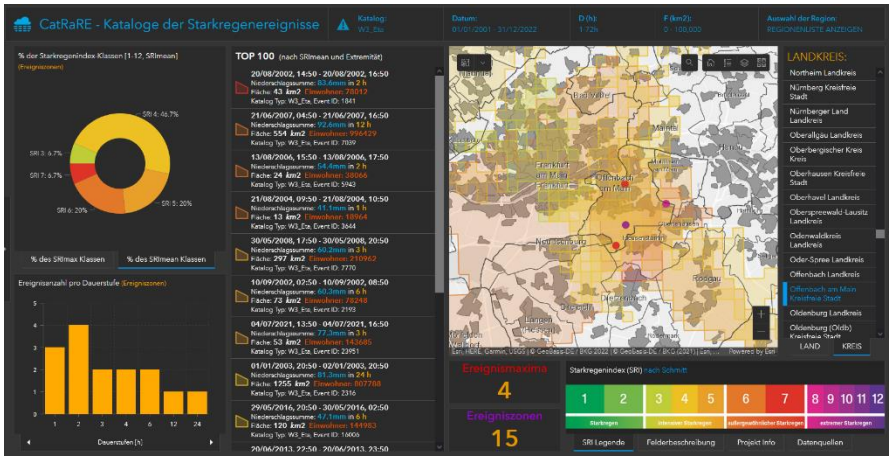

Fig 1: Screenshot of the online CatRaRE dashboard available at https://arcg.is/1HDqH5 showing the heavy precipitation events that have hit the German city of Offenbach between 2001 and 2022.

The catalogue's events are thus characterized by time and location, a specific duration, areal extent and mean precipitation intensities and combined with additional external attributes. The catalogue allows Germany-wide statistical analyses on spatial and temporal distributions of heavy rainfall events including the event-specific attributes like duration and area. Figure 2 shows the annual number and accumulated area of all heavy precipitation events of duration between 1 and 72 hours in Germany since 2001. Both attributes show large annual variations. In 2002 – the year with the huge flooding of the Elbe river – the maximum area has been observed, while in 2018 the highest number of events has been observed, although 2018 is known for the extreme precipitation deficit during summer. Number as well as area show an slightly increasing trend over the last 22 years. It will be interesting to monitor the further development and potential correlations with climate change.

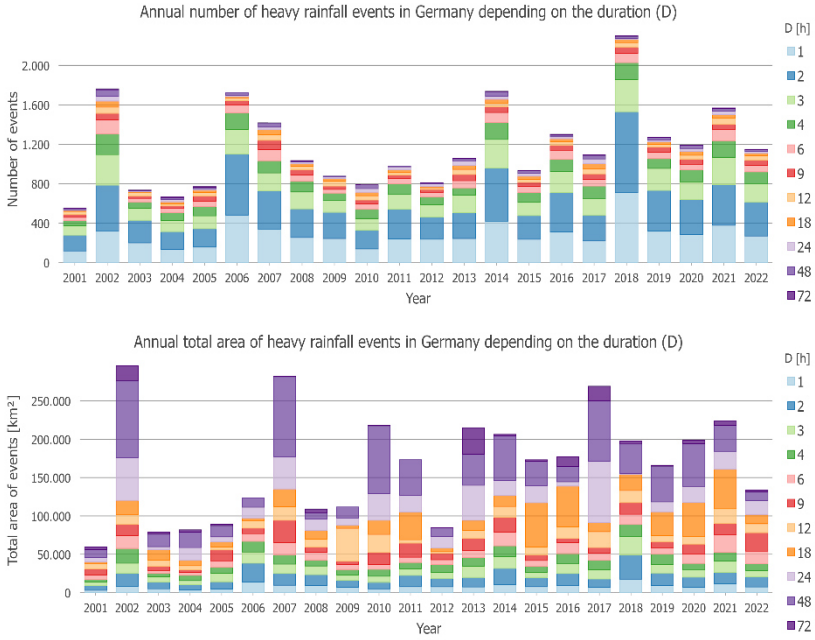

Fig 2: Annual number (top) and accumulated area (bottom) of extreme precipitation events in Germany according to CatRaRE.

CatRaRE has been used for several applications. These comprise studies of a potential urban effect on precipitation, statistics on urban areas in Germany affected by heavy precipitation events, and works towards hazard and risk mapping for prevention and impact-oriented forecasting. In this presentation we will introduce CatRaRE and present a selection of applications focusing on urban rain events.

References

Lengfeld, K., Walawender, E., Winterrath, T., and Becker, A. (2021), CatRaRE: A Catalogue of radar-based heavy rainfall events in Germany derived from 20 years of data, Meteorologische Zeitschrift, 30, 6, 469 - 487, DOI: 10.1127/metz/2021/1088.

Müller, M., and Kaspar, M. (2014), Event-adjusted evaluation of weather and climate extremes. – NHESS, 14, 473 - 483, DOI:10.5194/nhess-14-473-2014.

Winterrath, T., Brendel, C., Hafer, M., Junghänel, T., Klameth, A., Lengfeld, K., Walawender, E., Weigl, E., and Becker, A. (2018), RADKLIM Version 2017.002: Reprocessed gauge-adjusted radar-data, one-hour precipitation sums (RW), DOI: 10.5676/DWD/RADKLIM_RW_V2017.002.

Association between urban morphology and the spatial distribution of pluvial floodwater

Y. Zhu[1], S. Fatichi[2], P. Burlando[1]

1 Institute of Environmental Engineering, ETH Zurich, Switzerland
2 Department of Civil and Environmental Engineering, College of Design and Engineering, National University of Singapore, Singapore

*Corresponding author: yuezhu@ethz.ch

Abstract

With the ongoing effects of climate change, cities worldwide are witnessing more intense rainfall and frequent flooding events. Moreover, the growing global population induces a continuous expansion of urban areas, which, in turn, plays a crucial role in altering the permeability of land cover, further enhancing the occurrence of flood hazards in many cities. However, the relationship between urban morphology and pluvial flooding has received limited attention.

Using a cellular automata-based model (Guidolin et al., 2016), we conducted simulations to analyze the distribution of pluvial floods in an urban catchment characterized by diverse urban morphologies (Fig. 1). Subsequently, a series of regression models were adopted to uncover hidden relationships between urban landscape metrics and the spatial distribution of pluvial floodwater. The effects of different landscape metrics on the spatial distribution of pluvial floodwater were quantitatively measured. The analysis results indicate that, although the total area of impervious surfaces plays the most significant role in floodwater distribution, the morphology of building footprints and impervious surfaces also influence this process (Fig. 2). The findings of this study can provide insights for urban planners in promoting flood-resilient urban development.

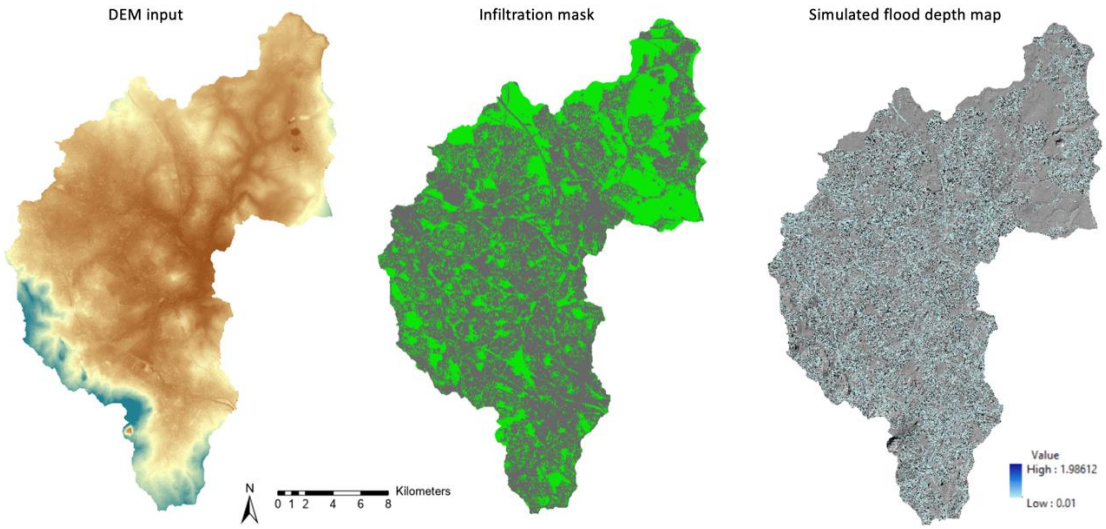

Fig. 1 The Inputs and outcomes of flood simulation

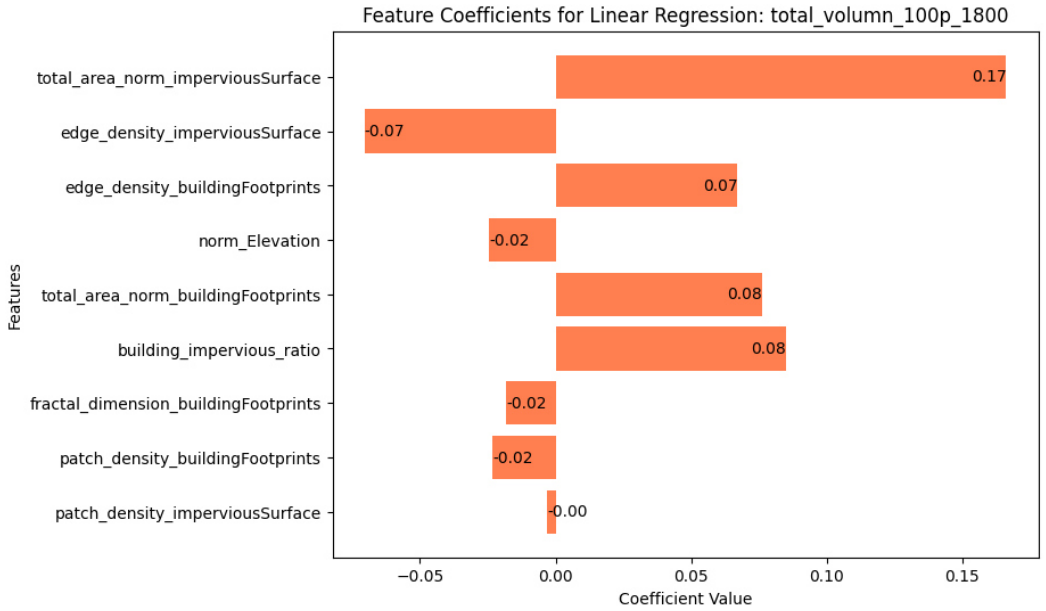

Fig. 2 Coefficients of linear Regression for the relationships between landscape metrics and flood inundation

References

Guidolin, M., Chen, A. S., Ghimire, B., Keedwell, E. C., Djordjević, S., & Savić, D. A. (2016). A weighted cellular automata 2D inundation model for rapid flood analysis. Environmental Modelling & Software, 84, 378-394.

Land-water-atmosphere interactions and urbanization effects on precipitation: insights from the coastal city of Shanghai

Qi Zhuang[1,2], Marika Koukoula[2], Nadav Peleg[2]

1 Department of Hydraulic Engineering, Tongji Univerisity, China.
2 Institute of Earth Surface Dynamics, University of Lausanne, Switzerland.

*Corresponding author: Qi.Zhuang@unil.ch

Abstract

Extreme precipitation is becoming more common and more severe due to urban expansion and global climate change. Urbanization also contributes to the increase in impermeable areas in cities. Due to these two factors, flash floods are becoming more frequent and more destructive in cities. Cities along the coast are particularly vulnerable to flooding as extreme rainfall is further influenced by the land-sea breeze and the complex interactions between the land, water, and atmosphere. Hence, improving the understanding of urbanization effects on precipitation in coastal cities is of great concern. We quantitatively analyze the effects of urbanization and land-water-atmosphere interactions on two types of precipitation, typhoon and convective rainfall, in the city of Shanghai (Fig. 1). In addition to being a coastal megacity in China, Shanghai is also surrounded by large lakes and rivers. The complex landscape effects on extreme precipitation are studied using the Weather Research and Forecasting (WRF) model, considering the urban canopy and different underlying land cover, such as the Taihu Lake and the East China Sea, and different urbanization and climate change scenarios. Implications of the results are valuable for urban design and flooding control management in Shanghai and are relevant to other coastal cities that are experiencing fast urbanization.

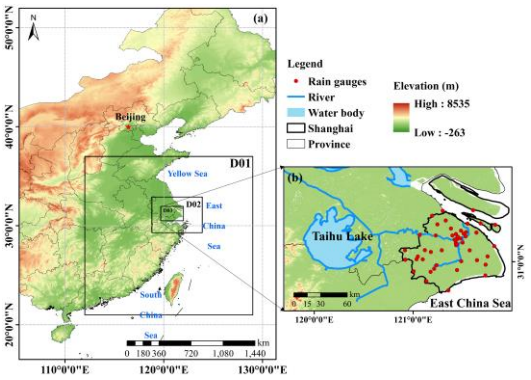

Fig. 1: Study region. (a) WRF simulation area of three nested domains. (b) The innermost domain (D03) with rain-gauge locations covers Shanghai areas.

Spatial downscaling of heavy rainfall with a multiple-point geostatistics model: Beijing case study

Wenyue Zou[1]*, Guanghui Hu[1] , Pau Wiersma[1] , Shuiqing Yin[2], Grégoire Mariethoz[1], Nadav Peleg[1]

[1] Institute of Earth Surface Dynamics, University of Lausanne, Lausanne, Switzerland
[2] State Key Laboratory of Earth Surface Processes and Resource Ecology, Faculty of Geographical Science, Beijing Normal University, Beijing 100875, China

*Corresponding author: wenyue.zou@unil.ch

Abstract

High-resolution gridded rainfall products at sub-daily and 10^0 km scales are required for hydrological applications in urban catchments. As most cities are ungauged, gridded rainfall data are often obtained through remote sensing. However, their spatial resolution is often too coarse (at 10^1 km) and requires to be downscaled to a finer resolution. The challenge is not only to downscale the rainfall intensity to a finer scale by considering areal reduction factors but also to downscale the spatial structure of the storm, as both elements are equally important to the assessment of the surface hydrological response. As a result of the lack of training data, the latter is difficult to obtain. Further development of the stochastic multiple-point geostatistics (MPS) framework is presented to downscale long-term satellite-derived gridded rainfall series using only a few years of high-resolution rainfall observations. We demonstrate how the MPS framework can be used to downscale the CMORPH rainfall from 8 to 1 km resolution for the period 1998 - 2019, taking the city of Beijing as a case study, with a specific focus on extreme rainfall events. The high-resolution CMPAS dataset (1 km, hourly), available for 2015-2020, is used as the source of the training images. We show that the downscaling framework preserves the observed mean areal rainfall (with a bias of 2%), reproduces the spatial coefficient of variance (with a bias of 2%), and extreme rainfall at the 99th percentile (with a bias of 6%). Additionally, it also adequately reproduces the rainfall spatial structure, preserving the variograms of the rainfall fields. Similarities were also observed comparing the 2- to 30-year return periods maps of the downscaled rainfall extreme with ground observations. The results indicate that the MPS method downscales rainfall intensities and preserves the spatial structure well, especially for heavy rainfall, even if limited data is available. The proposed downscale approach can be applied to other rainfall datasets and regions.